

Venus Tectonics: An Overview of Magellan Observations

SEAN C. SOLOMON,¹ SUZANNE E. SMREKAR,¹ DUANE L. BINDSCHADLER,² ROBERT E. GRIMM,^{3,4} WILLIAM M. KAULA,²
GEORGE E. MCGILL,⁵ ROGER J. PHILLIPS,^{3,6} R. STEPHEN SAUNDERS,⁷ GERALD SCHUBERT,² STEVEN W. SQUYRES,⁸
AND ELLEN R. STOFAN⁷

The nearly global radar imaging and altimetry measurements of the surface of Venus obtained by the Magellan spacecraft have revealed that deformational features of a wide variety of styles and spatial scales are nearly ubiquitous on the planet. Many areas of Venus record a superposition of different episodes of deformation and volcanism. This deformation is manifested both in areally distributed strain of modest magnitude, such as families of graben and wrinkle ridges at a few to a few tens of kilometers spacing in many plains regions, as well as in zones of concentrated lithospheric extension and shortening. The common coherence of strain patterns over hundreds of kilometers implies that even many local features reflect a crustal response to mantle dynamic processes. Ridge belts and mountain belts, which have characteristic widths and spacings of hundreds of kilometers, represent successive degrees of lithospheric shortening and crustal thickening. The mountain belts of Venus, as on Earth, show widespread evidence for lateral extension both during and following active crustal compression. Venus displays two principal geometrical variations on lithospheric extension: the quasi-circular coronae (75–2600 km diameter) and broad rises with linear rift zones having dimensions of hundreds to thousands of kilometers. Both are sites of significant volcanic flux, but horizontal displacements may be limited to only a few tens of kilometers. Few large-offset strike slip faults have been observed, but limited local horizontal shear is accommodated across many zones of crustal stretching or shortening. Several large-scale tectonic features have extremely steep topographic slopes (in excess of 20°–30°) over a 10-km horizontal scale; because of the tendency for such slopes to relax by ductile flow in the middle to lower crust, such regions are likely to be tectonically active. In general, the preserved record of global tectonics of Venus does not resemble oceanic plate tectonics on Earth, wherein large, rigid plates are separated by narrow zones of deformation along plate boundaries. Rather tectonic strain on Venus typically involves deformation distributed across broad zones tens to a few hundred kilometers wide separated by comparatively undeformed blocks having dimensions of hundreds of kilometers. These characteristics are shared with actively deforming continental regions on Earth. The styles and scales of tectonic deformation on Venus may be consequences of three differences from the Earth: (1) The absence of a hydrological cycle and significant erosion dictates that multiple episodes of deformation are typically well-preserved. (2) A high surface temperature and thus a significantly shallower onset of ductile behavior in the middle to lower crust gives rise to a rich spectrum of smaller-scale deformational features. (3) A strong coupling of mantle convection to the upper mantle portion of the lithosphere, probably because Venus lacks a mantle low-viscosity zone, leads to crustal stress fields that are coherent over large distances. The lack of a global system of tectonic plates on Venus is likely a combined consequence of a generally lesser strength and more limited horizontal mobility of the lithosphere than on Earth.

INTRODUCTION

The surface of Venus is replete with a diversity of tectonic features at a wide variety of scales, most remarkably well-preserved because of the absence of a water cycle and the consequently low rates of weathering and erosion [Arvidson *et al.*, 1991]. Over the past decade and a half the Pioneer Venus radar, Earth-based radar observatories, and the Ven

15-16 orbital imaging radars have provided views of large-scale tectonic features on Venus at ever increasing resolution [Pettengill *et al.*, 1980; Masursky *et al.*, 1980; Campbell *et al.*, 1983, 1984; Barsukov *et al.*, 1986]. The radar images from Magellan constitute an improvement in resolution of at least an order of magnitude over the best images previously available [Pettengill *et al.*, 1991]. A summary of early Magellan observations of tectonic features on Venus has been given by Solomon *et al.* [1991]. Data available at the time of that summary were restricted to the first month of mapping and represented only about 15% of the surface of the planet. At the time of this writing, Magellan images and altimetry are available for more than 90% of the Venus surface. Thus a more global perspective may now be taken on the styles of lithospheric deformation on Venus and their implications for the tectonic history of the planet.

It is important to recognize, however, that because many of the data have only recently been acquired, our understanding of the tectonic characteristics of Venus remains uneven. Areas viewed early in the Magellan mission that have been the focus of detailed studies, including Ishtar Terra [Kaula *et al.*, this issue], western Eistla Regio [Grimm and Phillips, this issue; Senske *et al.*, this issue], Alpha Regio [Bindschadler *et al.*, this issue (*a*)], and Lavinia Planitia

¹Department of Earth, Atmospheric, and Planetary Sciences, Massachusetts Institute of Technology, Cambridge.

²Department of Earth and Space Sciences, University of California, Los Angeles.

³Department of Geological Sciences, Southern Methodist University, Dallas, Texas.

⁴Now at Department of Geology, Arizona State University, Tempe.

⁵Department of Geology and Geography, University of Massachusetts, Amherst.

⁶Now at Department of Earth and Planetary Sciences, Washington University, St. Louis, Missouri.

⁷Jet Propulsion Laboratory, Pasadena, California.

⁸Center for Radiophysics and Space Research, Cornell University, Ithaca, New York.

[Squyres *et al.*, this issue (*a*)], have tended to become type areas for discussions of regional tectonics. While we make an effort here to generalize from these focused studies to other regions and to global implications, it should be stressed that such generalizations are preliminary and that there is a need for further detailed analyses of major tectonic provinces throughout the planet.

We begin with a discussion of Magellan observations of the tectonic characteristics of highland regions on Venus, with the aim of sharpening the competing theories for highland formation and evolution. We then consider complex ridged terrain, or tessera, and the extent to which these elevated blocks of intensely deformed crust may be genetically related to highlands. Next we treat the tectonics of plains and lowland regions, including deformation belts and coronae, and possible relations between such features and mantle dynamics. Finally, we comment on the implications of these observations for the global tectonics of Venus.

TECTONICS OF HIGHLAND REGIONS

The highlands of Venus exhibit a wide variety of tectonic features and topographic complexity, and much of the discussion of the global tectonics of Venus prior to the Magellan mission concentrated on models for highland formation and evolution. Magellan data are now available for all the major highland regions of Venus (Figure 1). In this section we synthesize these observations, summarize the principal competing theories for highland tectonics, and evaluate these theories in light of Magellan data.

Beta Regio

Beta Regio is a 2000 x 3000 km highland region centered at 30°N, 282°E (Figure 2). It is cut by a N-S trending trough, Devana Chasma, characterized by several kilometers of relief

and radar-bright and -dark linear features interpreted as normal faults facing toward and away from, respectively, the radar [McGill *et al.*, 1981; Campbell *et al.*, 1984]. On the basis of topographic and morphologic characteristics determined from Pioneer Venus, Arecibo, and Venera data, a large free-air gravity anomaly, and an apparent depth of compensation of long-wavelength topography of 300 km or more, Beta Regio has been interpreted to be a region of uplift, rifting, and volcanism overlying a site of upwelling of hot mantle material [McGill *et al.*, 1981; Phillips and Malin, 1983, 1984; Campbell *et al.*, 1984; Stofan *et al.*, 1989]. Near the southern boundary of Beta Regio is a volcanic edifice, Theia Mons, 350 km across and 5 km high (point T in Figure 2a). Theia Mons lies along the rift and is the source of flows that have infilled the adjacent part of the trough [Campbell *et al.*, 1984; Stofan *et al.*, 1989]. Rhea Mons, a shield-shaped topographic high at the northern end of Beta Regio (point R in Figure 2a), has also been interpreted as a volcanic construct on the basis of its similarity in topography and backscatter characteristics to Theia Mons [Masursky *et al.*, 1980; Campbell *et al.*, 1984; Stofan *et al.*, 1989].

Magellan data have provided both a more complete regional view of Beta Regio as well as greatly improved resolution (Figure 3), resulting in additional information on the structure and sequence of geologic activity in the region. The volcano Theia Mons is clearly superposed on the rift, but the edifice is also cut by later faulting and rifting. In the central region, faulting occurs over a broad region. To the north, the character of the terrain surrounding the rift differs from that to the south. In the south and central regions the rift is surrounded by plains characterized by fractures and volcanic flows, while near the northern end of the rift the surrounding region is composed of complex ridged terrain, or tessera (see below). The topography along the rift shows a great deal of variation (Figure 4), from a relatively deep (2 km or more), narrow (about 80 km) trough near Rhea Mons in

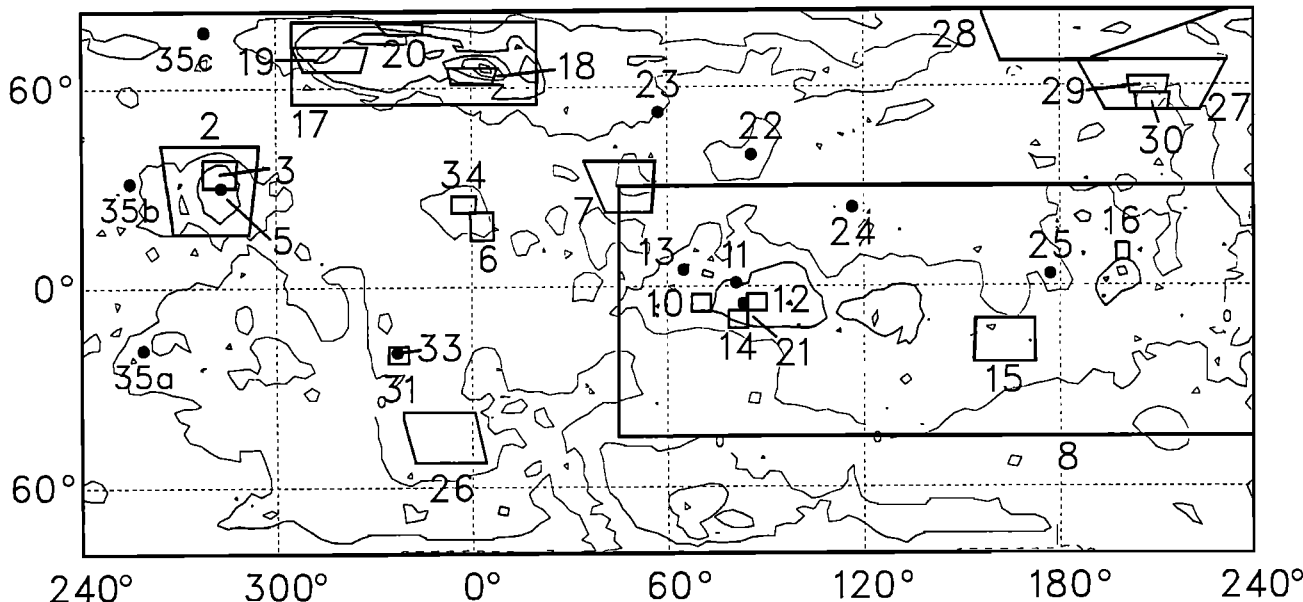


Fig. 1. Index map for subsequent images and topographic maps. The background depicts simplified Magellan altimetry. Contours of negative elevation are dashed; the zero contour is a thin line; contours of positive elevation are thick lines; 2-km contour interval. The altimetry datum here and in other altimetric maps and profiles (except where noted) is a planetary radius of 6051.9 km. Numbered boxes denote the outlines of other figures in this paper.



Fig. 2a. Magellan radar image of Beta Regio. The image is centered at 29.5°N , 281°E ; the width of the image is about 1850 km. This and all subsequent radar images are in sinusoidal equal-area projection; north is up, and the radar illumination direction is from the left; the incidence angle of the radar is about 40° for this image and in general is a function of latitude [Pettengill *et al.*, 1991]. Solid bars denote gaps in the image data. Letters denote features discussed in the text. Theia Mons, the large, radar-bright circular structure centered in the lower third of the image (point T), is located at the junction of several rift trends. Rhea Mons is centered at point R. Point A marks a chain of coronae and fractures that cut the central rift.

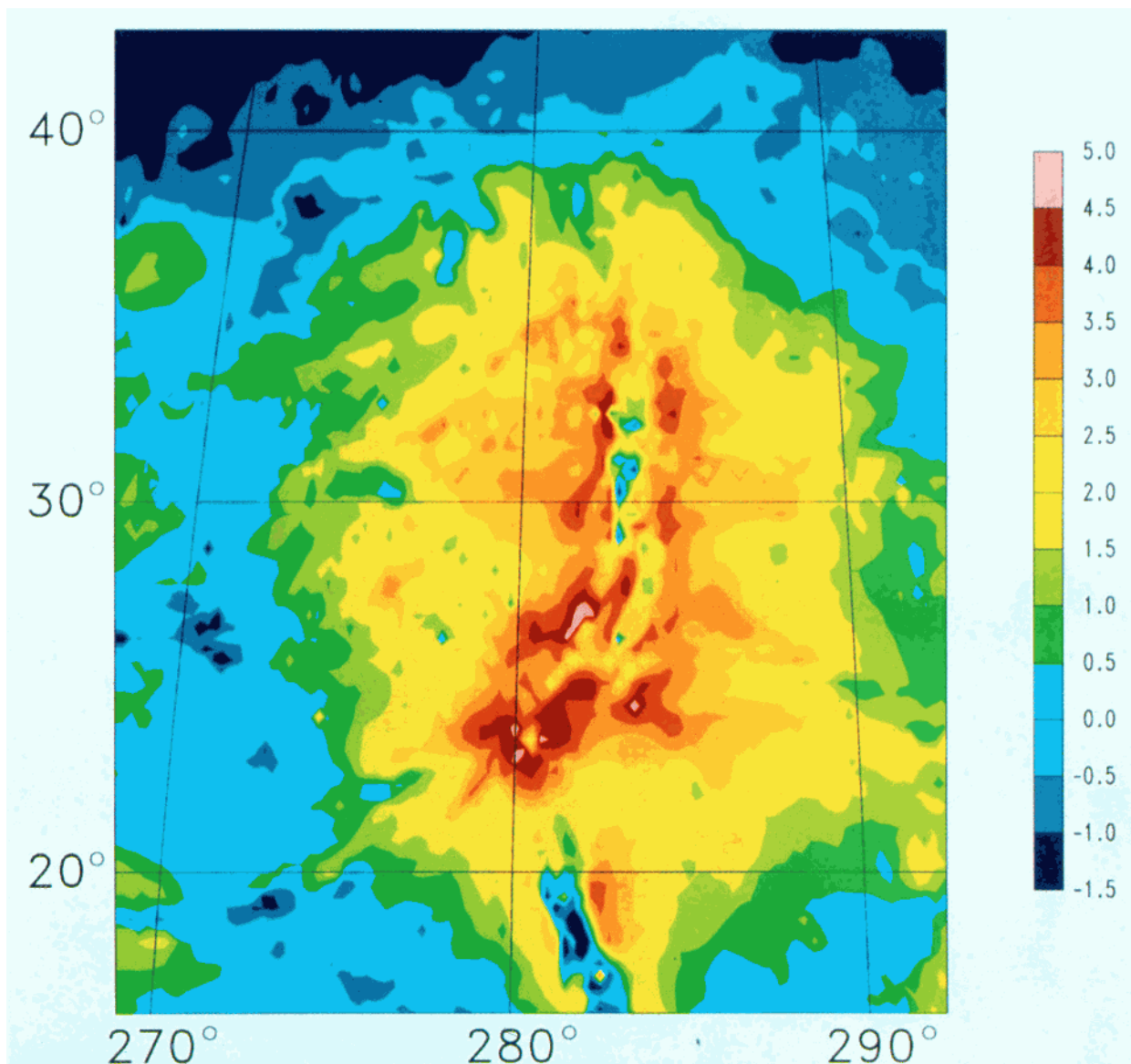


Fig. 2b. Altimetry of Beta Regio. Contours are of individual altimetry measurements, regridded at 0.3° intervals of latitude and longitude; 0.5-km contour interval. The map projection and boundaries are approximately the same as in Figure 2a.

northern Beta Regio (profile AA') to a broader trough (about 130 km wide) with blocks of higher-standing terrain in the center of the rift (profiles BB' and CC'). South of Theia Mons, between Beta and Phoebe regiones, Devana Chasma is characterized by greater relief (as much as 6 km) and more distinct flanking highs than within Beta Regio (profiles DD' and EE', Figure 4).

The tessera terrain in northern Beta Regio is dominated by generally NE trending ridges and grooves spaced 1–2 km apart (e.g., point A, Figure 3); the predominant trend is more nearly N–S in portions of tessera to the east of Devana Chasma (e.g., point B, Figure 3). This dominant tectonic fabric is cut by grooves and lineations oriented in many directions. Normal faults and graben extending from the rift cut across the tessera fabric, and blocks of tessera can be identified within the rift. In many places, the tessera terrain is embayed by smooth, radar-dark plains material interpreted to be volcanic in origin.

Magellan images of Rhea Mons indicate that the topographic high is actually a region of tessera terrain, with

some smooth plains deposits of possible volcanic origin near the summit (point C, Figure 3). Features previously interpreted as flows [Stofan et al., 1989] correspond to lobate regions of complexly deformed terrain. Stofan et al. [1989] had used the apparent rifting of Rhea as evidence that volcanism had preceded rifting in Beta Regio and that the thermal anomaly postulated to have been associated with the rift moved southward over time. From recent Arecibo images [Senske et al., 1991] and Magellan data, it now appears that rifting in Beta Regio occurred concurrently with volcanism at Theia Mons. As noted above, flows from Theia infill the rift and superimpose and are channelled by faults, but the summit region and the flanks are also cut by rift-related extensional faults. A volcanic origin for Rhea Mons is in doubt, and a southward progression of magmatic activity in Beta Regio is no longer supported by the observations.

Faults within the rift vary in morphology, from long (>100 km), relatively straight faults with extremely steep scarps, as seen at the western rift valley wall, to more sinuous faults in



Fig. 3. Magellan radar image of northern Beta Regio centered at about 33.5°N, 283°E. This image, about 900 km wide, shows a region of complex ridged terrain that has been rifted apart. On the western flank of the rift in the lower half of the image is the topographic high known as Rhea Mons. Letters denote features discussed in the text.

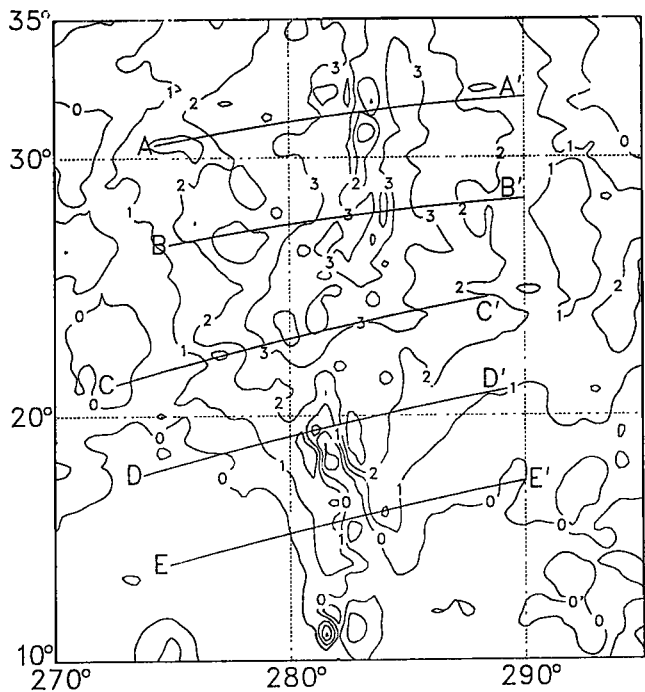


Fig. 4a. Topographic contour map (Mercator projection) of the Devana Chasma rift system showing the locations of the profiles in Figure 4b; altimetry data points were regressed at 0.5° intervals of latitude and longitude; 1-km contour interval.

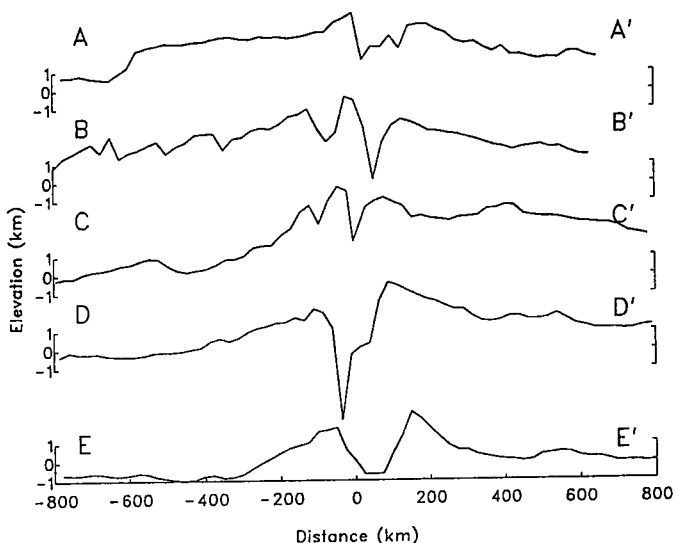


Fig. 4b. Five profiles of topography across Devana Chasma within and south of Beta Regio. Profiles have been constructed from individual altimetry measurements located within 15–25 km of evenly spaced points along a great circle; multiple measurements within the sampling radius are weighted inversely by distance; 50:1 vertical exaggeration.

the center of the rift, to smaller sinuous graben (Figure 5). The impact crater Somerville, located at 30°N, 282.5°E in central Beta Regio, has apparently been split by rifting (Figure 5). The crater was originally approximately 37 km in diameter. The majority of the crater lies on the western flank of the rift, but a small portion of its rim is located on a high-standing block in the rift center. The crater has been extended by about 10 km. This feature thus provides a measure of horizontal displacement and strain accumulated during the time since the crater formed. The average horizontal extensional strain across the crater is about 0.3, but the observed strain is not uniform across the structure and this value need not be representative of the average accumulated strain across the rift as a whole.

On the basis of the identification of tessera terrain in northern Beta Regio and in flanking regions to the east, *Senske et al.* [1991] proposed that Beta Regio may represent a block of tessera terrain disrupted by a mantle plume. Identification of fragments of tessera to the west of Beta Regio and the detailed characteristics of the tessera terrain in northern and eastern Beta Regio as seen in Magellan data are not inconsistent with this hypothesis. No tessera fragments can be identified in southern Beta Regio, but they may be covered by volcanic deposits. Theia Mons sits at the junction of several tectonic trends [*Stofan et al.*, 1989], similar to the situation at major edifices in Eistla and Atla Regiones [*Schaber*, 1982; *Senske et al.*, this issue]. This geometry is similar to the arrangement of volcanism along terrestrial rifts, where rifts tend to propagate and link up between regions of hotspot-related volcanism [*Dewey and Burke*, 1974]. To the north of Beta Regio, a zone of faults and graben that connect a chain of coronae (e.g., point A, Figure 2a) cuts faults extending from Devana Chasma and may represent a late stage of tectonic activity in the region.

Eistla Regio

Eistla Regio is a discontinuous series of rises trending approximately WNW-ESE between longitudes 340°E and 55°E at latitudes 10–25°N. Western and central Eistla Regio are each characterized by broad rises, rift zones, large volcanic structures, strong positive gravity anomalies, and apparent depths of compensation of 100–200 km [*Janle et al.*, 1987; *Senske*, 1990; *Smrekar and Phillips*, 1991; *Grimm and Phillips*, this issue]. Preliminary interpretations of volcanic and tectonic features seen in early Magellan data from western Eistla Regio have been made by *Head et al.* [1991] and *Solomon et al.* [1991]. Detailed discussions of the geology of western and central Eistla Regio, and radar images of the region, are given by *Grimm and Phillips* [this issue] and *Senske et al.* [this issue]. Eastern Eistla Regio was not viewed during the first cycle of Magellan imaging and is not discussed further here.

Western Eistla Regio is dominated by the large volcanoes Sif and Gula montes, which measure 200–300 km in diameter and 1.5–2 km in relief and are the sources of volcanic flows typically extending to distances of 300 km. Extensive fracture systems are associated with these volcanoes, particularly Gula Mons. The most prominent set of fractures is Guor Linea, which extends to the SE of Gula Mons for 1000 km (Figure 6a). Many of these fractures occur along

the walls and floor of a linear trough located along the crest of a broad linear rise. Where best developed the trough is 50–75 km wide, marked by steep walls, and typically several hundred meters deep, although depths in excess of 1 km are present (Figures 6b and 6c). On the basis of its dimensions, relief, fault characteristics, and orientation with respect to Gula Mons, Guor Linea is interpreted as a rift system resulting from the stretching and thinning of the lithosphere [*Solomon et al.*, 1991].

Detailed analysis reveals that at least three sets of fractures may be distinguished within the Guor Linea region [*Grimm and Phillips*, this issue]. The most recent fractures (also the longest and widest), strike nearly E-W and are associated with a deep trough that crosscuts the main trend of the rift system (e.g., point C in Figure 6a). Earlier fractures strike approximately NW-SE and are the principal structures of the rift. Some of the latter fractures well outside the rift valley occur in en echelon patterns consistent with a component of right-lateral shear superimposed on the overall extensional strain (e.g., point B in Figure 6a). The age relationship between these two fracture systems suggests that N-S extension has prevailed most recently but that earlier extension was oriented NE-SW. Alternatively, the earlier faults may have been originally more nearly east-west but rotated clockwise to their present positions, consistent with the sense of the en echelon systems. A third, more faint set of fractures strikes approximately N-S (e.g., point A in Figure 6a); superposition relationships suggest that this system formed early and provided mechanical boundaries for younger NW striking faults but was later reactivated and cuts both NW striking faults and Gula Mons.

Fractures associated with Gula and Sif montes and with other volcanic structures to the NW of Gula Mons have been documented and described by *Solomon et al.* [1991], *Grimm and Phillips* [this issue], and *Senske et al.* [this issue]. Fractures approximately radial to Gula Mons, aside from those of the Guor Linea system, are found to the SW, NW, and east of the volcano. To the NW, the radial fractures merge into a set of faults concentric to the 230-km-diameter Idem-Kuva corona (see later section). The fracture systems associated with Sif Mons are less well developed than those associated with Gula Mons. Radial fractures are best developed to the north, NW, and west. Fine-scale, NNW striking fractures in the NW quadrant have an en echelon appearance, consistent with right-lateral shear, although this geometry could simply be due to truncation against NW striking fractures [*Grimm and Phillips*, this issue].

Central Eistla Regio contains an abundance of volcanic features, many of which have been faulted and fractured. These include Sappho Patera, a 300-km-diameter volcanic structure marked by concentric fractures; a prominent volcano at about 11°N, 14°E, that has been extensively dissected; and several partially buried coronae flanking the main rise. Fractures on the rise trend mostly N-S, whereas those to the east and west (the latter constituting the eastern terminus of Guor Linea) strike E-W.

Eistla Regio was favorably located for the measurement of gravity from Pioneer Venus orbiter tracking data [*Sjogren et al.*, 1983]. *Grimm and Phillips* [this issue] inverted line-of-sight spacecraft accelerations to determine the two-dimensional free-air gravity anomaly for the Eistla region.

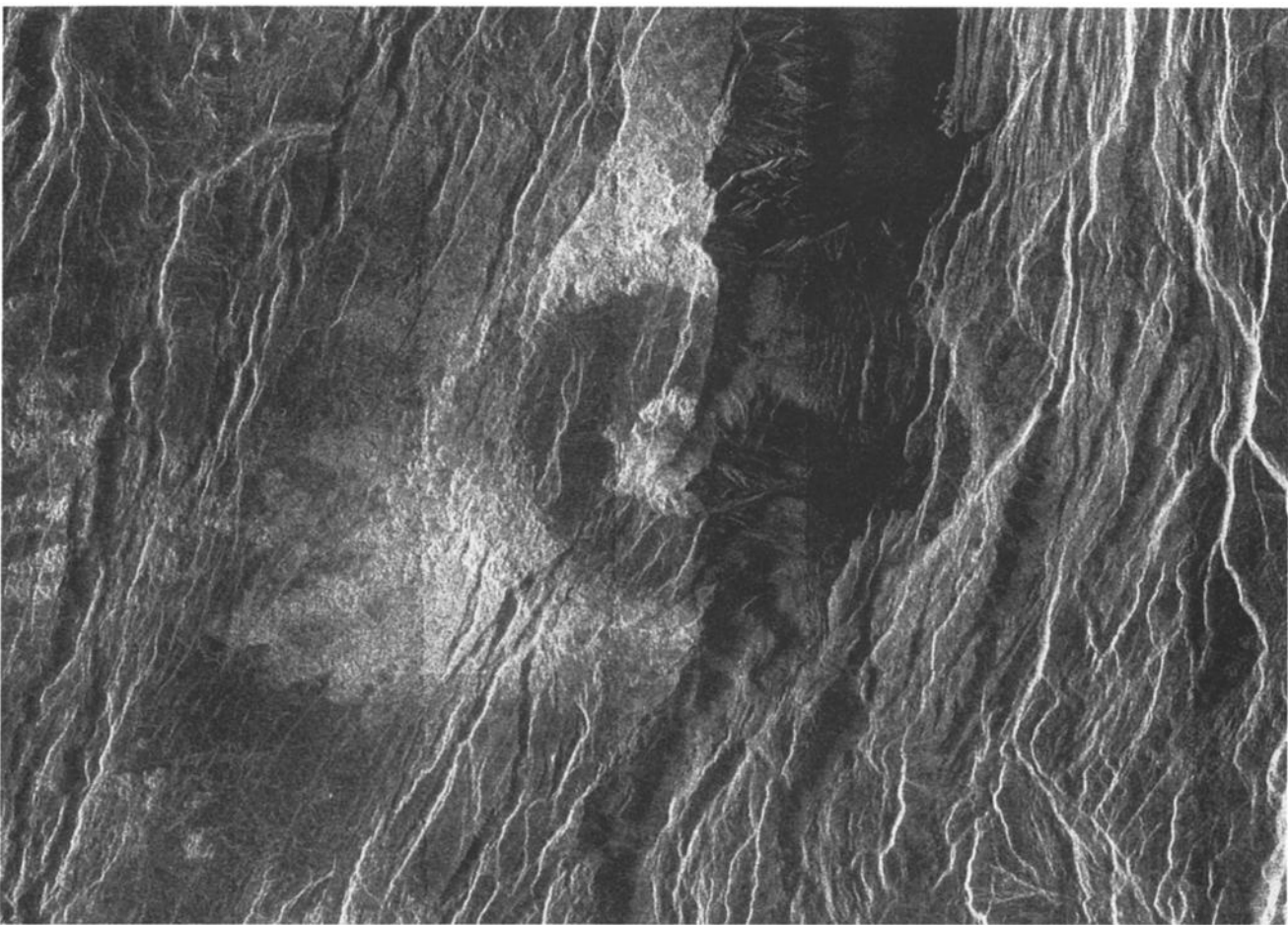


Fig. 5. Magellan radar image of the impact crater Somerville, located within Devana Chasma in central Beta Regio. The image is centered at about 30°N, 283°E and is about 100 km wide. The crater was originally 37 km in diameter; the eastermost fragment of the crater rim has been separated by about 10 km from the main portion of the crater. The floor of the rift valley is marked by numerous linear to sinuous faults and graben.

From the gravity and topography they then determined the mass anomalies on two internal horizons, one at 20 km depth representative of the crust-mantle boundary and one at 200 km depth beneath the lithospheric thermal boundary layer. They converted the deeper set of mass anomalies to equivalent density anomalies, and they solved for the mantle flow that would be driven by these anomalies. On the basis of this flow model, both western and central Eistla are sites of strong mantle upwelling. The western locus of upwelling is stronger beneath Gula Mons than beneath Sif Mons; the upwelling zone extends to the SE beneath Guor Linea. The solution for the shallow set of mass anomalies suggests that the crust beneath western Eistla Regio, particularly Guor Linea, is thinner than average for the region. Crustal thinning is not indicated at Sappho Patera; thickened crust is allowed in this area for some models. Near-surface convective flow is strongly directed to the SW along the southern margin of Eistla Regio; strong northerly flow is predicted directly to the north of Gula Mons but is weaker elsewhere.

The large gravity anomaly of western Eistla Regio indicates that the rise overlies a site of strong mantle upwelling and surface uplift. The larger component of crustal compensation and somewhat weaker flow-related density anomaly at central Eistla Regio may imply that the

crust was thickened magmatically and that the mantle upwelling is presently waning. The strong mantle signal beneath Guor Linea suggests that rifting is in response to mantle convection rather than the passive result of lithospheric stretching. The geometry of most recent faulting in Guor Linea agrees well with the infinitesimal strains predicted from the flow model. Furthermore, if the strikes of earlier faults and the en echelon sense of fractures outside the rift valley of Guor Linea are the result of shear-induced rotation, the clockwise sense of this rotation is consistent with the prediction that the strongest flow is directed to the southwest. An asymmetry in large-scale mantle flow at Eistla Regio may thus be manifested in the regional tectonics.

Bell Regio

Bell Regio is a broad dome approximately 1500 km in diameter (Figures 7a and 7b). It is elongated in the N-S direction and includes distinct northern and southern rises. One large shield volcano, Tepev Mons, and several smaller volcanic centers in southern Bell Regio were identified from Venera 15 and 16 radar images [Barsukov et al., 1986; Markov et al., 1987; Janle et al., 1987]. Volcanic flows and the corona Nefertiti are found in northern Bell Regio. A set of N-S trending fractures located in central Bell Regio was

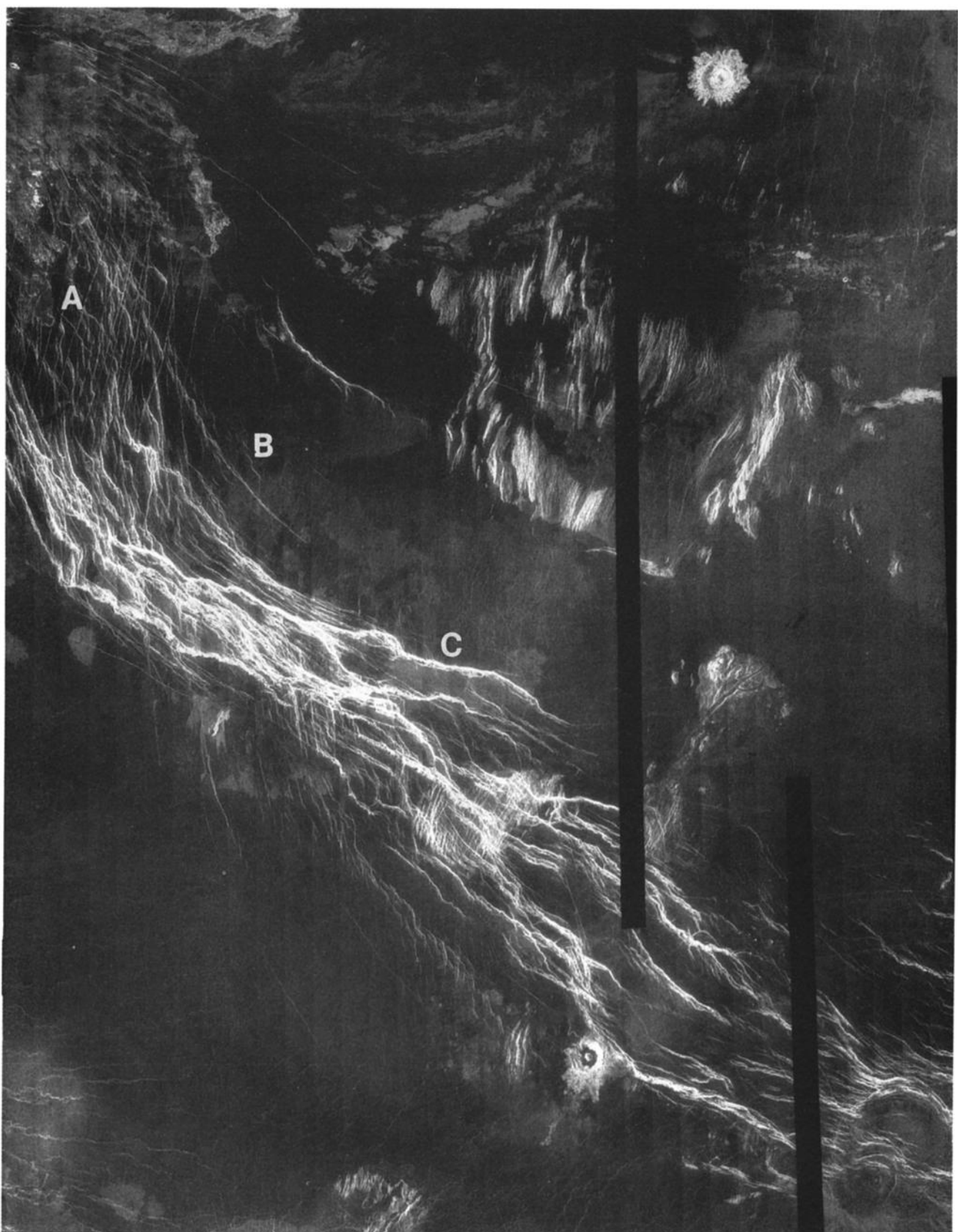


Fig. 6a. Magellan radar image of Guor Linea, a rift system southeast of Gula Mons in western Eistla Regio. The image is centered at 18°N , 3°E and is about 700 km wide. Letters denote features discussed in the text.

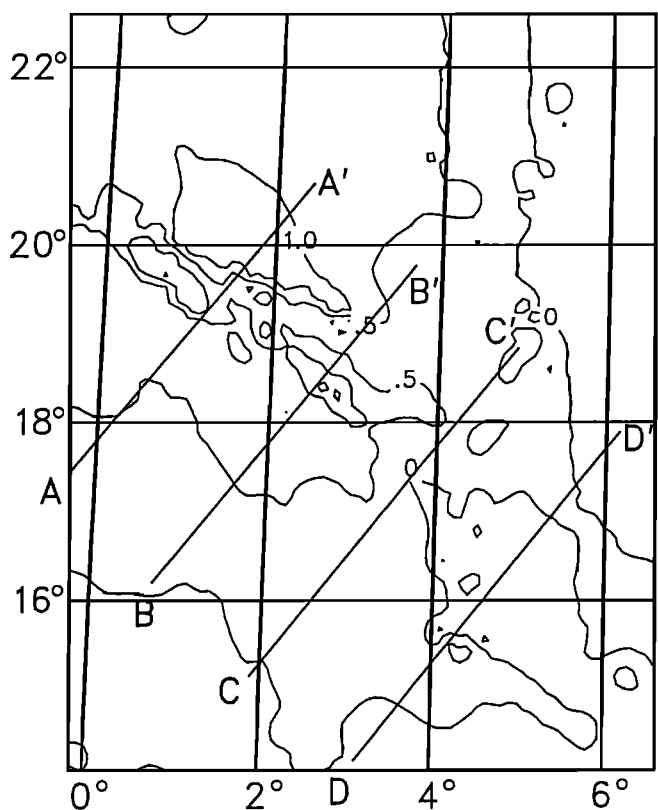


Fig. 6b. Altimetric map of the Guor Linea region showing locations of the profiles in Figure 6c; altimetry data points were regressed at 0.1° intervals of latitude and longitude; the contour interval is 0.5 km.

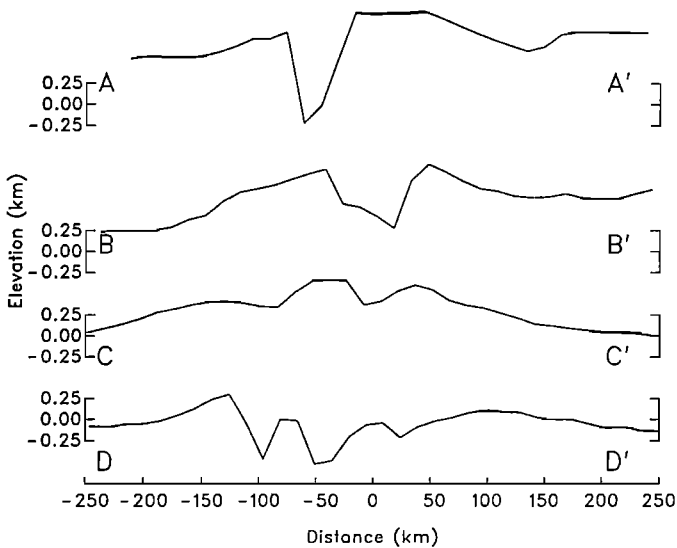


Fig. 6c. Topographic profiles across Guor Linea constructed as in Figure 4 from altimetric measurements located within 15-25 km of points along the profile; 70:1 vertical exaggeration.

identified as a rift system [Janle et al., 1987]. From Pioneer Venus gravity data, the apparent depth of compensation at Bell Regio was found to be in the range of 100-200 km [Janle et al., 1987; Smrekar and Phillips, 1991]. On the basis of these characteristics, Bell Regio was suggested to be a site of mantle upwelling, or hotspot.

Magellan radar and altimetry data reveal new details of the volcanic and tectonic processes at Bell Regio. Of the volcanic centers in southern Bell Regio, Tepev Mons (point T in Figure 7a) is the most striking. The volcano rises approximately 5 km above the local plains and is elongated in the E-W direction (Figure 7b). Eastern Tepev Mons is a volcanic peak that is radar-dark at the summit, while western Tepev Mons contains a shallow, 40-km-diameter, radar-dark caldera (Figure 7c). To the southeast lie a 15-km-diameter caldera with a raised rim and a 30-km-diameter "pancake" dome. Broad, relatively flat-topped domes were first identified in the Magellan radar data and are interpreted to have been formed by more viscous, possibly more evolved lavas than are typical for Venus [Head et al., 1991]. Numerous volcanic flows are associated with each volcanic center; the most recent flows in southeastern Bell Regio appear to emanate from the 15-km-diameter caldera and extend for hundreds of kilometers. Numerous pits, collapse features, and lava channels also occur in this area.

A set of narrow, concentric graben lie approximately 100 km north of the center of Tepev Mons (Figure 7c). One wide trough occurs at a distance of only 50 km. These graben may be the result of flexure of the lithosphere in response to the Tepev Mons load. A depression to the north of the volcano, identified from a single Venera altimetric profile, was suggested to be a flexural moat [Janle et al., 1988]. A similar depression is seen in the Magellan altimetry (Figure 7b), but it may be simply due to the presence of other rises to the north and west of Tepev Mons, as suggested earlier [Solomon and Head, 1990b]. The volcanic flows that form an annulus around much of Tepev Mons (Figure 7c) may be evidence of ponding in a flexural moat.

Southeastern Bell Regio consists of a gentle rise that forms a volcanic center (point A in Figure 7a) distinct from Tepev Mons. Lava flows are generally radar-dark, in contrast to the bright flows to the west (Figure 7a). A set of pit chains and collapse features are centered at 30°N, 48.5°E (point B in Figure 7a). Most of the features radiate out from the center; a few features form concentric arcs. To the south, between 25° and 27°N, are several short, concentric graben that appear to be associated with the same volcanic center (point C in Figure 7a).

Northern Bell Regio has lesser relief and more limited volcanism than southern Bell Regio. A group of small volcanic domes lies between 33° and 35°N and 50°-54°E (point D, Figure 7a). Numerous flows extend outward from the elongated corona Nefertiti (37°N, 48°E, point N, Figure 7a). The corona is defined by an irregular set of concentric fractures, with N-S trending fractures dominating the structure. To the south of Nefertiti are several graben that are extremely faint in the Magellan radar data. These troughs are much more apparent in Venera 15 and 16 radar data, perhaps because of the lesser angle of incidence of the radar, and were interpreted as evidence for rifting [Janle et al., 1988]. The extension represented by these graben is small in comparison to rifting observed in Atla, Beta, and Eistla Regiones (e.g., Figures 2 and 6). To the west are numerous lineations and small coronae (e.g., point E, Figure 7a). Many of the lineations appear to be compressional ridges, while far to the west they form troughs which radiate out from the coronae.

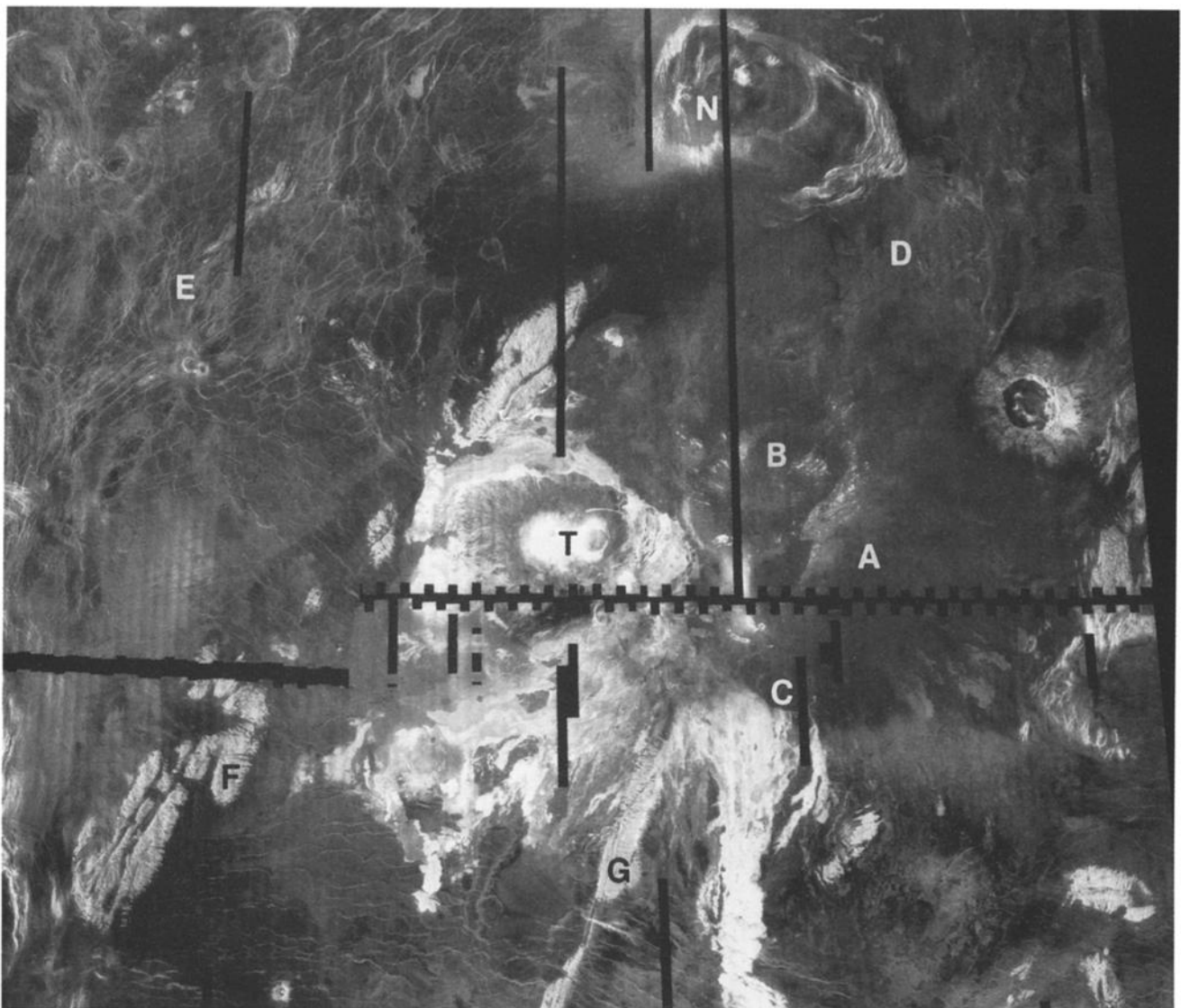


Fig. 7a. Magellan radar image of Bell Regio, centered at 30°N, 45°E. The image is about 1845 km wide. Numerous radar-bright and -dark flows can be associated with the volcanic centers in the southern region. Small blocks of complex ridged terrain are also visible and appear to be older than the volcanic deposits. Letters denote features discussed in the text.

A series of blocks of complex ridged terrain, or tessera, are seen to trend NE from 26°N, 37°E to 33°N, 45°E (e.g., point F, Figure 7a). Only the northern block of complex ridged terrain was identified in the Venera 15 and 16 data [Markov et al., 1987; Janke et al., 1987]. Another block of complex ridged terrain with a similar trend extends southward from south-central Bell Regio (e.g., point G, Figure 7a). Smaller, isolated regions of tessera are also apparent in the southeastern portion of Figure 7a. Two sets of lineations occur within the radar-bright tessera blocks, one trending NE and one trending NW. In some areas, a third E-W trend is also present. In all areas, the NE trending lineations, which consist of long, narrow graben, constitute the most recent deformation. Volcanic flows embay the edges of tessera blocks and cover the floors of many of the larger NE trending graben. In a few locations, the NE trending graben also cut the adjacent volcanic plains. As at Beta Regio, the complex ridged terrain is the oldest terrain type. This tessera terrain either predates the volcanism and the formation of the broad topographic rise or represents the earliest stage of deformation associated with the hotspot.

Two impact craters in the vicinity of Bell Regio were identified in Venera 15 and 16 radar data [Markov et al., 1987]. Potanina (31.5°N, 53°E) has a diameter of approximately 85 km and appears to be partially embayed by volcanic flows associated with Bell Regio. Voynich (35.5°N, 56°E, not visible in Figure 7a) may also be partially embayed; alternatively, the crater may have formed as an asymmetric structure. In addition to these previously identified craters, two other impact craters are visible in Magellan images of southern Bell Regio. A 20-km-diameter central-peak crater lies at 23°N, 40.5°E. It is unclear whether volcanic flows cover some of the ejecta associated with this crater; an E-W trending ridge appears to cut the northern extent of the ejecta blanket. A 60-km-diameter crater on the southern flank of Bell Regio (26.5°N, 42.5°E) is nearly buried by volcanic flows.

In summary, Bell Regio, like Beta Regio, is a broad topographic rise and has a large apparent depth of compensation, moderate deformation, and extensive volcanism. Bell Regio differs from Beta Regio and closely related highlands, however, in that there is little evidence for

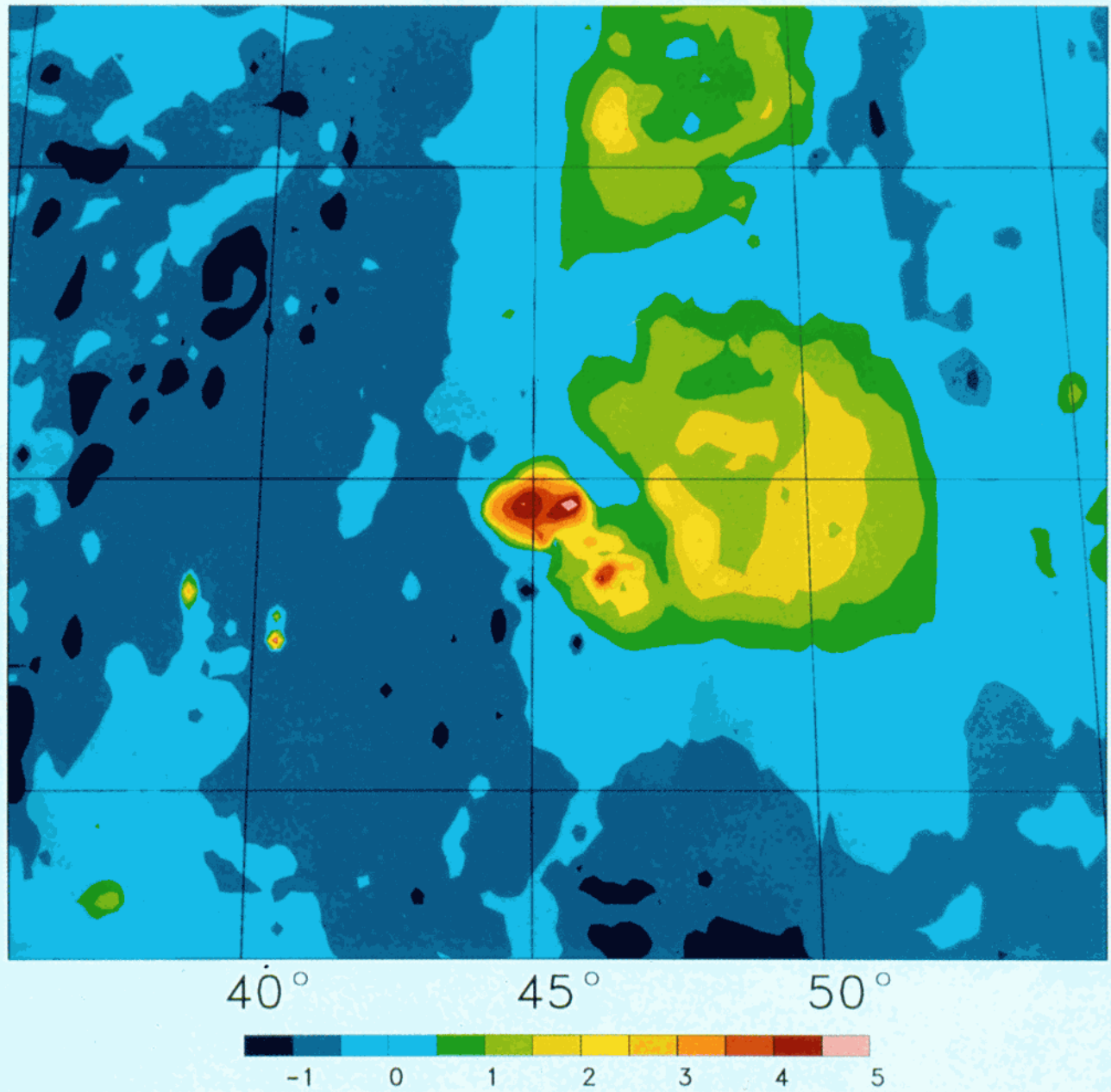


Fig. 7b. Altimetric map of Bell Regio; map projection and boundaries are approximately as in Fig. 7a; 0.5-km contour interval. The altimetric data points were regridded at 0.2° intervals of latitude and longitude.

extensional strain. The variety of volcanic features in Bell Regio suggests that there have been numerous episodes of volcanism, possibly spanning an extended interval of geological time. Volcanic modification of at least two impact craters may imply that volcanism in the area is younger than average for the Venus surface.

Aphrodite Terra

Aphrodite Terra is the largest highland region on Venus, spanning the equator from approximately 45° to 210°E (Figure 8a). The physiographic character of Aphrodite Terra changes dramatically across its length. Western Aphrodite is made up of the highland plateaus Ovda and Thetis regions (45° to 110°E and 110° to 140°E, respectively), which have average elevations of about 3–4 km (Figure 8b). Between 140°E and 190°E, eastern Aphrodite Terra has an average

elevation of only 1–1.5 km and is dominated by a series of ENE trending, elongated ridges and troughs (Figure 8b). Diana and Dali chasmata (approximately 140° to 175°E) are the most prominent of the troughs; we refer to this area as the chasmata region. Atla Regio, located in easternmost Aphrodite Terra, has an average elevation of about 3 km (Figure 8b) but contains the volcanic peaks of Ozza and Maat montes, which rise up to 6 and 9 km, respectively.

The Pioneer Venus gravity data also indicate distinct differences among segments of Aphrodite Terra [Herrick et al., 1989; Smrekar and Phillips, 1991; Kiefer and Hager, 1992]. Apparent depths of compensation increase generally from west to east. Herrick et al. [1989] found apparent depths of compensation of 75 km, 125 km, 250 km, and 240 km for Ovda Regio, Thetis Regio, the chasmata area, and Atla Regio, respectively. Some variation is also apparent across

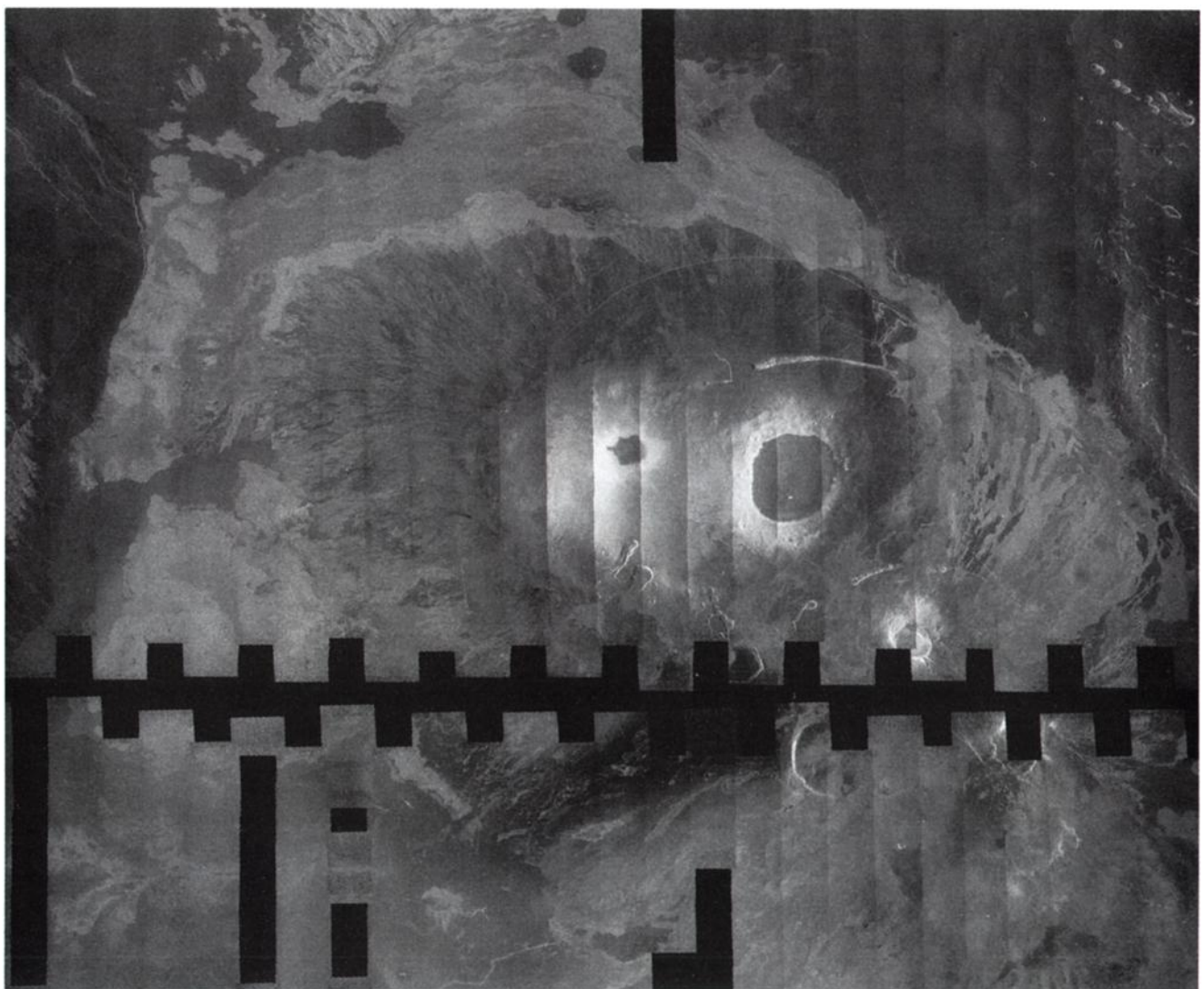


Fig. 7c. Radar image of the Tepev Mons area showing several volcanic constructs. Tepev Mons, in the center of the image, is distinguished by several sets of concentric graben as well as lava flows apparently ponded in a flexural moat. The image is centered at 29.5°N, 45°E and is approximately 450 km wide.



Fig. 8a. False-color radar mosaic of Aphrodite Terra (52.5°E-240°E, 45°S-30°N); cylindrical equidistant projection. In this image, gaps in the Magellan imaging data were filled with Pioneer Venus data.

TABLE 1. Definition of Map Units in Aphrodite Terra

Symbol	Unit	Type Area (Figure)	Definition
TI	interior block terrain	10	Irregular raised blocks, more or less equidimensional, 15–75 km across, separated by curvilinear troughs. Blocks are highly fractured by graben, but regionally there are few long fractures.
TR	linear ridge terrain	11,12	Linear, rounded ridges crosscut perpendicularly by narrow troughs, probably graben. Generally foldlike appearance. Ridges typically 8–15 km wide and 30–60 km long. In some cases, ridges are curved and irregular, typically with fewer cross-cutting fractures.
TL	linear trough terrain	13	Generally appears cross-fractured, with at least one well-developed system of straight, parallel troughs, ten to hundreds of kilometers long and a few hundred meters to a few kilometers wide, interpreted to be graben.
T	other tessera		Similar to TR and TI but low-lying and not as radar-bright.
S	shield volcano		Topographic domes with radial volcanic flows, often with associated rifts.
C	crater material		Includes all subunits of craters: ejecta, wall, floor, and peaks.
P	plains, undivided		Smooth, radar-dark planar surface; interpreted to be volcanic.
F	festoon		Volcanic flow which appears to be thicker and to have been more viscous than typical lava flows on Venus.
Stipple	fractured terrain	14	Swarms of radar-bright lineations interpreted to be extensional fractures.

the chasmata area. Between 160°E and 190°E, the apparent depth of compensation is less well constrained than in other areas of Aphrodite Terra, indicating that the gravity and topography are less well correlated.

The only radar imaging observations of Aphrodite Terra prior to Magellan were those made by Pioneer Venus. As in other areas of Venus, the regions of high topography in Aphrodite Terra are radar-bright and are consistent with both increased roughness and the presence of high-dielectric materials [Pettengill et al., 1988; Klose et al., this issue]. On the basis of reflectivity and rms slope inferred from Pioneer Venus data, Bindschadler et al. [1990a] concluded that Ovda and Thetis regiones are likely to be areas of significant deformation, similar to the complex ridged terrain, or tessera, seen in higher-resolution Venera and Arecibo images (see later section). While not as radar-bright as the regions of high topography, many of the chasmata appear bright in comparison to their surroundings [Senske, 1990]. Although Pioneer Venus radar images were not of sufficiently high resolution to allow volcanic flows to be resolved, the peaks of Maat and Ozza montes were interpreted as volcanic centers because of the similarity of morphological and gravity characteristics in Atla Regio to those of Beta Regio [Senske, 1990].

Magellan radar data show that the patterns of deformation across Aphrodite Terra are varied and highly complex (Figure 8a), and, indeed, the notion that Aphrodite should be regarded as a single large-scale geological entity is questionable. As a guide to the discussion of structural differences among the various segments of this highland, a preliminary geologic map of Aphrodite Terra is shown in Figure 9. There is no basis, of course, at present for determining lithology and stratigraphy from the Magellan radar images except in limited cases. We utilize instead the concept of geomorphic or structural units, distinguished on the basis of tectonic imprint as seen in the radar images. The map units adopted for Aphrodite Terra are given in Table 1.

Western Aphrodite: Ovda and Thetis regiones. Magellan data confirm the earlier suggestion from Pioneer Venus data [Bindschadler et al., 1990a] that Ovda and Thetis regiones are characterized by highly deformed terrains. The primary units found in Ovda and Thetis Regiones are interior block and linear ridge units, with regions of linear trough terrain near the northern and portions of the southern boundaries (Figure 9). Fractures are present on most of the margins of both Ovda and Thetis regiones. Overall, these tectonic patterns indicate early crustal shortening, followed by more modest lateral extension. Type examples from Ovda Regio illustrate the characteristics of the principal map units for Aphrodite.

A region of interior block terrain in eastern Ovda Regio is shown in Figure 10. The primary structures are broad domes and ridges, approximately 20 km in width and interpreted as compressional in origin. These features are separated by radar-dark regions interpreted to be later volcanic flows. In this region, fractures radiating out from a structure near the southern limit of the image cut the domes and ridges. Such crosscutting of domes and ridges by later fracturing is typical of the interior block terrain and indicates a general sequence of crustal shortening followed by modest extension.

The interior regions of Ovda Regio, and portions of Thetis Regio, are composed primarily of linear ridge terrain (Figure 11). In many areas, the ridges are continuous over hundreds of kilometers and have a typical spacing of 10–20 km. The ridges are similar in appearance to fold and thrust belts and are interpreted as products of crustal shortening. Fractures typically cut the ridges, often at right angles (Figure 11). In other regions, the ridges are much more irregular. An example from central Ovda Regio is shown in Figure 12. On the right side of the area shown, ridges are continuous over greater distances and are curved. These patterns may be the result of deformation of originally more linear ridges. On the left side of Figure 12, the ridges are broken up into short segments, suggesting that this area might represent an early

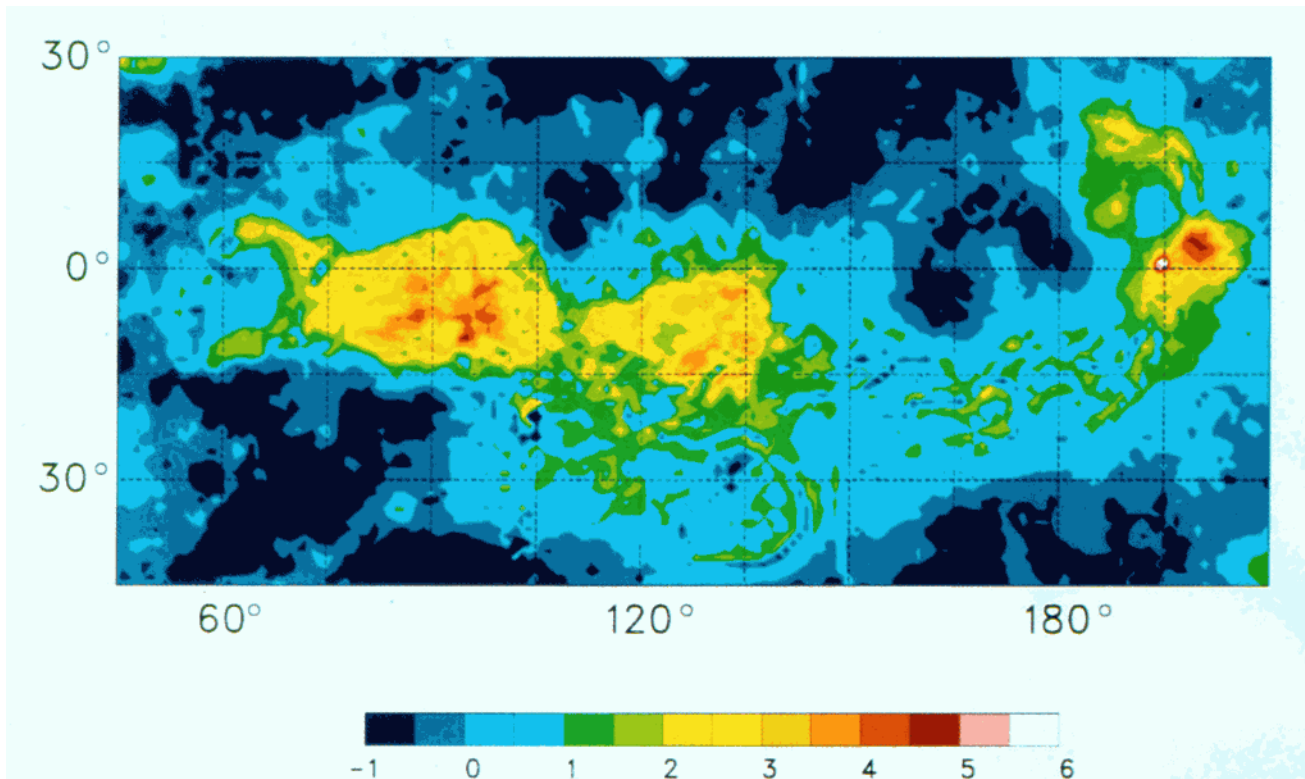


Fig. 8b. Altimetric map of Aphrodite Terra; map projection and boundaries are approximately as in Figure 8a; 0.5-km contour interval. The individual altimetric measurements were regridded at intervals of 1° in latitude and longitude.

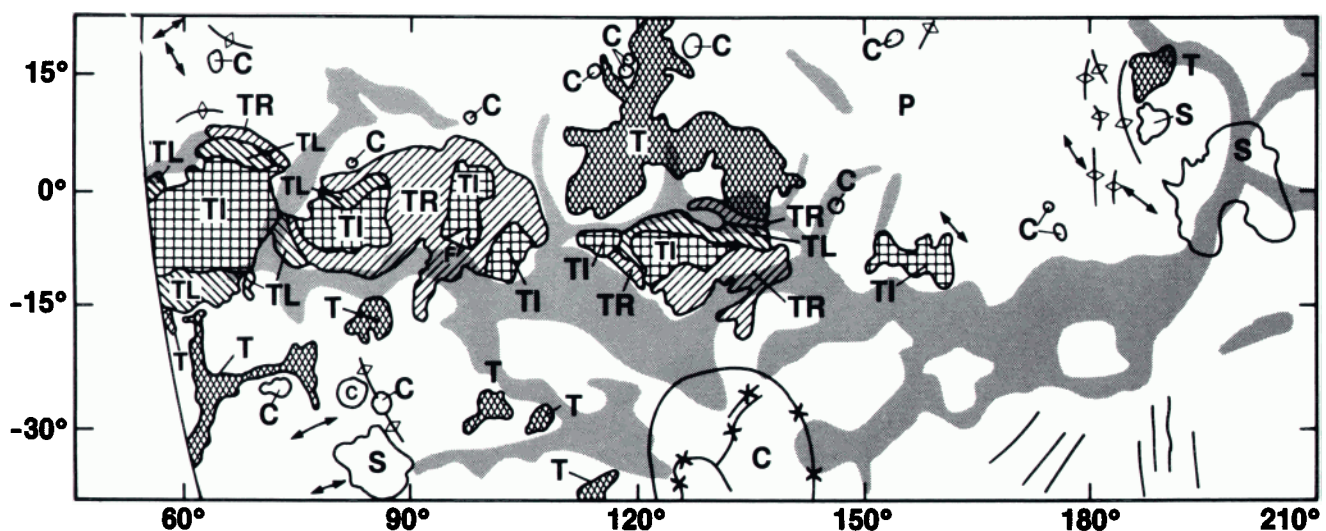


Fig. 9. Preliminary geological map of Aphrodite Terra (by R. S. Saunders). Map units are defined in Table 1. Double ended arrows indicate the general trend of lineations in a given area. Lines with diamonds indicate ridges, those with crosses indicate troughs, and unmarked line segments indicate lineations; all such lines are generalized and denote families of like features with similar trends. The line on the left marks the map boundary.

stage in the development of interior block terrain. As in other highland areas, much of the highest terrain is marked by radar-bright material (lower portion of the image).

In regions of linear trough terrain, narrow graben are the predominant structure. These graben are several kilometers in width and tens of kilometers in length and generally represent the latest stage of significant regional strain (Figure 13). Ridges similar to those in the linear ridge terrain are visible in Figure 13, but are much more dissected. Smooth, radar-dark patches, interpreted as lava flows, embay many of the graben, often filling in the lows between the NE trending ridges.

The margins of Ovda and Thetis regiones are dissected by fracture sets that often continue into the surrounding plains. A part of the southern edge of Ovda Regio is shown in

Figure 14. In this region the ENE trending fractures near the bottom of the image crosscut both linear ridge terrain (upper right) and linear trough terrain (upper left). These fractures are continuous for tens to hundreds of kilometers and are typically 1 km wide. They represent the most recent stage of deformation in Ovda and Thetis regiones, which appears to have overlapped in time with plains-forming volcanism.

Chasmata area. The linear to arcuate troughs in the chasmata area are among the deepest found on Venus. The troughs are hundreds of kilometers to 1000 km in length and tens of kilometers to 100 km in width and are typically bounded on one side by a ridge comparable in height to the depth of the trough [McGill *et al.*, 1983; *Ford and Pettengill*, this issue, Plate 4]. The change in elevation from the bottom of a trough to the top of an adjacent ridge can be

as great as 7 km over a horizontal distance of only 30 km. The area around the troughs is highly deformed, as illustrated in Figure 15. Diana Chasma is located in the upper left of Figure 15, and Dali Chasma runs approximately E-W along the lower half. Most of the small-scale deformation is manifested as fractures, many of which are paired and form graben. Fractures generally have an ENE trend and lie along a line connecting eastern Thetis and Atla regions. Much of the region shown in Figure 15 is mapped as fractured terrain (Figure 9) because of the dominance of these fractures. Locally fractures can radiate outward from a central point, such as in the two coronae in the upper central and lower right portions of Figure 15. Ridges, which appear to be compressional in origin, also occur in this region. On the left side of Figure 15, a N-S band of lineations, dominantly ridges, can be seen along a double trough [Ford and Pettengill, this issue] connecting Diana Chasma with what appears to be the western terminus of Dali Chasma. This pair of troughs has been variously interpreted as a fold-and-thrust belt [Suppe

and Connors, this issue] and as a transform zone accommodating strike-slip motion and linking the two chasms [McKenzie et al., this issue].

On the basis of the Pioneer Venus altimetry and radar data, this region and areas having chasms with similar morphological characteristics, such as Hecate Chasma southwest of Beta Regio, were interpreted as regions of extension [Schaber, 1982] or crustal spreading [Head and Crumpler, 1987, 1990; Senske, 1990]. The chasms in central Aphrodite and Hecate do show similarities in terms of widths and relief to chasms interpreted as rift structures in Beta Regio (Devana Chasma, Figures 2-5) and Atla Regio (see below), but these latter chasms tend to be more symmetric in cross section and linear in plan view. McKenzie et al. [this issue] have suggested that the chasmata region may be an area of lithospheric subduction, on the basis of a similarity of arcuate planforms, asymmetric topographic profiles, and relief to those of deep-sea trenches on Earth.

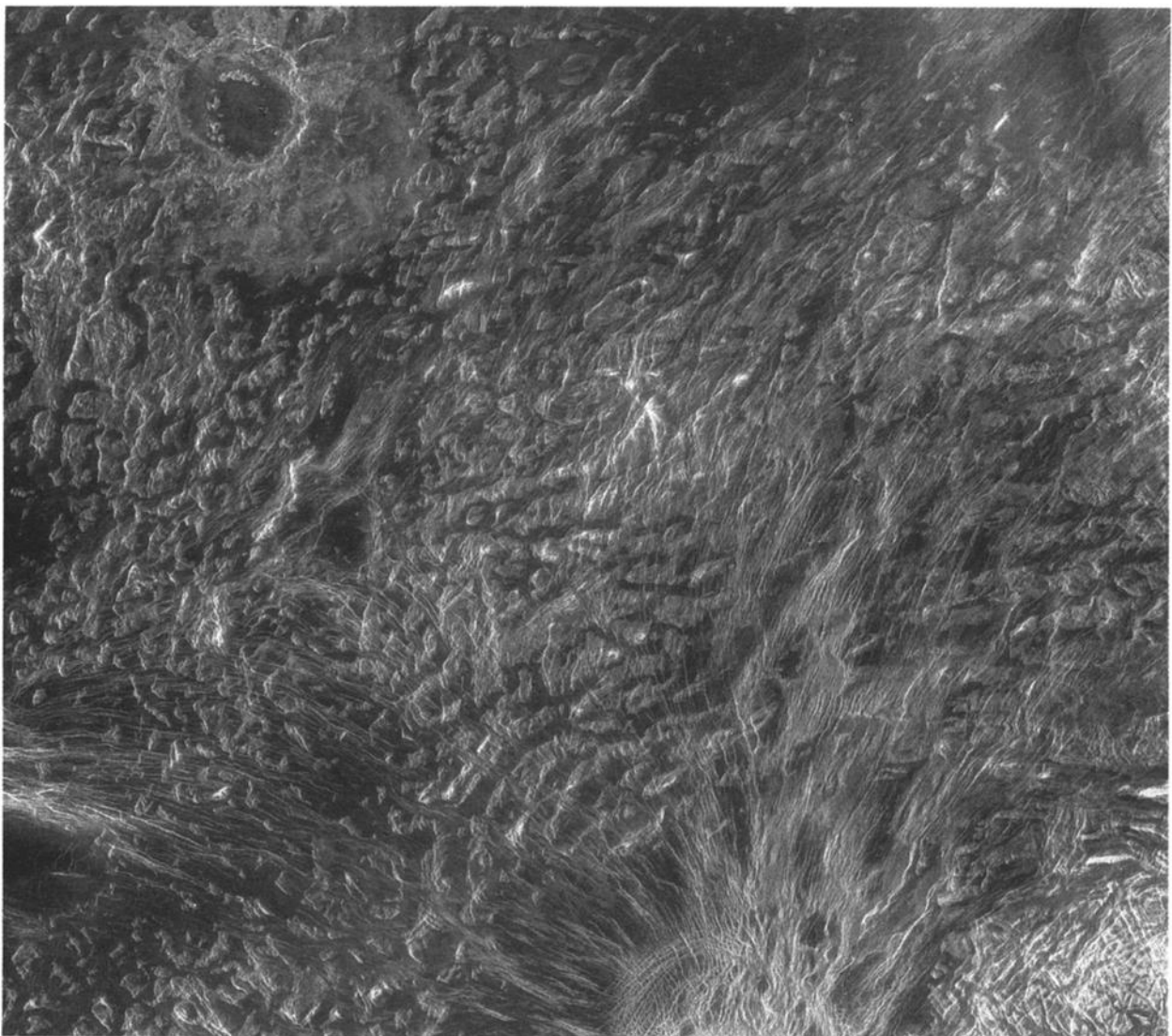


Fig. 10. Magellan radar image from eastern Ovda Regio. The image is centered at 5°S, 70°E and is 600 km wide. The region is a type area for the interior block terrain (T1) of Figure 9. The earliest discernible event in this region was the formation of irregular broad domes and ridges about 20 km across. The valleys between these ridges then were flooded by radar-dark lava flows. An extensive fracture system radial to the circular feature at the bottom of the image postdates the domes, ridges, and flooded valleys. An impact crater 60 km in diameter is visible in the upper left.

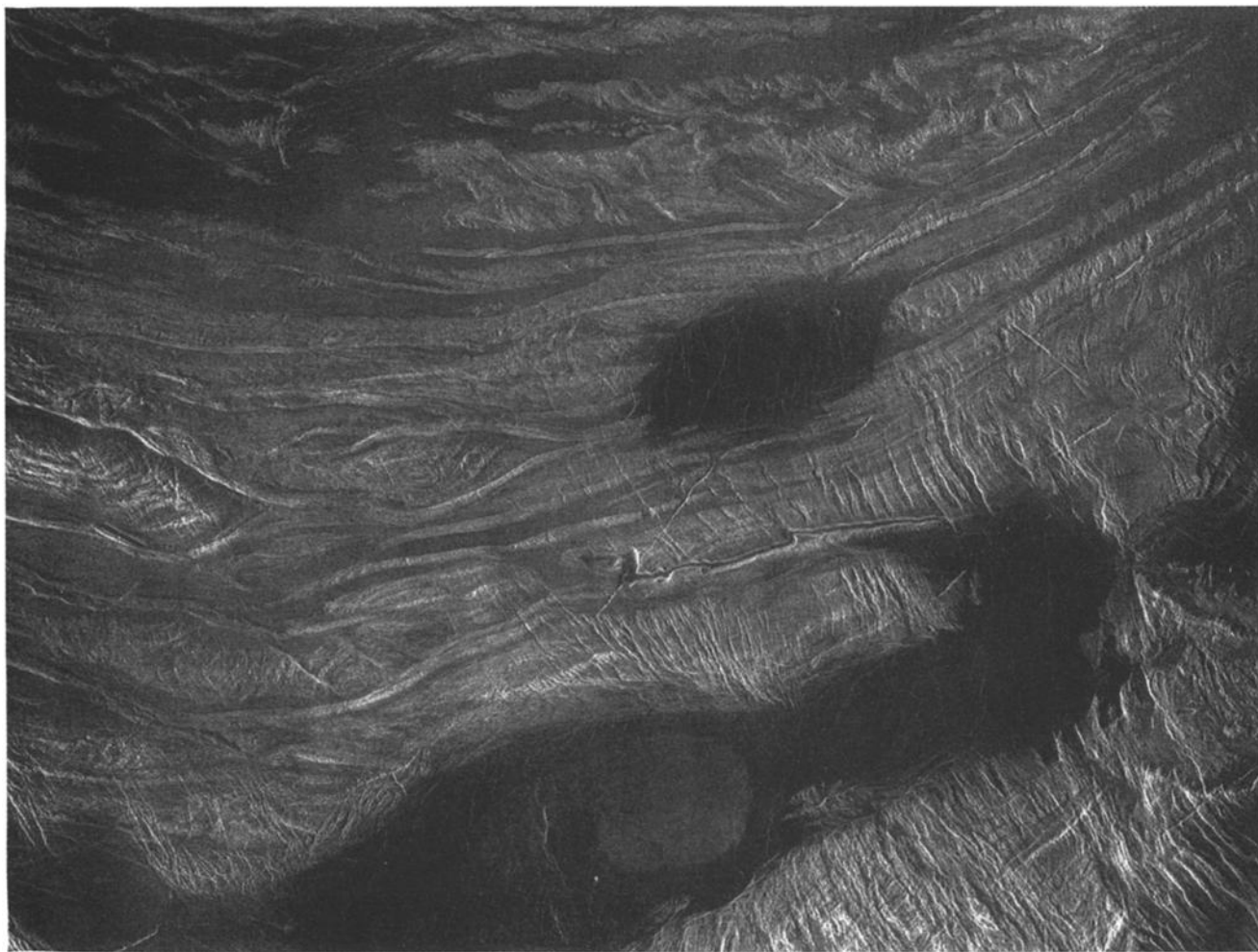


Fig. 11. Magellan radar image of the northern boundary of Ovda Regio. This image is centered at 1°N, 81°E and is 300 km wide. The region shown is a type area for the linear ridge terrain (TR) of Figure 9. The dominant features in the image are low-relief, rounded, linear ridges, typically 8–15 km in width and 30–60 km long. The ridges lie mostly along a 100- to 200-km-wide slope across which the elevation drops 3 km from Ovda Regio to the plains to the north. Some ridges have been cut by orthogonal extensional fractures. Radar-dark material, either volcanic or aeolian, fills the regions between some ridges. The curvilinear, banded nature of these ridges is suggestive of N-S crustal shortening.

Atla Regio. Atla Regio is a broad, highland dome (Figures 8a and 8b) with numerous volcanic centers and rifts, similar in many ways to Beta Regio. A regional-scale radar image of Atla Regio is given by Bindschadler *et al.* [this issue (b)]. The area is mapped as a complex of shield volcanos and fractured terrain (Figure 9; see also Senske *et al.* [this issue]). Maat Mons is the most central and highest (approximately 9 km in elevation) of the major volcanic constructs in Atla Regio. Volcanic flows and radial graben and fractures extend for hundreds of kilometers out from its center. Numerous episodes of volcanism and fracturing are apparent, with flows infilling and embaying older fractures and fractures crosscutting flows. The summit of Maat Mons is marked by a region of radar-dark material [Klose *et al.*, this issue; Senske *et al.*, this issue] approximately 100 km across. Pits, flows, and small domes are visible within the dark region, which is bounded to the west and south by several concentric graben, 5–10 km in width. A 100-km-wide field of small volcanic domes lies to the north of the summit.

Ozza Mons lies to the northeast of Maat Mons. Overlapping volcanic flows, tens to hundreds of kilometers in length and of varying radar brightness, surround Ozza Mons

[Senske *et al.*, this issue]. Except for the outline of what appear to be several summit calderas, 10–30 km in diameter, fractures are not present in the vicinity of this volcano. To the south lies a secondary volcanic center, which is elongated along a NE trend. Volcanic flows are abundant in this area, but fractures are the dominant features. While some fractures are radial and concentric, most trend NE and are continuous with the system of fractures and graben that connect Atla Regio with the chasms to the southwest.

In addition to these main volcanic centers, there are a wide variety of smaller features. Several pancake domes, small domes, pits, and local lava flows are visible throughout Atla Regio. Sapas Mons, another large shield volcano, lies near the western margin of the region. Numerous impact craters occur in the area (Figure 9); many of these craters have been modified by volcanic flows or by fractures.

Despite the abundance of volcanism, systems of fractures are the most prominent features in Atla Regio. Four major fracture systems extend outward from the center of the region (Figure 9). These fracture systems appear as radar-bright lineations in Figure 8a. One of these systems, Ganis Chasma, connects Maat Mons to Nokomis Montes to the

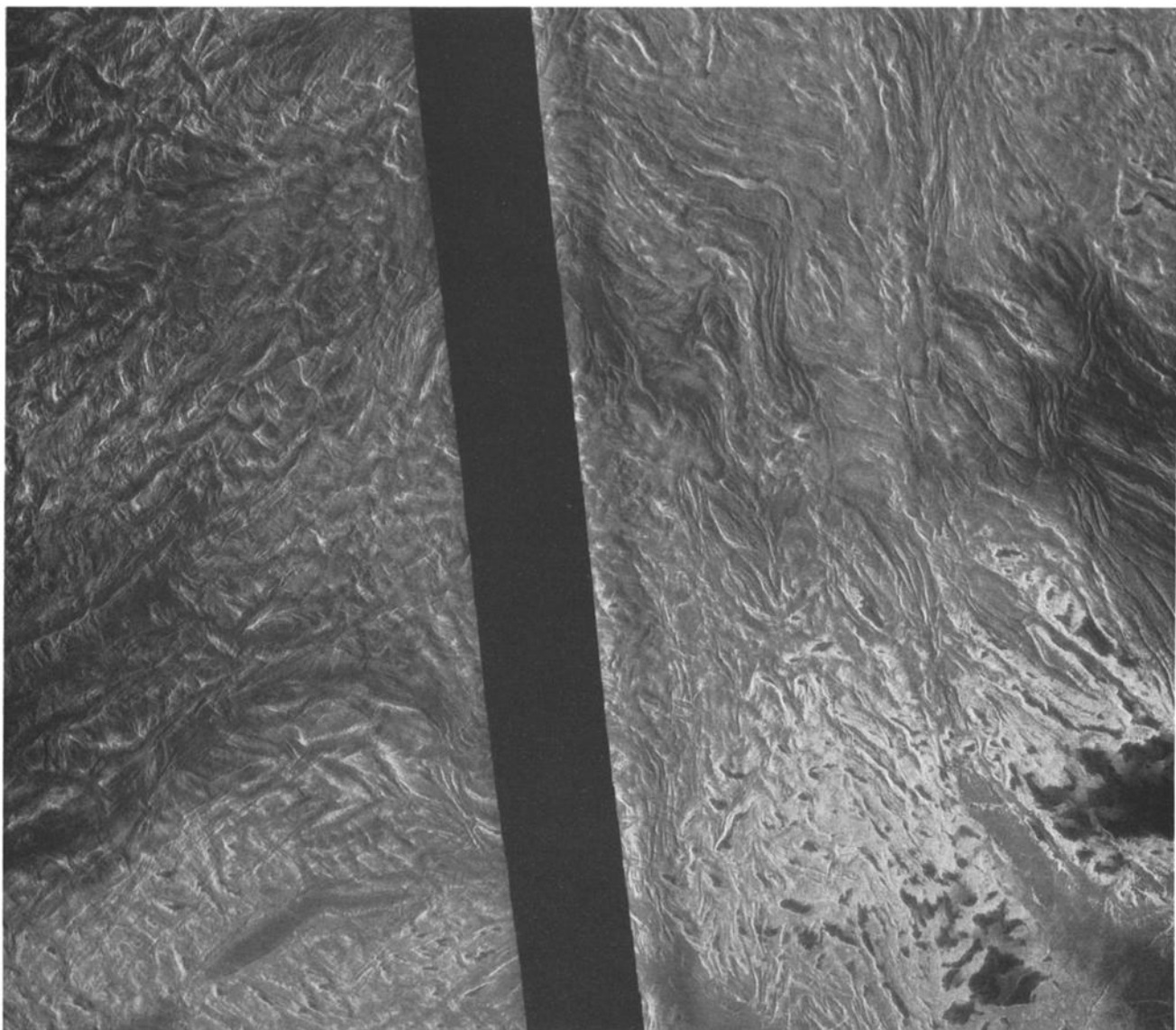


Fig. 12. Magellan radar image of a highly deformed region in central Ovda Regio. This image is centered at 5°S, 87°E and is approximately 530 km wide. This area of complex ridged terrain, or tessera, consists of contorted to sigmoidal ridges interpreted to have been polydeformed by compression. The sigmoidal folds in the upper right portion of the image suggest that initial compression formed a ridge belt which was subsequently deformed by an approximately orthogonal compressional stress field; this area illustrates the irregular facies of the linear ridge terrain best expressed on the margins of Ovda Regio (see Figure 11). The area in the left half of the image is characterized by ridges broken into short segments and may represent an early stage in the development of interior block terrain (see Figure 10).

northeast (Figure 16). Ganis Chasma is approximately 1000 km in length, 300 km in maximum width, and 1-1.5 km in relief. The graben that make up the fracture system are 1-10 km in width, tend to have irregular sides, and typically crosscut each other, forming a branching pattern. Volcanic flows both bury and are cut by the fractures. Although individual fractures and graben could not be resolved prior to Magellan, Ganis Chasma and the other chasms extending out from Atla Regio were interpreted as rifts [Schaber, 1982; Senske, 1990] on the basis of their orientation with respect to the volcanic centers and their topography and by analogy with similar systems in Beta Regio. Magellan data generally confirm this interpretation.

Ishtar Terra

The highland Ishtar Terra, centered at 65°N, 5°E, stands more than 2 km above mean planetary radius and extends

3700 km E-W and 1500 km N-S. The discussion in this paper is confined to the part west of 30°E, exclusive of Fortuna Tessera. Ishtar Terra contains a rich variety of landforms, as revealed in its topography (Figure 17) and in regional-scale radar images [Kaula et al., this issue]. The broad plateau, Lakshmi Planum, lies at its center (Figure 17). Its margins are the four mountain belts Danu, Akna, Freyja, and Maxwell montes and the steep scarps Vesta Rupes and north and south scarps forming, respectively, the southwestern, southeastern, and northeastern edges of the plateau. Regions of complex ridged terrain, or tessera, occur in plateaus outboard of the mountain belts. Outboard and at the base of the north and south scarps are two basins (referred to as the south and north basins), containing material similar to plains found elsewhere on Venus. Magellan image and altimetry data reveal many new details of the tectonic characteristics of these five types of physiographic features.



Fig. 13. Magellan radar image of a type area in Ovda Regio for the linear trough terrain (TL) in Figure 9. This image is centered at 5°N, 65°E and is 210 km wide. Closely spaced, narrow troughs trend N to NNW and intersect wide, generally older ridges and valleys trending approximately NE. Older troughs trending WNW are recognizable in only a few areas. The presence of radar-dark, apparently smooth plains suggests that infilling of the troughs and valleys was one of the most recent events. West to NW trending fractures cut some of the dark plains and indicate postemplacement deformation. A small volcanic dome is visible near the center of the image.

Upland plains: Lakshmi Planum. The surface of Lakshmi Planum contains several broadly defined units of distinguishable age [Kaula et al., this issue]. The ridged terrain units, characterized by intersecting ridges and troughs, are older than the extensive smooth plains units; caldera-associated and margin-associated (both mountain- and scarp-associated) deformation constitutes the most recent tectonic activity. The ridged terrain units (centered near 65°N, 345°E) extend for hundreds of kilometers and are

heavily embayed by the lava flows that make up the smooth plains. The predominant trends of their lineations are not related to other structural trends observed in the adjacent plateau margins or mountain belts.

The smooth plains are dominant in the southern, less elevated portion of Lakshmi Planum, near 60°N. Many of the troughs within these plains parallel the nearest plateau margin or mountain belt. The most pronounced are those paralleling the most prominent marginal features; most

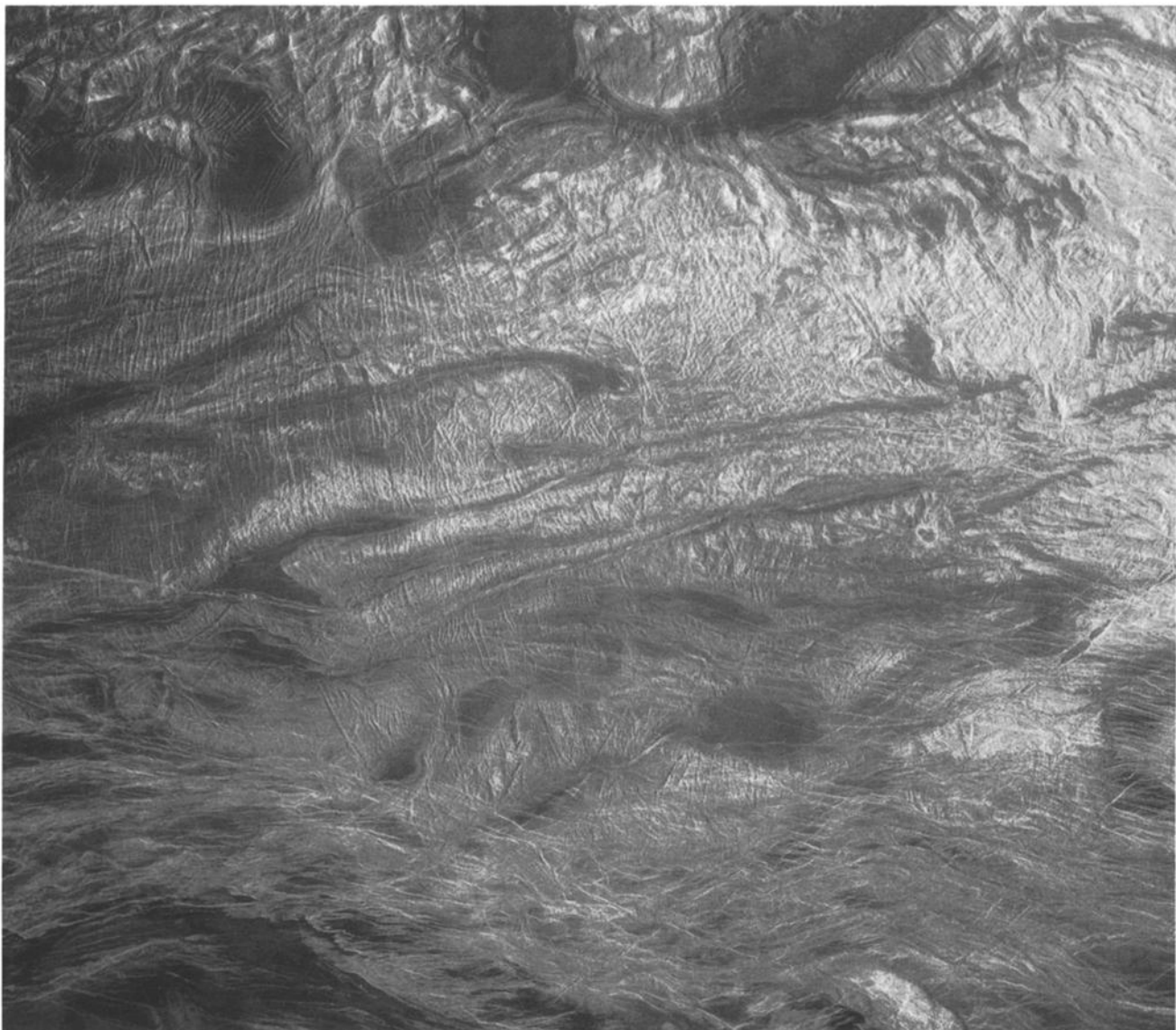


Fig. 14. Magellan radar image of an area in Ovda Regio; the southern portion of the image depicts the fractured terrain (mapped with stippling) of Figure 9. The image is centered at about 10°S, 82°E and is 600 km wide. The area is dominantly one of complex ridged terrain, or tessera. The dark regions lacking structure have been flooded by lava and stand lower than the surrounding tessera.

notable are the Rangid Fossae paralleling the western front of Maxwell Montes near 62°N, 357°E (Figure 18a). Those paralleling Vesta Rupes and the north and south scarps are narrow but distinct, while those paralleling Danu Montes are less distinct. The two large calderas, Colette (centered at 66°N, 323°E, diameter approximately 100 km) and Sacajewea (centered at 64.5°N, 336.5°E, diameter approximately 200 km) paterae, dominate the volcanic and deformational history of central Lakshmi Planum [Roberts and Head, 1990]. Smaller calderas, such as Siddons (61.5°N, 340°E), are also present.

Mountain belts: Maxwell, Freyja, Akna, and Danu montes. All of the mountain belts are made up of ridges, tens to hundreds of kilometers in length (e.g., Figures 18a and 19a). These ridges were interpreted as compressional folds and thrust faults on the basis of Arecibo and Venera images [Campbell et al., 1983; Phillips and Malin, 1984; Barsukov et al., 1986; Crumpler et al., 1986]. In the more intensely folded parts of the belts, the ridge spacing is quite variable.

These spacings are typically 3–10 km but range from less than 1 km to 20 km. The length scales are consistent with a weak layer of accommodation at a few kilometers depth [Zuber, 1987]. All the belts have radar-bright crests (Figures 18a and 19a), a consequence of high intrinsic reflectivity as well as roughness [Klose et al., this issue]. In Maxwell Montes, the brightness extends over a wide area, about 500 by 500 km.

The mountain belts appear to be younger than the adjacent plains of Lakshmi Planum. The upland plains material of Lakshmi Planum does not embay the feet of these mountain belts. Rather the deformation associated with mountain development appears to involve the plains, indicating that horizontal shortening continued to times more recent than the youngest lava flows [Kaula et al., this issue]. Only Maxwell and Akna montes have trenches or foredeeps, but these are less than 1 km deep (Figures 18c and 19c), of modest depth compared with oceanic trenches on Earth. Topographic gradients on the front slopes of the mountain belts are typically quite high. The slopes in western Maxwell

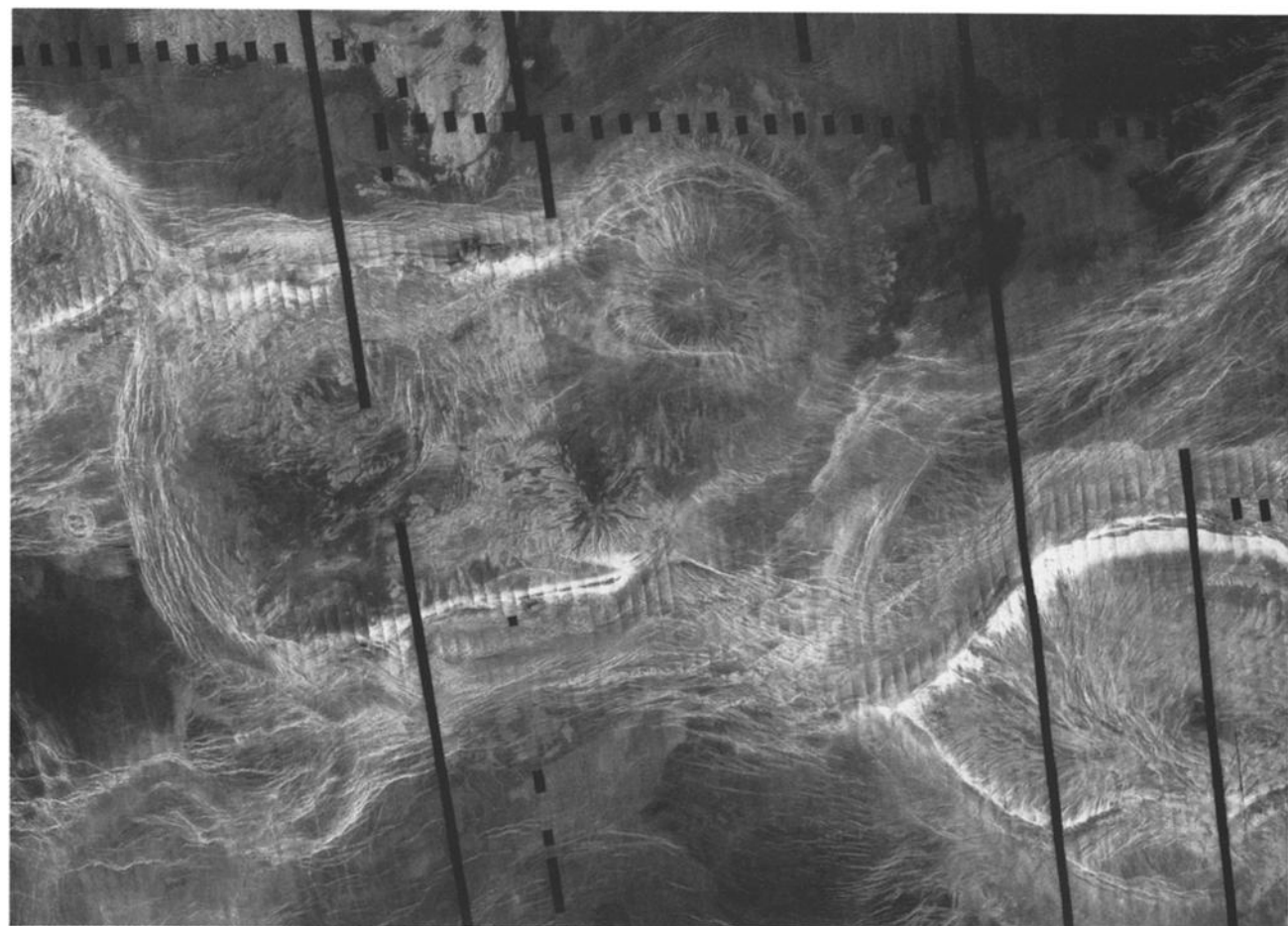


Fig. 15. Magellan radar image of the Diana and Dali Chasmata area of central Aphrodite Terra. The image is centered at about 16°S, 163°E and is about 1900 km wide. Diana Chasma is located in the top left and runs WSW to ENE; Dali Chasma runs approximately E-W across the lower half of the image. The topography of this region is shown in Plate 4 of *Ford and Pettengill* [this issue]. The imaged region includes two coronae marked by radial fractures and concentric deformational structures: Miralaidji, in upper center, and Latona, at lower right. A belt of ridges linking the two chasm systems runs N-S along the left side of the image. The brightest areas are linear highs that asymmetrically flank one side of each major trough segment. A highly fractured impact crater, approximately 40 km in diameter, is located at the far center left.

Montes (Figure 18c) and eastern Akna Montes (Figure 19c) are locally in excess of 30°.

Evidence for volcanism and extension within the mountain belts and along the plateau scarps is variable. Only in Danu Montes do lava channels extend downslope into the plains of Lakshmi Planum. Danu Montes and Vesta Rupes also have the most extensional features, although extension, likely the result of gravitational spreading, is found in all of the mountain belts and plateau margins [Smrekar and Solomon, this issue]. All mountain belts display evidence for volcanism on their outboard slopes, although in the case of Maxwell Montes the only flows are those apparently triggered by the formation of the Cleopatra impact crater. Both Danu Montes and Freyja Montes have aligned collapse pits, indicating that magmatism has been facilitated by extension.

Complex ridged terrain: Fortuna, Itzpapalotl, Atropos, and Clotho tesserae. Adjacent to all of the mountain belts are highly deformed regions of appreciably lower elevations that extend outward by 100–1000 km and descend to the lowland plains. The widths of these outboard regions of complex ridged terrain, or tessera, correlate with the heights of the adjacent mountain belts. The geometry and intensity

of deformation differ among the tessera regions. To the east of Maxwell Montes, in the central ridged tessera of western Fortuna [Vorder Bruegge and Head, 1989], the dominant fabric is a sequence of N-S trending arcuate ridges spaced 15–25 km apart. Atropos Tessera, to the west of Akna Montes (Figure 19a), is similar to central Fortuna Tessera, in that most of the ridges are parallel to those in the adjacent mountain belt. Itzpapalotl Tessera, north and northeast of Freyja Montes, shows more variety: within 200 km of the crest are radar-dark, presumably smooth areas 30 km in width. But beyond these smooth areas is yet more rugged tessera (Figure 20a), until an abrupt drop of 2 km at Uorsar Rupes (Figure 20c). In Clotho Tessera there are lineations at appreciable angles to the main trends. These crosscutting trends commonly extend into the lowlands.

Smooth scarps: Vesta Rupes and northern and southern scarps. The margins of Lakshmi Planum along longitudes 338°–353°E in the north and 340°–5°E in the south are strikingly smooth compared with the mountain belts, despite abrupt changes in elevation. The smooth scarps also contrast with the mountain belts in that their shapes are convex toward the upland plain. The exception is Vesta Rupes, which is more nearly linear and not as smooth.



Fig. 16. Magellan radar image of the Ganis Chasma area of Atla Regio in eastern Aphrodite Terra. The image is centered at 10°N, 199°E and is approximately 400 km wide. A series of overlapping graben, 1–10 km in width, make up the N-S trending rift system. The rift is up to 300 km wide and extends for 1000 km.

The northern scarp is about 900 km in length and makes a smooth bend of slightly more than 90° near 67°N, 344°E. The north-south arm of this sweep is the smoother, but it is nonetheless marked throughout by fine-scale troughs less than 1 km wide, over a width of 40–80 km, contrasting with the radar-dark plains of the plateau and the anastomosing lineations of the basin. In the east-west arm, to the east of 345°E, however, the scarp is cut by many troughs 1–3 km

wide at 4–12 km intervals. In the southeast, the plateau margin is broken up into three scallops (Figure 17). There is a marked decrease from west to east in the number of troughs parallel to the scarp, but the topographic drop remains the same. The number of upland troughs at appreciable angles to the scarps increases appreciably from west to east.

Despite their generally smooth character, the scarps include some areas of disrupted terrain. On the northern

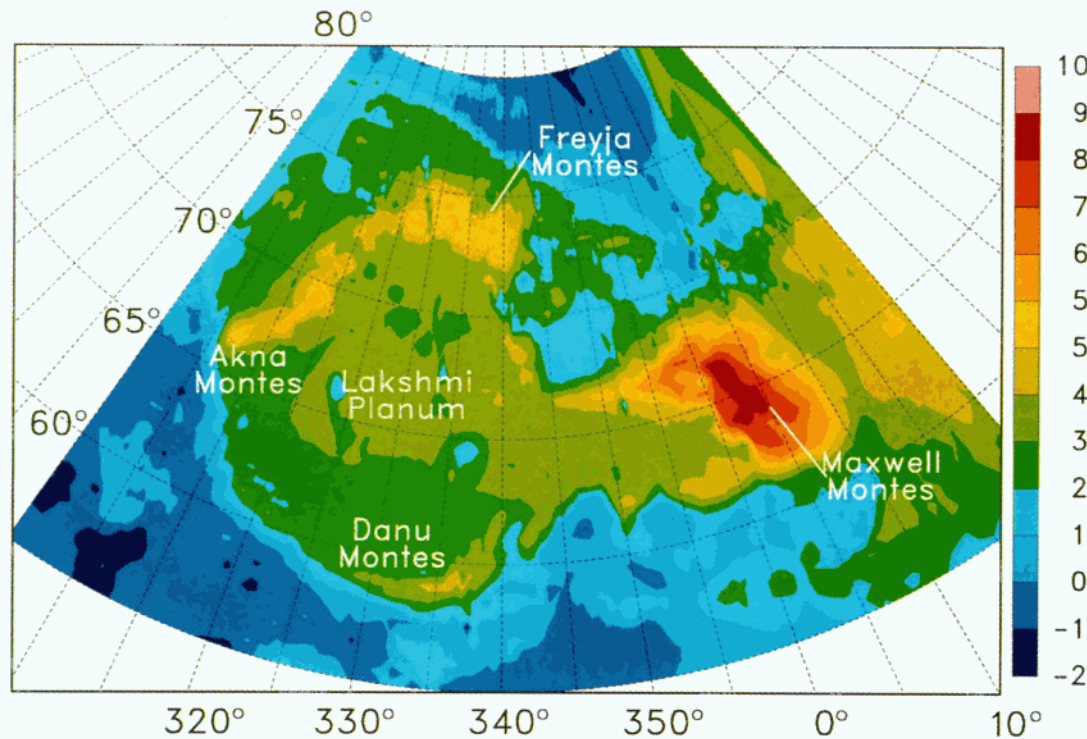


Fig. 17. Magellan altimetric map of Ishtar Terra (polar stereographic projection). Individual altimetric data points have been regridded at a 0.5° interval of latitude and longitude; 1-km contour interval.

scarp are a series of troughs at the eastern extreme, 345.5°–348°E, at the nose of the northwest arm of Maxwell Montes. In the southeast, there are numerous troughs and lineations in the cusp between the central and west basins. On both the northern and southern scarps these distorted terrains are of limited extent, locally less than 150 km, and do not appear to be related to trends in the basins below. Vesta Rupes, particularly its western reach, is dissected by numerous graben, faults, and lava channels, features which may be a result of gravitational spreading of the plateau margin [Solomon et al., 1991; Smrekar and Solomon, this issue].

Basins: North and south. The basins below the scarps are similar in appearance to the lowland plains that dominate the surface of Venus. However, they stand about 0.5 km above mean planetary radius in the south and 2.5 km in the north. They contain a variety of lineations, suggestive of long histories of deformation and changes in stress orientations. In the north basin, the most recent deformation appears to be associated with either Freyja Montes to the west or Maxwell Montes to the southeast, but in the south basin the most recent deformation appears more local in scale and not directly related to the major forces shaping Ishtar Terra.

Inferences. Ishtar Terra contains features which have been attributed both to mantle upwelling and mantle downwelling beneath other highland regions on Venus. The mountain belts are clearly zones of lithospheric compression and crustal shortening and thickening, and the most straightforward hypothesis to account for their presence is that Ishtar Terra overlies a center of downwelling mantle flow [Bindschadler et al., 1990b; Kiefer and Hager, 1992]. On the basis of the extensive volcanism in Lakshmi Planum

and elsewhere in Ishtar Terra and the relatively large apparent depth of compensation of long-wavelength topography, however, it has also been suggested that Ishtar Terra overlies a center of mantle upwelling [Pronin, 1986; Basilevsky, 1986; Grimm and Phillips, 1991].

The complex and varied patterns of deformation in the major physiographic provinces of Ishtar Terra suggest that neither the downwelling nor the upwelling mantle flow models, in their simplest forms, are likely to be of much predictive utility in accounting for the tectonic history of the region. Ishtar is probably similar to continental regions on Earth in that the recent dynamics, which largely determine topographic and geoidal elevations, are strongly influenced by the geometry of zones of weakness and the presence of old, relatively stable blocks. There are several indicators of an age sequence of events in Ishtar Terra consistent with this view [Kaula et al., this issue]. The volcanic flows of Lakshmi Planum are more recent than the ridged terrain they embay, suggesting that the latter units are relicts of a craton whose resistance to deformation led to the transfer of deformation elsewhere. All four mountain belts appear to have continued to undergo crustal shortening and deformation since the time of emplacement of most of the youngest volcanic flows in the adjacent plains of Lakshmi Planum, since they are not embayed by these plains. The high elevations and steep slopes found in all of the mountain belts suggest that these features have been recently, or are still, active. Details in the structural patterns of some of the mountain belts and their outboard plateaus suggest shifts in the magnitude and direction of thrusting; the E-W trending western arm of Freyja Montes, for instance, experienced more

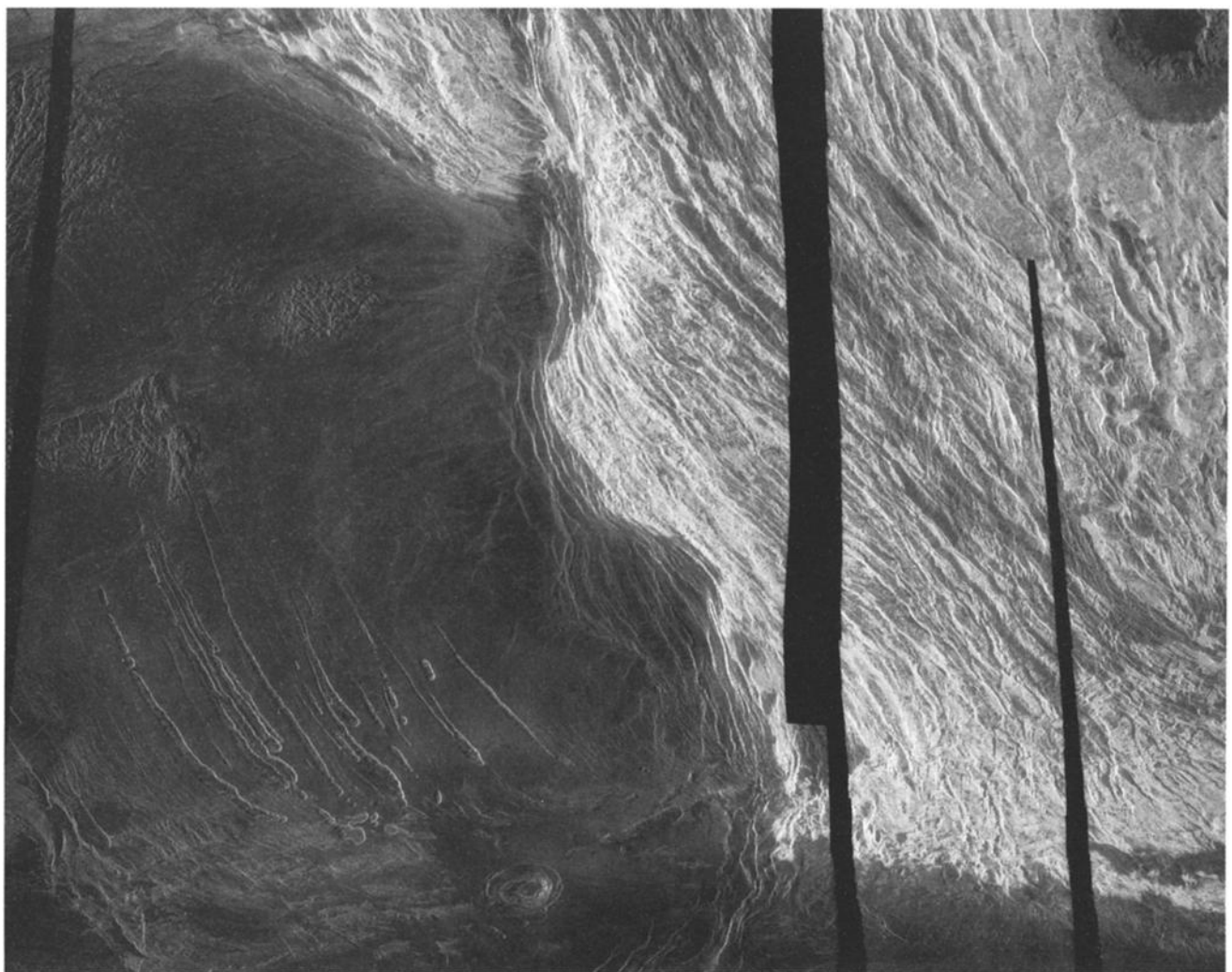


Fig. 18a. Magellan radar image of western Maxwell Montes. The image centered at 64°N , 0°E ; the width of the image is about 560 km. The radar-bright, NW-trending ridges and troughs form the steep western slope of Maxwell Montes. A portion of the impact crater Cleopatra is visible in the upper right. At lower left, a series of linear to scalloped troughs and pit chains (Rangrid Fossae) cut the radar-dark volcanic deposits of Lakshmi Planum. Partially embayed inliers of ridged terrain are visible in the portion of Lakshmi Planum at upper left.

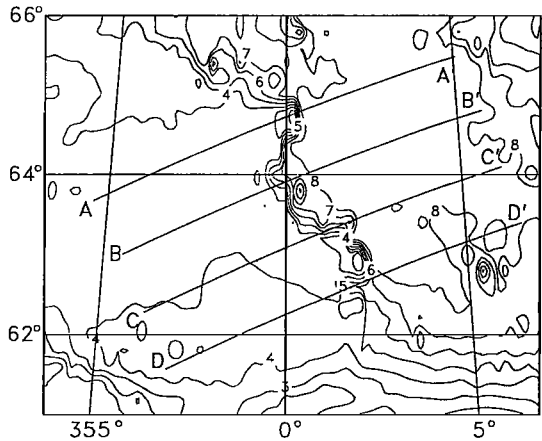


Fig. 18b. Altimetric map of western Maxwell Montes showing the locations of the profiles in Figure 18c; map projection and boundaries are approximately as in Figure 18a; individual altimetric data points have been regressed at a 0.2° interval of latitude and longitude; the contour interval is 1 km.

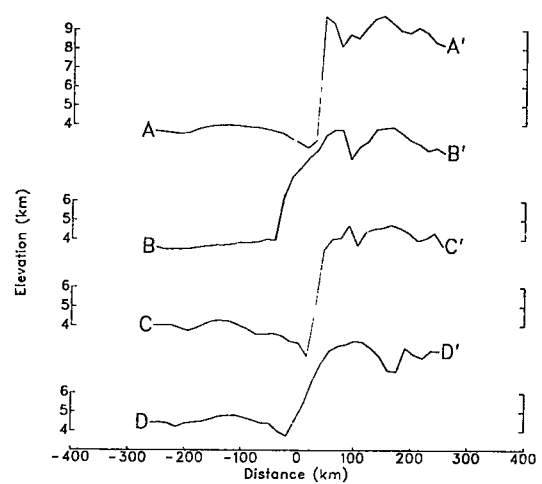


Fig. 18c. Topographic profiles across the western front of Maxwell Montes, with the northernmost profile at the top. Profiles have been constructed as in Figure 4 from altimetric measurements located within 15 km of points along the profile; vertical exaggeration 35:1.

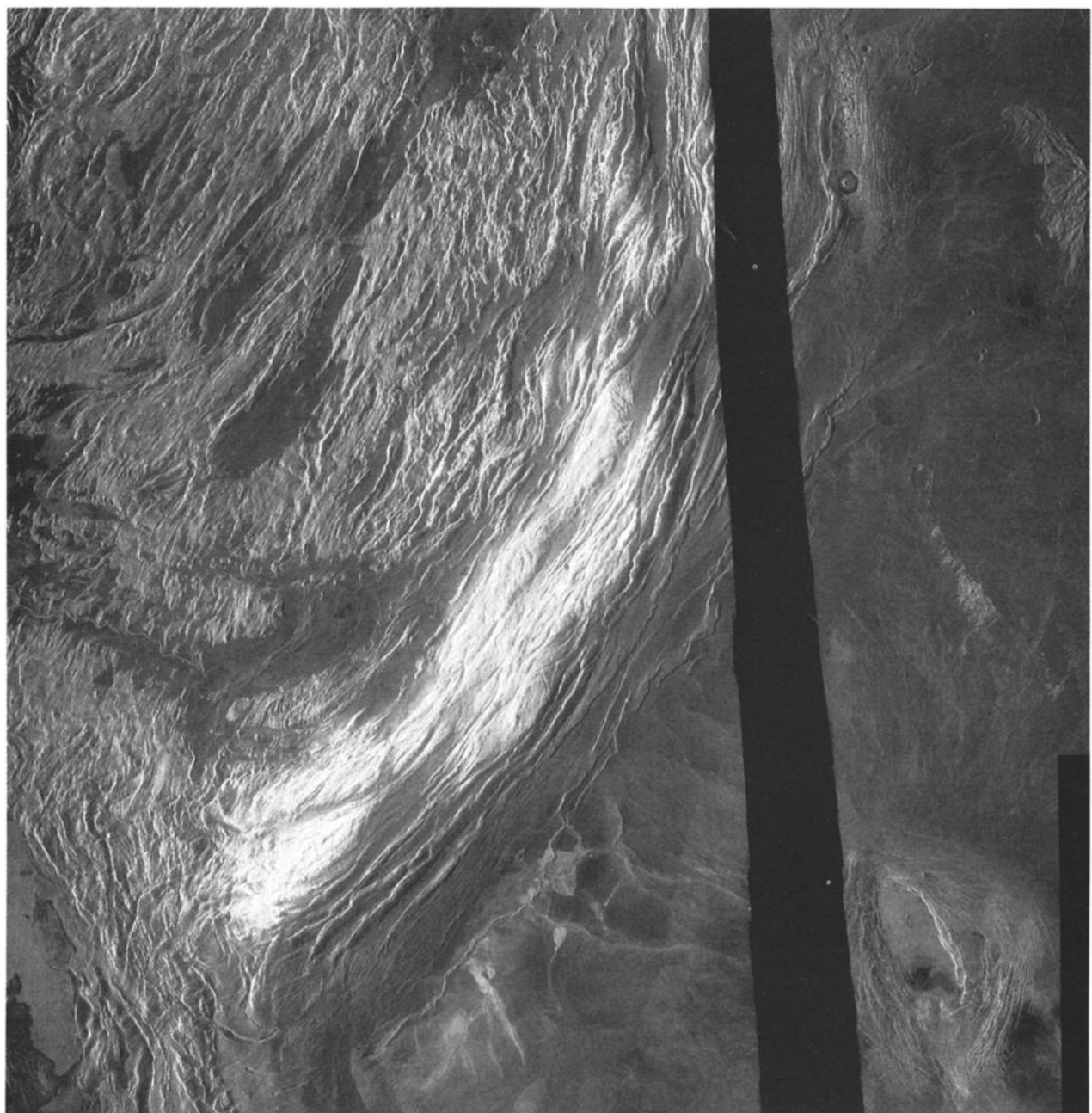


Fig. 19a. Magellan radar image of southern Akna Montes. The image is centered at 69.5°N, 320.5°E; the width of the image is about 675 km. The highest part of the mountains in the image shown is the radar-bright area in the lower left. Note that the thrusting and folding associated with mountain formation continues onto the adjacent volcanic plains of westernmost Lakshmi Planum.

recent deformation than did the N-S trending eastern arm. Some structural patterns in the plateaus outboard of Freyja and Danu montes appear to be younger than the deformation associated with the formation of the adjacent mountain belts. In the south basin, these patterns seem related to Maxwell Montes, but in the north, in central Itzpapalotl Tessera and beyond, they appear to be unrelated to Ishtar Terra. In the portion of Ishtar Terra imaged early by Magellan, the crater density is very close to the global mean, corresponding to an average crater retention age of about 500 Ma [Phillips *et al.*, 1991a]. Thus it is reasonable that the preserved sequence of volcanic and deformational events in Ishtar Terra spans a geological time interval comparable to that represented by units and features elsewhere on the Venus surface.

Models for Highland Formation and Evolution

Hypotheses for the origin of highland features are useful in the context of Magellan data only if they are quantitative in the sense that they are able to predict surface strain, topography, or gravity. Matching predicted deformation to that inferred from Magellan data can prove difficult, however, because many terrains appear to have undergone multiple stages of deformation that are far more complex than the predictive capabilities of available models. This problem is exacerbated by the fact that temporal sequences of deformational events are often difficult to establish. Further, specific geological features have been subject to strain associated with their local evolution but are also recorders of

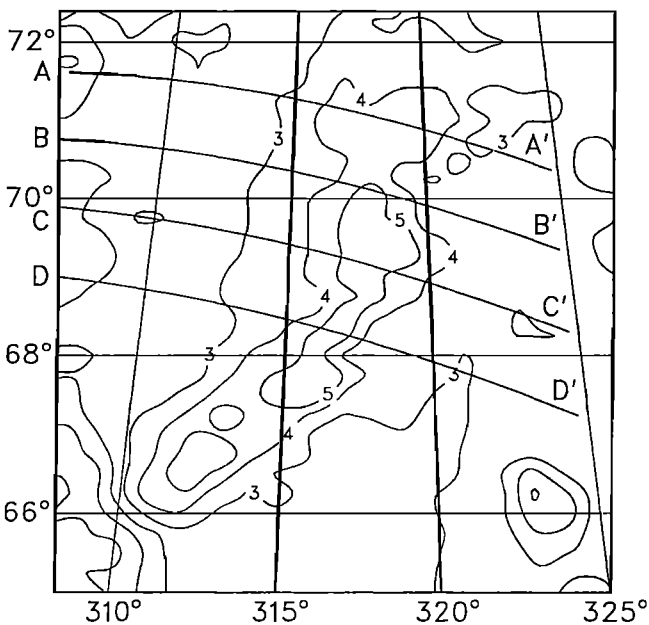


Fig. 19b. Altimetric map of southern Akna Montes showing the locations of the profiles in Figure 19c; map projection and boundaries are approximately as in Figure 19a; individual altimetric data points have been regridged at 0.25° in latitude and 1° in longitude; the contour interval is 1 km.

strain from larger-scale tectonic episodes, and it can be difficult to separate these two components.

Highland classification. For the discussion of models for highland formation and evolution on Venus it is convenient to define three classes of highlands on the basis of tectonic styles, regional morphology, and gravity characteristics (Table 2). In the discussion of models, we consider the applicability of models to each highland class. We then explore how each model links the highland classes as well as other features on Venus.

Beta-type highlands are characterized by broad topographic rises, moderate extensional deformation, shield volcanism, and large ratios of geoid to topography, implying apparent depths of compensation (ADC) of long-wavelength topography in excess of 100 km. Highlands in this class include Beta, Atla, Eistla, and Bell regiones. Ovda-type highlands are topographic plateaus distinguished by intense tectonic deformation, limited volcanism, and moderate values of the ADC (less than 100 km). Ovda and Thetis regiones are in this class. Ishtar Terra is a unique region on Venus, so this single highland belongs to the Lakshmi-type class. Lakshmi Planum is a plateau, with narrow mountain belts on its periphery, moderate volcanism, and a large ADC.

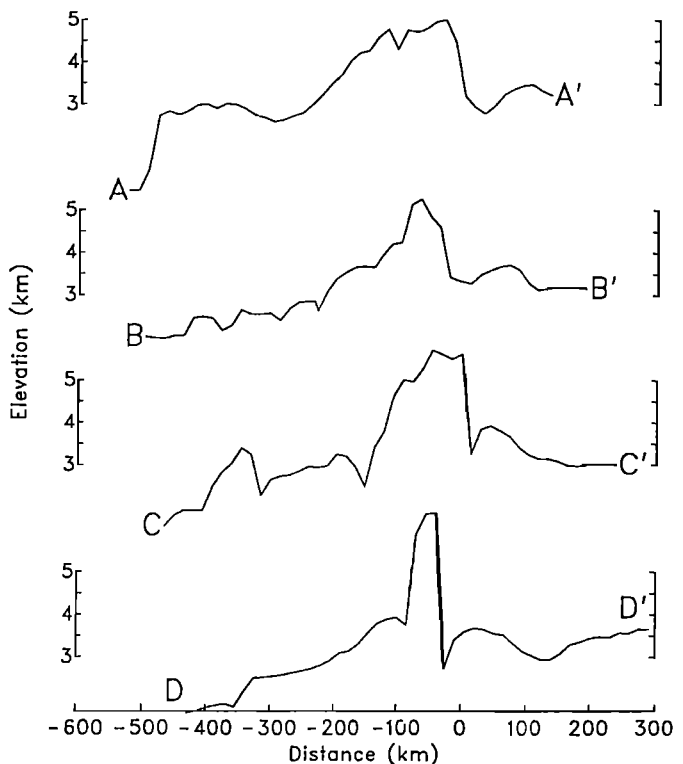


Fig. 19c. Topographic profiles across the eastern front of Akna Montes. Profiles have been constructed as in Figure 4 from altimetric measurements located within 15 km of points along the profile; for small segments near the western end of these profiles where data are sparse, the nearest three points, also weighted inversely by distance, were used to estimate the topography; vertical exaggeration 65:1.

Model premises. Models for highland formation and evolution operate on the basis of several premises, often implicit, which merit mention: (1) Venus has an internal heat production similar to that of the Earth [Solomon and Head, 1982; Phillips and Malin, 1984]. (2) Because of the high surface temperature, the elastic lithosphere of Venus is only a few tens of kilometers thick [Solomon and Head, 1984]. (3) For a crust 10–30 km in thickness [Grimm and Solomon, 1988; Banerdt and Golombek, 1988; Zuber and Parmentier, 1990] there are two elastic lithospheres, one in the upper crust and one in the upper mantle. (4) The weak lower crust can detach along a ductile decollement [Smrekar and Phillips, 1988]. (5) Mantle flow fields directly couple stress into the lithosphere and are responsible for some of the tectonic deformation observed [Phillips, 1986, 1990]. (6) Large apparent depths of isostatic compensation (ADCs) imply dynamic support of topography [Phillips et al., 1981]. (7) Crust will thicken or thin in response to induced stresses

TABLE 2. Highland Types and Properties

	Beta Type	Ovda Type	Lakshmi Type
Examples	Beta, Eistla, Atla	Ovda, Thetis	Lakshmi
ADC	> 100 km	< 100 km	~ 180 km
Tectonics	extensional	complex	mountain belts
Volcanism	extensive, shields	limited	moderate: plains and shields
Topography	broad rise	plateau	plateau with peripheral mountain belts

ADC, apparent depth of compensation

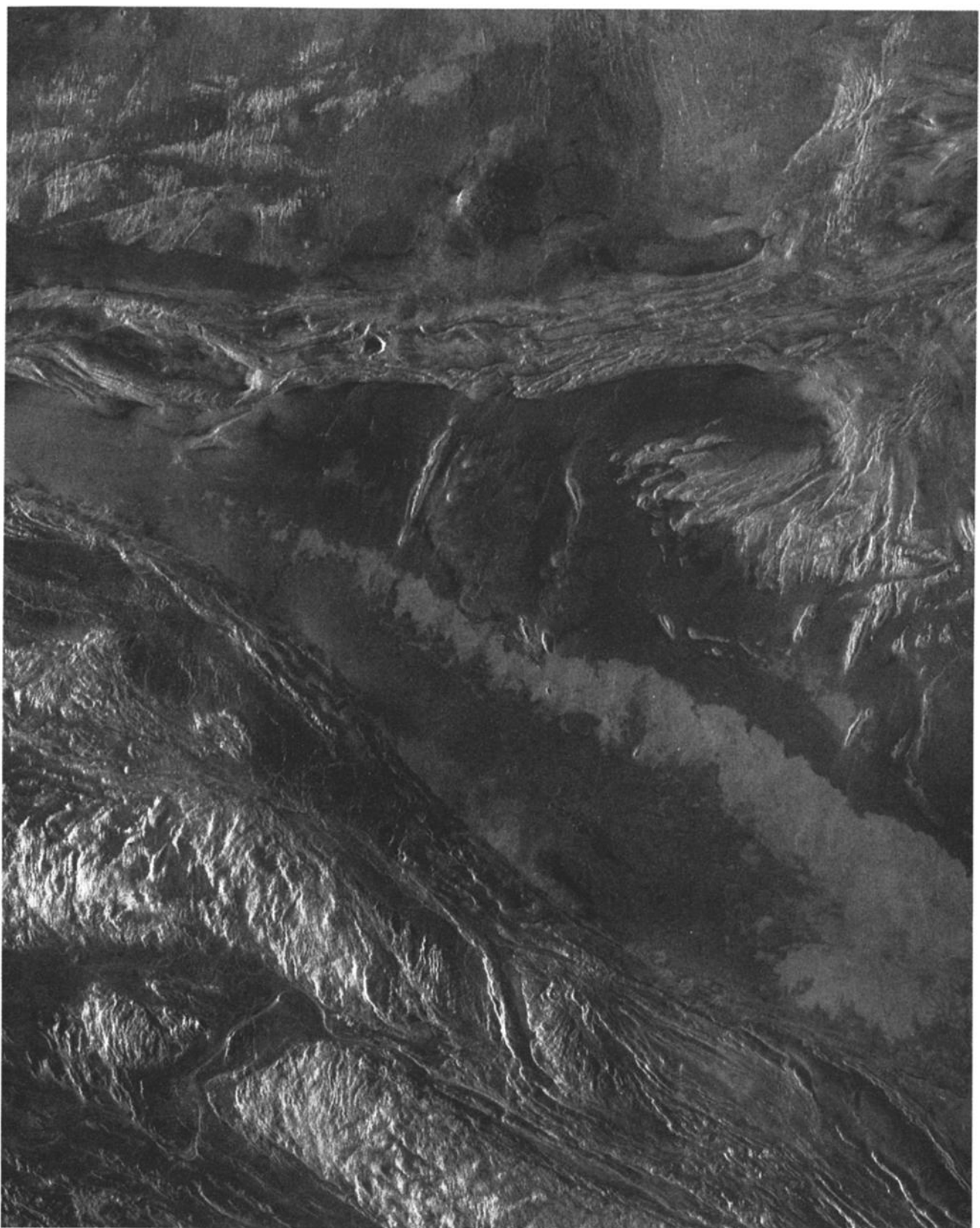


Fig. 20a. Magellan radar image of the Uorsar Rupes region. The image is centered at 78°N, 336°E and is about 250 km wide. The Uorsar Rupes scarp runs from center left to lower right in the image. Its base is embayed by relatively young, undeformed volcanic plains material. At lower left in the image is Itzpapalotl Tessera, the highly deformed plateau outboard of Freyja Montes.

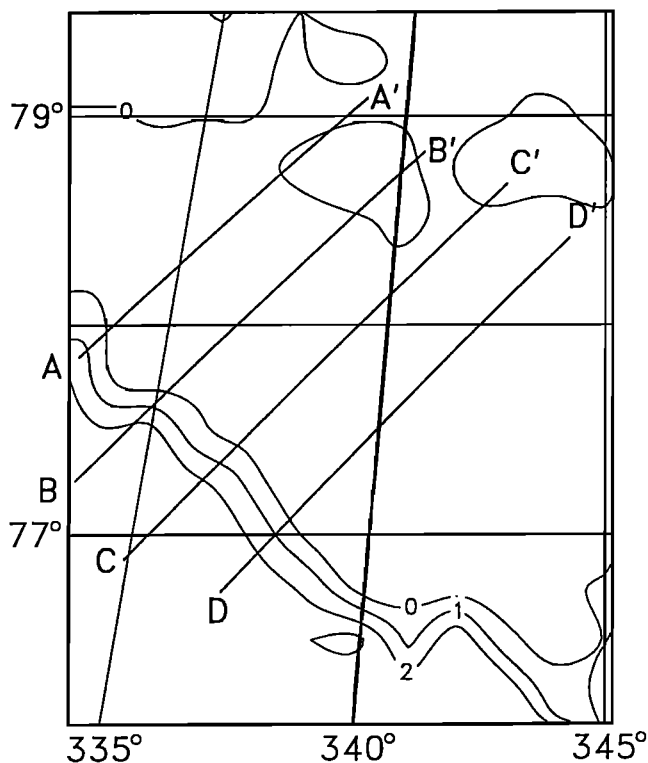


Fig. 20b. Altimetric map of the Uorsar Rupes region showing the locations of the profiles in Figure 20c; map projection and boundaries are approximately as in Figure 20a; individual altimetric data points have been regridged at 0.25° in latitude and 1° in longitude; the contour interval is 1 km.

on a geologically reasonable time scale (~ 500 m.y.) [Bindschadler and Parmentier, 1990]. (8) In the interpretation of dynamic models, deformation that appears to be compressional in nature arises from downwellings; deformation that appears to be extensional in nature arises from upwellings. (9) Lithosphere is not able to move large distances horizontally because there is no low-viscosity zone [Phillips, 1986; Phillips et al., 1991b]. (10) Subduction zones driven by lithosphere with a large negative buoyancy do not exist on Venus, at least on a global scale [Phillips et al., 1991b]. Obviously, the validity of any model relies on the correctness of these underlying premises.

Models. Geophysical models for the origin of highland features on Venus are directly related to convective flow fields in the mantle. Mountains could form from either upwelling flow (plumes or hotspots), downwelling from the upper thermal boundary layer (coldspots), or accretion resulting from horizontal translation of the lithosphere. There is little evidence for terrestrial-style plate tectonics on Venus in the sense that a rigid lithosphere is uncoupled from the underlying mantle and motion is driven by the potential energy stored in subduction zones. Large-scale horizontal motion, if it exists, may be driven by direct coupling of mantle convection into the lithosphere [Head and Crumpler, 1990]. More likely, horizontal translation is limited [Grimm and Solomon, 1989; Solomon et al., 1991; Phillips et al., 1991b]. Convergence can arise from direct shear coupling into the lithosphere by mantle flow or by secondary, inward flow of the crust in response to lithospheric depression caused by mantle downwelling. Convergence can also be driven by the impingement of a mantle plume on the base of the

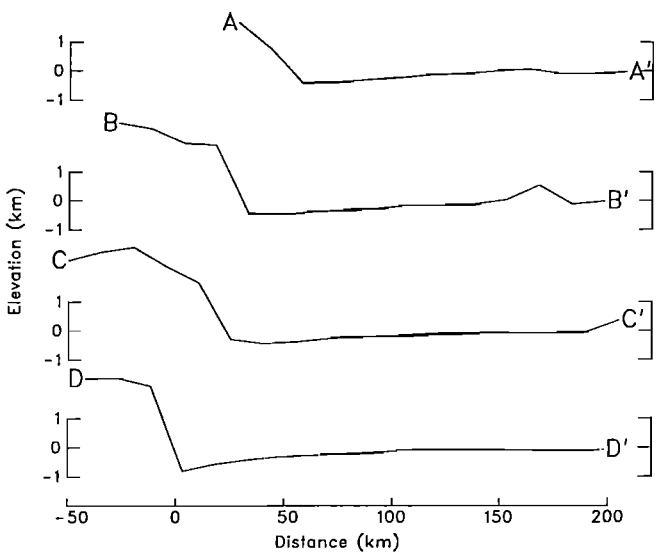


Fig. 20c. Topographic profiles across Uorsar Rupes, with the northeasternmost profile at the top. Profiles have been constructed as in Figure 4 from altimetric measurements located within 15 km of points along the profile; vertical exaggeration 13:1.

lithosphere, provided there are lateral heterogeneities in lithospheric strength [Grimm and Phillips, 1990, 1991]. Thus vertical convective motion may lead to significant amounts of horizontal shortening, giving rise to folded mountain belts and to lithospheric thrust faulting and subduction-like morphology. No matter what the mode of origin, the existence of significant positive topographic relief will lead to extensional strain, as observed in the peripheral mountain belts of Lakshmi Planum [Solomon et al., 1991; Smrekar and Solomon, this issue].

The hotspot model [Phillips and Malin, 1983, 1984; Morgan and Phillips, 1983] was developed on the basis of Pioneer Venus data as a mechanism by which Venus loses its internal heat in the absence of seafloor spreading. Beta Regio was taken as the "type" hotspot by analogy to terrestrial hotspot characteristics such as a broad topographic dome, shield volcanism, and extensive rifting. East Africa was considered to be an especially good analogy [McGill et al., 1981]. Further, the ADC for Beta Regio is 300 to 400 km, an observation taken as evidence for the dynamic support of long-wavelength topography. Other regions in the equatorial highlands, by virtue of their large ADC values, were also proposed to be hotspots.

The evolution of an upwelling mantle plume and the attendant hotspot has been discussed in detail by Herrick and Phillips [1990] and Phillips et al. [1991b]. A hotspot evolutionary sequence is characterized by (1) a broad domal uplift resulting from a rising mantle plume, (2) massive partial melting in the plume head and generation of a thickened crust or crustal plateau, (3) collapse of dynamic topography as the plume wanes, and (4) spreading of the plateau by lower crustal creep. The ADC during this sequence gradually shoals as the plume wanes and the crust thickens by volcanism and magmatic intrusion. Phillips et al. [1991b] postulated that Beta Regio, Thetis Regio, Ovda Regio, and the complex ridged terrain of Alpha Regio represent successive stages of the hotspot cycle. They regarded Ishtar Terra as a special case wherein a plume has impinged on a

tessera block, and the lateral variation in lithospheric strength, from tessera to nontessera, is able to focus flow-induced stresses, giving rise to peripheral mountain belts [Grimm and Phillips, 1990, 1991].

Whether the mantle is heated from below or heated from within, the upper thermal boundary layer of a convecting mantle is unstable and nucleates cold, downwelling flow. This return flow can take the form of sheets or quasi-cylindrical plumes [Schubert, 1992]. The idea that plume-like downwelling could give rise to elevated topography has been advanced by Bindschadler and his colleagues [Bindschadler and Parmentier, 1990; Bindschadler et al., 1990b, this issue (b)] to explain compressional deformation associated with highland features. This class of models depends on the occurrence of induced secondary crustal flow over geologically reasonable time scales. A coldspot evolutionary sequence is characterized by (1) downward surface displacement in response to a sinking plume, (2) inward crustal flow, leading to crustal thickening and formation of a crustal plateau on a time-scale of several hundred million to a billion years, (3) rebound of the crustal plateau to increased elevation as the cold plume is assimilated by the mantle, and (4) collapse and spreading of the crustal plateau. For models of this hypothesis explored to date, the ADC during the coldspot cycle is increasingly positive and is unbounded at the point when the topography passes through zero in its second-stage evolution; thereafter it is negative and asymptotically increases to a small positive value. The inconsistency between predicted values of the ADC during the later stages of the coldspot model and the values calculated from observed topography and gravity on Venus has been the chief focus of criticism of this hypothesis [e.g., Grimm and Phillips, 1991].

The tectonic cycle during coldspot evolution is one of compressional strain focusing near the margins of the growing plateau. Later the crustal plateau is in extension as it spreads laterally. A possible sequence of the coldspot cycle is represented by the Atalanta Planitia lowland, Ovda Regio, Thetis Regio, and Alpha Regio. Ishtar Terra is again a special case wherein the downwelling is particularly vigorous or longlasting.

Magellan constraints on models. Magellan data have revealed that the highlands are tectonically complex and varied and that only Beta, Eistla, Bell, and Atla regiones satisfy all of the morphological and geological characteristics originally attributed to Venusian hotspot terrain. The hypothesis that Beta-type highland overlies a mantle plume or hotspot is entirely consistent with Magellan data. Ovda-type highlands pose two problems for the hotspot model. First, observed tectonic deformation indicates that a large amount of strain has taken place, although the sign of the strain is often ambiguous. It is incumbent upon proponents of the hotspot model to demonstrate that such deformation can occur. Phillips et al. [1991b] suggested, but did not test, the following strain mechanisms during the hotspot cycle: (1) extensional deformation during uplift, (2) strain associated with ductile detachments, which may lead to the development of compressional features on the slopes of uplifts or the resulting crustal plateaus, (3) membrane compressional strain acting on the new crustal block as dynamic topography subsides, (4) extensional and compressional strain associated with collapse and spreading

of the crustal block, and (5) thermoelastic strain as the hotspot cools, particularly in the new crustal cap. Additionally, if the crustal root of a plateau can transform to eclogite, then lithospheric delamination could lead to significant strain in the plateau. The superposition of several sources of stress would lead to complex deformation of a crustal plateau.

The second problem is that in the early phase of the hotspot cycle, extensive volcanism and large shield volcanoes are expected. In the regions postulated to represent the more evolved stages of the cycle (e.g., Alpha Regio), evidence for such volcanism is not seen. The model thus requires that tectonic deformation be sufficiently severe so as to render these early volcanic units and structures unrecognizable at present.

The chief difference between the hotspot and coldspot models is the importance of secondary crustal flow in the latter class of models. Models of convection-induced crustal flow predict that the crust should thin over centers of upwelling [Bindschadler and Parmentier, 1990], leading ultimately to the formation of lowlands displaying evidence for significant extensional strain (i.e., isostatic effects eventually dominate dynamic effects). As discussed in a later section, such evidence has not been found in the Magellan observations of lowlands on Venus, a result which raises questions for the coldspot model for highlands insofar as secondary crustal flow is required to create elevated terrain. Furthermore, models of convection-induced crustal flow over both coldspots and hotspots predict that after the topography passes through zero in its second-stage evolution the topography and free-air gravity will be anticorrelated for a geologically extended period. Such an anticorrelation is not observed on Venus. Most models for convection-induced crustal deformation carried out to date, however, do not include the effects of magma generation in the upwelling mantle and associated volcanism and crustal thickening, processes which could considerably alter the relation between topography, preserved tectonic features and mantle flow in upwelling regions.

COMPLEX RIDGED (TESSERA) TERRAIN

Arguably the most complicated of the tectonic terrains on Venus are regions of complex ridged terrain, or tesserae. Tesserae are broad, commonly equidimensional uplands characterized by intersecting sets of linear features [Basilevsky et al., 1986]. Typical spacings between these features were observed in Venera 15-16 images to be 10-20 km. Large regions of complex ridged terrain (more than 1000 km across) are typically relatively steep-sided plateaus that (as with even the smallest tesserae) are elevated above their surroundings. Compared with rifted highland areas with abundant volcanism such as Beta and Atla regiones, the gravity and geoid anomalies over large tessera terrains are modest in magnitude and the apparent depths of compensations are less, often significantly, than 100 km [Smrekar and Phillips, 1991; Phillips et al., 1991b].

On the basis of Venera 15-16 data, complex ridged terrain (CRT) was known to cover at least 10% of Venus north of 30°N [Sukhanov, 1986; Bindschadler and Head, 1989]. The unusually rough surfaces of CRT at meter and submeter scales [Bindschadler and Head, 1988, 1989] allowed its

distribution to be predicted over most of the planet from Pioneer Venus data [Bindschadler et al., 1990a]. It was suggested that complex ridged terrain dominates several highland regions, including Ovda, Thetis, and Phoebe regiones, and covers significant portions of eastern and northwestern Beta Regio, northern Asteria Regio, Lada Terra, and the Nokomis Montes region.

Three morphologic types of CRT were distinguished on the basis of Venera 15-16 data: linear ridged terrain, trough and ridge terrain, and disrupted terrain [Bindschadler and Head, 1991]. These classes of CRT were characterized, respectively, by subparallel ridges and troughs and cross-strike lineations, subparallel troughs and orthogonal ridges and troughs, and more chaotic patterns of generally shorter structural elements. Disrupted terrain is the most commonly observed, with linear ridged terrain less abundant, and trough and ridge terrain relatively rare [Bindschadler and Head, 1991]. Linear ridged and disrupted terrains were thought to be related, with the former attributed to compressional deformation and penecontemporaneous shear deformation. Continued shearing and extensional deformation were suggested to lead to the formation of disrupted terrain. Structures in the trough and ridge terrain include both long, broad (up to ~1000 by 50 km) linear troughs, and smaller, discontinuous ridges and troughs (<40 km long, ~5-10 km wide). Both sets of structures were interpreted as extensional; the low resolution of Venera data made it impossible to resolve their relative ages.

Magellan Observations of Complex Ridged Terrain

On the basis of Magellan image data the area of known tesserae on the surface of Venus has essentially tripled. Most of this terrain is found within highland regions. In particular, CRT is found in Ovda, Thetis, Phoebe, Beta, and Asteria regiones and in the Lada Terra and Nokomis Montes regions, as predicted [Bindschadler et al., 1990a], and it appears to be the most areally extensive highland tectonic unit [Bindschadler et al., this issue (b)]. Ovda Regio and the westward extension of Aphrodite Terra comprise the largest contiguous region of CRT on the planet, covering approximately 10^7 km².

Magellan data indicate that most major regions of complex ridged terrain are characterized by compressional ridges and troughs, spaced some 10-20 km apart, upon which are superposed numerous generally younger graben and related extensional structures having widths and spacings ranging down to the limit of resolution (~200 m). Most individual features are continuous for no more than 100 km, although groups of structures may retain consistent orientations for up to ~1000 km. The compressional ridges are commonly found near and parallel to the tessera boundaries. Magellan images of complex ridged terrain suggest that both linear ridged terrain and disrupted terrain (essentially equivalent to the interior block terrain defined above as a map unit for Aphrodite Terra) remain useful as classifications and that interpretations of the styles of deformation based on Venera data [Bindschadler and Head, 1991] were largely correct. Interpretation of the trough and ridge terrain (essentially equivalent to the linear trough terrain defined as a map unit for Aphrodite Terra) as wholly extensional, however, may have been incorrect. Instead, Magellan data suggest that in

many areas trough and ridge terrain is similar in morphology and probably in origin to linear ridged terrain.

Here we summarize aspects of the morphology of five major tesserae: Alpha, Ovda, Thetis, and Tellus regiones and Laima Tessera. Alpha Regio is the first major tessera terrain to be the subject of detailed mapping and geological analysis using Magellan data [Solomon et al., 1991; Bindschadler et al., this issue (a)]. Ovda and Thetis regiones, constituting western Aphrodite Terra, have been discussed in an earlier section. Tellus Regio was the type area for disrupted terrain and Laima Tessera the type region for trough and ridge terrain [Bindschadler and Head, 1991].

Alpha Regio. Alpha Regio is a 1300 by 1500 km upland region composed almost solely of complex ridged terrain and located in the midsouthern latitudes of Venus (17°S to 35°S, 356°E to 12°E). It is approximately circular in planform and reaches maximum elevations of more than 2 km above mean planetary radius; regional-scale radar images and altimetry maps are given by Solomon et al. [1991] and Bindschadler et al. [this issue (a)]. Most of the interior is characterized by elevations near the datum, while the surrounding plains lie approximately 500 m lower. The highest elevations within Alpha Regio are all found near the periphery of the highland and are expressed as rugged topographic peaks and high plateaus. The more central portions of the region stand at least 1 km below the highest peaks. The gravity anomaly resolved in Pioneer Venus data is centered near the eastern border of Alpha Regio and implies an apparent depth of compensation probably less than 100 km [Bindschadler et al., this issue (a), (b)].

The structural fabric of Alpha Regio is composed primarily of broad ridges and troughs (10-20 km wide), fine-scale ridges (<3 km wide), linear disruption zones, and interrelated graben, grooves, troughs, and scarps. Bindschadler et al. [this issue (a)] interpreted the broad and fine-scale ridges to be contemporaneous compressional structures which were ubiquitously crosscut by (and are thus older than) both linear disruption zones and graben and associated grooves, troughs, and scarps. Linear disruption zones are interpreted as the result of small amounts of strike-slip or shear deformation and represent structures of intermediate age. Graben and associated structures are extensional and constitute the youngest structures. In addition, these workers noted that broad ridges are commonly found within the highest elevations and tend to align with the nearest boundary between the CRT and the surrounding lowlands.

Ovda, Thetis, and Tellus regiones. Magellan images of the large areas of complex ridged terrain in Ovda, Thetis, and Tellus regiones display all of the principal variants of tessera terrain. Linear ridged terrain (e.g., Figure 11) occurs throughout large portions of Ovda Regio and along the northern and southern boundaries of Thetis Regio (Figure 9). Parallel linear ridges spaced approximately 10-20 km apart and commonly continuous along strike for over 100 km are crosscut by numerous scarps and graben typically 5-10 km in width. Scattered linear dark regions often occupy local troughs and are likely regions of comparatively less deformed volcanic plains. The ridges are interpreted to be the result of crustal compression and shortening. The generally younger graben tend to trend at high angles to the linear ridges; a few graben can sometimes be seen at low angles or even parallel to the ridges. Areas where graben are best developed are

equivalent to the linear trough terrain (Figure 13) defined as a map unit for Figure 9.

Magellan images illustrate a morphologic transition from linear ridged terrain and linear trough terrain to disrupted terrain. A partially disrupted ridge fabric can be seen in central Ovda Regio (Figure 21). Here, graben are less abundant than in the regions shown in Figure 11 or 13, and both broad-scale (~ 10 km spacing) and fine-scale ridges (< 3 km spacing) are apparent. This terrain is similar to much of Alpha Regio [Bindschadler et al., this issue (a)], although the broad ridges in Ovda Regio are more prominent. Individual ridges are rarely continuous over as much as 100 km and commonly no more than 50 km, significantly less than in Figure 11 or 13. As in Alpha Regio, the discontinuous nature of the broad ridges may be due to shearing which postdated or was contemporaneous with ridge formation, or it may result from interference folding.

An area within Tellus Regio that may represent the end result of the disruption process is shown in Figure 22. Here the terrain is dominated by NW-SE trending graben and scarps. A few elongate to domical topographic ridges trend NE-SW in the central portion of the image, but they are sufficiently dissected by extensional structures that they are not recognizably similar to landforms seen in other regions. Other parts of Tellus Regio more clearly manifest compressional ridges [Bindschadler et al., this issue (a)], however, and we suggest that the ridges in this region may be remnants of such structures.

Laima Tessera. Laima Tessera was the type area for trough and ridge terrain, interpreted on the basis of Venera 15-16 data as being extensional in nature [Bindschadler and Head, 1991] or formed by a process analogous to terrestrial seafloor spreading [Head, 1990b]. Magellan images of the region (Figure 23) cast doubt on the former interpretation and rule out the latter. In this portion of Laima Tessera the NE-SW trending structures are graben that clearly crosscut and are thus younger than the more continuous NW-SE trending structures (Figure 23). This relationship is inconsistent with suggestions that the graben are analogous to abyssal hills on the seafloor and the NW-SE trending structures to fracture zones [Head, 1990b; Head and Crumpler, 1990], since abyssal hills would not be expected generally to crosscut transform faults [Bindschadler and Head, 1991]. Moreover, many of the NW-SE trending structures appear in Magellan data as relatively symmetric ridges and are similar to compressional ridges seen in Ovda Regio (Figures 11-12) and elsewhere. Although distinct NW-SE trending graben are present within Laima Tessera, they are less common than ridgeform structures.

Models for Tessera Formation and Evolution

Prior to Magellan a number of processes were suggested as potential contributors to the formation of complex ridged terrain, including mantle downwelling and attendant crustal thickening [Bindschadler and Parmentier, 1990], crustal spreading analogous to terrestrial seafloor spreading [Head and Crumpler, 1990; Head, 1990b], relaxational tectonics associated with the near-surface dynamics of a mantle plume head [Herrick and Phillips, 1990; Phillips et al., 1991b], and gravitational spreading or relaxation [Smrekar and Phillips,

1988; Bindschadler and Head, 1991]. The complexity and diversity of CRT are such that each of these processes, either alone or in combination, might have been important for particular regions. CRT are linked to both the hotspot and coldspot models for highland formation and evolution. For the former models, CRT plateaus are of magmatic origin, the result of crustal thickening by vertical differentiation. For the latter models, crustal thickening takes place by subsolidus convective flow in the lower crust. On the basis of a global examination of CRT characteristics indicated by data available prior to Magellan, Bindschadler and Head [1991] favored compressional deformation and crustal thickening driven by mantle downwelling, followed by gravitational relaxation, as the dominant combination of formational processes.

Magellan data indicate that most large tessera regions display a generally older set of ridge structures on which are superposed a younger set of graben and extensional fault structures. Thus a sequence of deformational events, as previously inferred [Bindschadler and Head, 1991], appears to characterize such terrain. An early phase of compression and crustal shortening was followed by a more recent phase of lateral extension, probably by gravitational spreading of the elevated terrain. Examination of CRT, such as Alpha Regio [e.g., Bindschadler et al., this issue (a)], reveals that while some deformation may be associated with the formation or modification of the tessera itself, especially near its boundaries, other deformation can be traced into the surrounding regions and has no special geometric relationship with the tessera terrain. Some of the younger graben, especially the largest ones, were evidently active both near the end of CRT deformation and at the beginning of lowland plains deposition (see discussion below of plains deformational sequence).

As suggested on the basis of the earliest Magellan data [Solomon et al., 1991], regions of high topography and thick crust may preferentially strain in response to regional stress because of the tendency for crust to weaken with increasing thickness. Thus tesserae may simply be long-lived blocks of thickened crust that have been subject to repeated episodes of tectonic deformation, often exogenic in origin and related to large-scale stresses. Further, elevated regions are apt to record a longer history of deformation than the plains because they are less susceptible to volcanic burial. By this argument, the level of deformation observed in any highland or CRT block depends in part on its age. Differences in tectonic deformation observed between, say, Eistla and Ovda regiones could be due, at least in part, to a greater age for the crustal thickening event for the latter region.

TECTONICS OF PLAINS AND LOWLAND REGIONS

The plains, which constitute more than 80% of the surface of Venus [Masursky et al., 1980], are generally low-relief areas with surface deposits of volcanic origin [Sukhanov et al., 1989; Head et al., 1991]. While a few plains regions viewed by Magellan are nearly devoid of tectonic features, most areas of plains show considerable evidence for deformation in a variety of forms and patterns [Saunders et al., 1991; Solomon et al., 1991]. These patterns are sometimes consistent over distances of hundreds of kilometers or more. Most of these deformational features

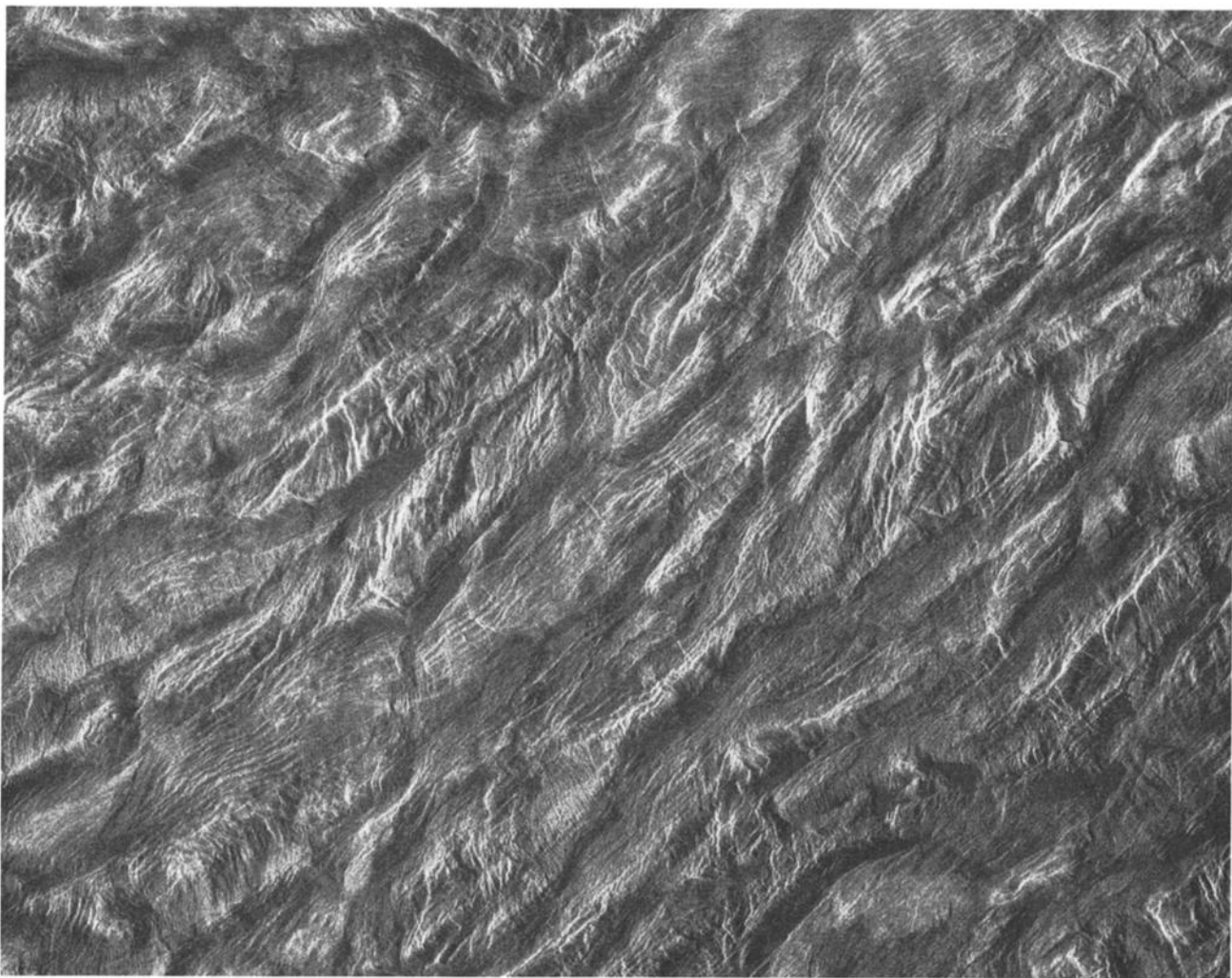


Fig. 21. Magellan radar image of a region in west central Ovda Regio, approximately 150 km wide and centered at 5.3°S, 83.2°E. The area shown is to the immediate west of that in Figure 12. Both broad-scale (10- to 20-km spacing) and fine-scale (< 3 km spacing) ridges are evident. Ridges are much less continuous than in type areas for linear ridged terrain (e.g., Figure 11).

represent modest levels of horizontal strain, of order 10^{-2} or less. Superposition relationships among volcanic units and constructs and tectonic features demonstrate a continuing interplay between deformation and volcanism in most plains regions.

An example of a common pattern of plains deformation is depicted in Figure 24. Superimposed on a reticulate plains unit [Saunders et al., 1991] in Niobe Planitia are a series of N-S trending radar-bright lineations. The largest of these lineations are seen to be steep-walled, flat-floored depressions, or graben. Lengths of individual graben are 5–40 km, and widths are typically 1 km to a few hundred meters or less. The characteristic spacing between graben is a few kilometers. The graben walls appear to cut, and are therefore younger than, the fine lineations defining the reticulate pattern of the plains. On the kilometer scale, the walls have a crenulate or saw-tooth pattern, which may indicate that the fractures defining the reticulate pattern in the plains locally influenced the trend of normal faulting during graben formation. These graben document that a modest amount of east-west extension was the most recent tectonic activity in this region. The narrowness of the graben implies a shallow depth of deformation (only a few hundred meters if they are

true graben and their bounding normal faults dip inward at 60°). The enigma of these and similar shallow structures is that their trends persist over large distances, implying the existence of structurally coherent sheets that are both very thin and areally extensive.

An example of another type of pattern commonly seen in the plains [Solomon et al., 1991] are the linear to sinuous, regularly spaced ridges shown in Figure 25 and located in Rusalka Planitia. In morphology, relief, and spacing the features appear similar to wrinkle ridges observed in lunar maria and Martian ridged plains and attributed to modest levels of horizontal compression and shortening [Plescia and Golombek, 1986; Watters, 1988]. Most of the wrinkle ridges in this region strike NW-SE. The spacing between ridges, while somewhat variable, is approximately 20 km; this spacing is consistent with deformation of the entire thickness of the strong upper crustal layer [Zuber, 1987; Zuber and Parmentier, 1990] in response to NE-SW compression.

Deformation Belts

Many areas of plains on Venus include structural or topographic features that occur as linear belts of



Fig. 22. Magellan radar image of a region of heavily disrupted terrain in north central Tellus Regio. The imaged region is approximately 120 km wide and centered on 39.5°N, 85.7°E. Terrain is dominated by north to NW trending graben and scarps, but numerous other types and trends of structures are present.

concentrated deformation [Barsukov *et al.*, 1986; Campbell *et al.*, 1991]. These deformation belts fall into three main morphological classes: (1) broad topographic ridges characterized by complex arrays of faults and fractures; (2)

narrow, narrow ridges; and (3) long, narrow belts consisting of a single sharply defined ridge, commonly with superposed smaller ridges. The first class includes most of the bright bands seen on Arecibo radar images of the southern hemisphere of Venus [Campbell *et al.*, 1991]. The second



Fig. 23. Magellan radar image of a region in northwestern Laima Tessera, approximately 150 km wide and centered on 52.3°N, 57.2°E. NE trending structures are interpreted as graben; NNW trending structures are interpreted as compressional in origin.



Fig. 24. Magellan radar image of modest extensional deformation of a reticulate plains units in Niobe Planitia. East-west extension has produced the N-S trending graben visible throughout the image. A number of low-relief volcanic constructs can also be seen. The image is centered at 23.7°N, 116.5°E and is about 110 km wide.

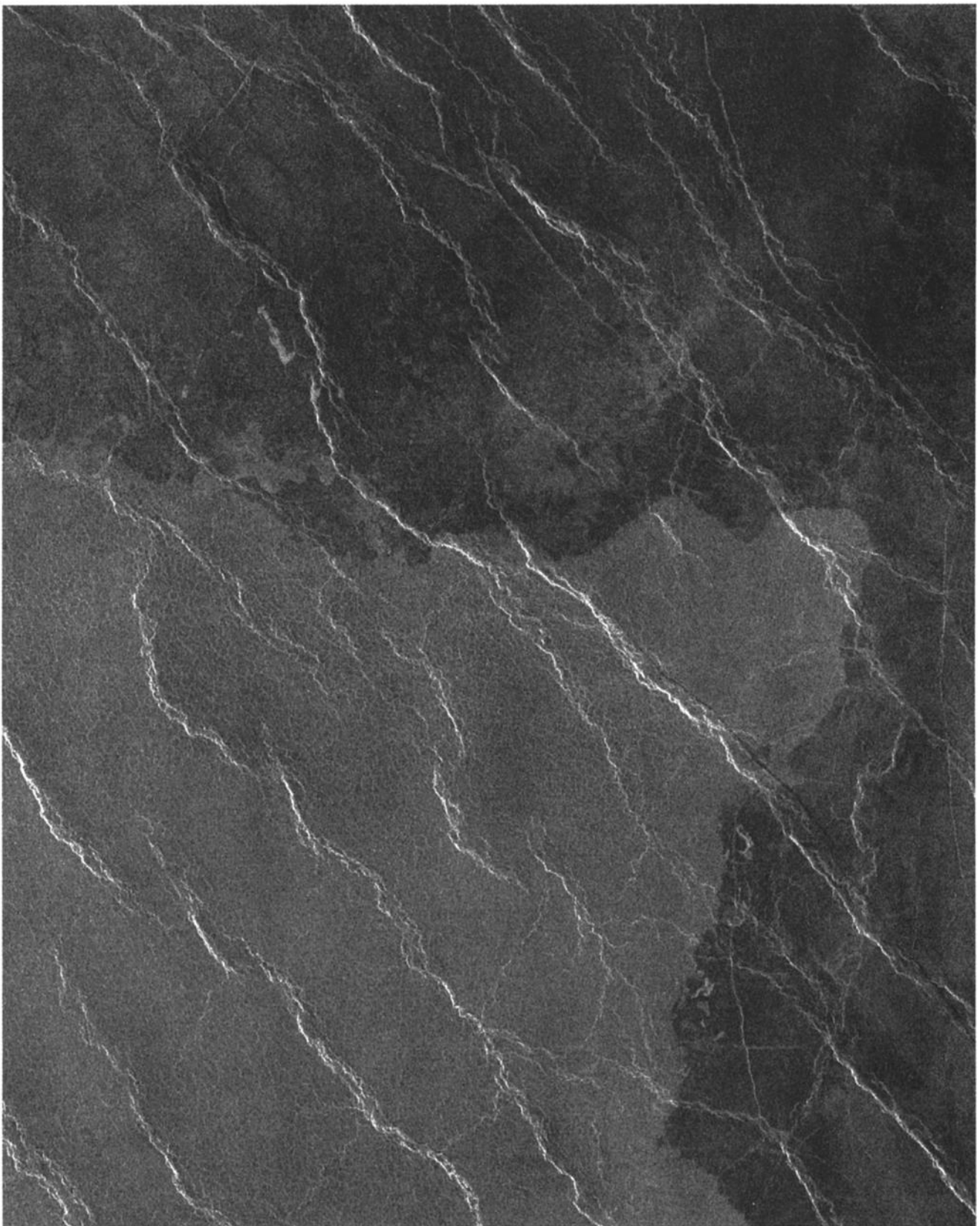


Fig. 25. Magellan radar image of modest compressional deformation of two plains units in Rusalka Planitia. NE-SW compression has produced the radar-bright, NW-SE trending wrinkle ridges. The wrinkle ridges appear to postdate both the brighter, reticulate plains unit in the lower left of the image and the darker and younger smooth plains unit at the top and right. The image is centered at 3.4°N, 176.9°E and is about 155 km wide.

class coincides with ridge belts as defined from *Venera* images of the northern hemisphere and has been further divided into a number of subclasses [Basilevsky *et al.*, 1986; Kryuchkov, 1988; Frank and Head, 1990]. The third class is a relatively limited population of ridges surrounding very large coronalike structures [Frank and Head, 1990]. In general, belts in class 1 are broad enough and of sufficient relief to be easily resolved by Magellan altimetric data [Solomon *et al.*, 1991; Squyres *et al.*, this issue (*a*)], although their topographic relief is not evident in radar images at high incidence angle. In contrast, belts in class 2 show less or even no relief at a scale sufficient to be resolved by Magellan altimetric data, but the relief of the individual narrow ridges making up the belts is evident in images regardless of incidence angle. For class 1 belts we use the term "fracture belts" [Squyres *et al.*, this issue (*a*)] in order to distinguish them from the class 2 belts, which are the true "ridge belts" of earlier papers.

Class 1 and class 2 belts commonly occur together, either as clearly distinct belts with different trends, or combined into single composite belts. Within composite belts the ridges may have the same trend as the fracture belt or have a trend markedly oblique to the associated fracture belt. Probably because of the low incidence angle, class 1 and class 2 belts are not easily separated in *Venera* images. Even on Magellan images the distinction is not easily made everywhere. In places, however, such as in Lavinia Planitia [Squyres *et al.*, this issue (*a*)], the stratigraphic and structural data are sufficient to infer not only that class 1 and class 2 belts are truly different features but also that they are of different ages.

Deformation belts are not distributed uniformly on the Venusian plains. Instead, they are concentrated in or near broad topographic lowlands. The two highest concentrations of plains deformation belts are in Lavinia Planitia and in Atalanta and Vinmara planitiae. The deformation belts in Lavinia are approximately centered on the long-wavelength topographic low. In the Atalanta-Vinmara region, however, most belts are well to the east of the long-wavelength topographic low. Deformation belts are also seen at lower concentrations southeast of Alpha Regio (where one attains a length of well over 2000 km), to the north of Bereghinya Planitia, and south of Aino Planitia.

Lavinia Planitia. The plains deformation belts that have been most thoroughly studied are those of Lavinia Planitia [Solomon *et al.*, 1991; Squyres *et al.*, this issue (*a*)]. The belts have widths of up to nearly 200 km and lengths that can be in excess of 1000 km (Figure 26). The belts form a very complex pattern, meandering, bifurcating, and merging along their lengths.

Belt formation in Lavinia Planitia had an extended history, as shown by crosscutting relationships among the belts and with surrounding plains units. Several volcanic units are found on the plains that separate the belts. At some locations the youngest materials present are deformed into belts, but at others (e.g., point A in Figure 26) belts clearly have been partially buried subsequent to their formation by thick volcanic flow units. There are also instances where a belt has formed and been partially buried by volcanic material, and then a younger belt has formed that transects the older belt and deforms the volcanic unit (e.g., point B in Figure 26).

Magellan images show that both ridge belts and fracture belts are present in Lavinia Planitia. Examples of ridge belts are seen at points C and D in Figure 26 (see also Figures 8 and 13 of Squyres *et al.* [this issue (*a*)]). The ridges can vary considerably in width both from one to the next in a given belt and along the length of a single ridge. The maximum ridge width observed in the Lavinia Planitia region is about 10 km, and more typical widths are a few kilometers. Some ridges appear symmetric in cross section, while others appear steeper on one flank than the other. A smooth, archlike profile is most common, but some ridges show a narrow, rugged, secondary ridge superimposed on the crest or on one flank. Ridges commonly bifurcate and merge along strike, producing a complex anastomosing pattern. Estimates of the heights of individual ridges, derived from measurement of radar foreshortening effects on the images, are typically 200–300 m [Squyres *et al.*, this issue (*a*), Figure 9].

An example of a fracture belt is shown at point E in Figure 26; higher-resolution examples are shown in Figures 10 and 15 of Squyres *et al.* [this issue (*a*)]. In contrast to the ridge belts, fracture belts are dominated by a complex pattern of linear to arcuate faults and fractures. Many faults appear singly, but others are paired to form grooves with widths ranging from a few kilometers down to the resolution limit of the images. The faults commonly display complex anastomosing and crossing patterns that indicate repeated or progressive deformation. Where fracture belts change trend, or where belts bifurcate or merge, the pattern of faults is especially intricate. In a few locations, two distinct scales of deformation are observed in fracture belts. Faults are spaced very closely (typically a few hundred meters) almost everywhere they are present in fracture belts. However, in a few locales these closely spaced faults are concentrated into bands of intense deformation that are separated by blocks of nearly undeformed material. The bands typically are spaced 20–30 km apart. It was reported by Solomon *et al.* [1991] that these bands of intense deformation coincided with local highs in the altimetry, but with revisions to the altimetry this conclusion is now in question [Squyres *et al.*, this issue (*a*)].

Several belts in Lavinia Planitia show evidence for horizontal shear parallel to the length of the belt [Solomon *et al.*, 1991; Squyres *et al.*, this issue (*a*)]. This evidence includes linear features that make S-shaped bends as they cross belts, rhombohedral downdrops within fracture belts, and patterns developed within ridge belts that can be interpreted as large-scale analogs of kinematic indicators seen in terrestrial shear zones. In all cases the amount of shear appears to be relatively minor and to be distributed across the belt rather than localized on major strike-slip faults.

Most of the deformation belts in the Lavinia Planitia area have clear topographic signatures [Solomon *et al.*, 1991; Squyres *et al.*, this issue (*a*)]. The belts stand several hundred meters above the surrounding plains. Elevation can be quite variable along the length of a belt, and the highest elevations commonly appear in complex, intensely deformed regions at belt bends and junctions. There is no evidence for bounding depressions at belt margins, and none of the belts are topographic depressions. While both ridge belts and fracture belts are elevated, fracture belts appear to display a few hundred meters greater relief than ridge belts. This difference may not, however, be real. The echo-fitting

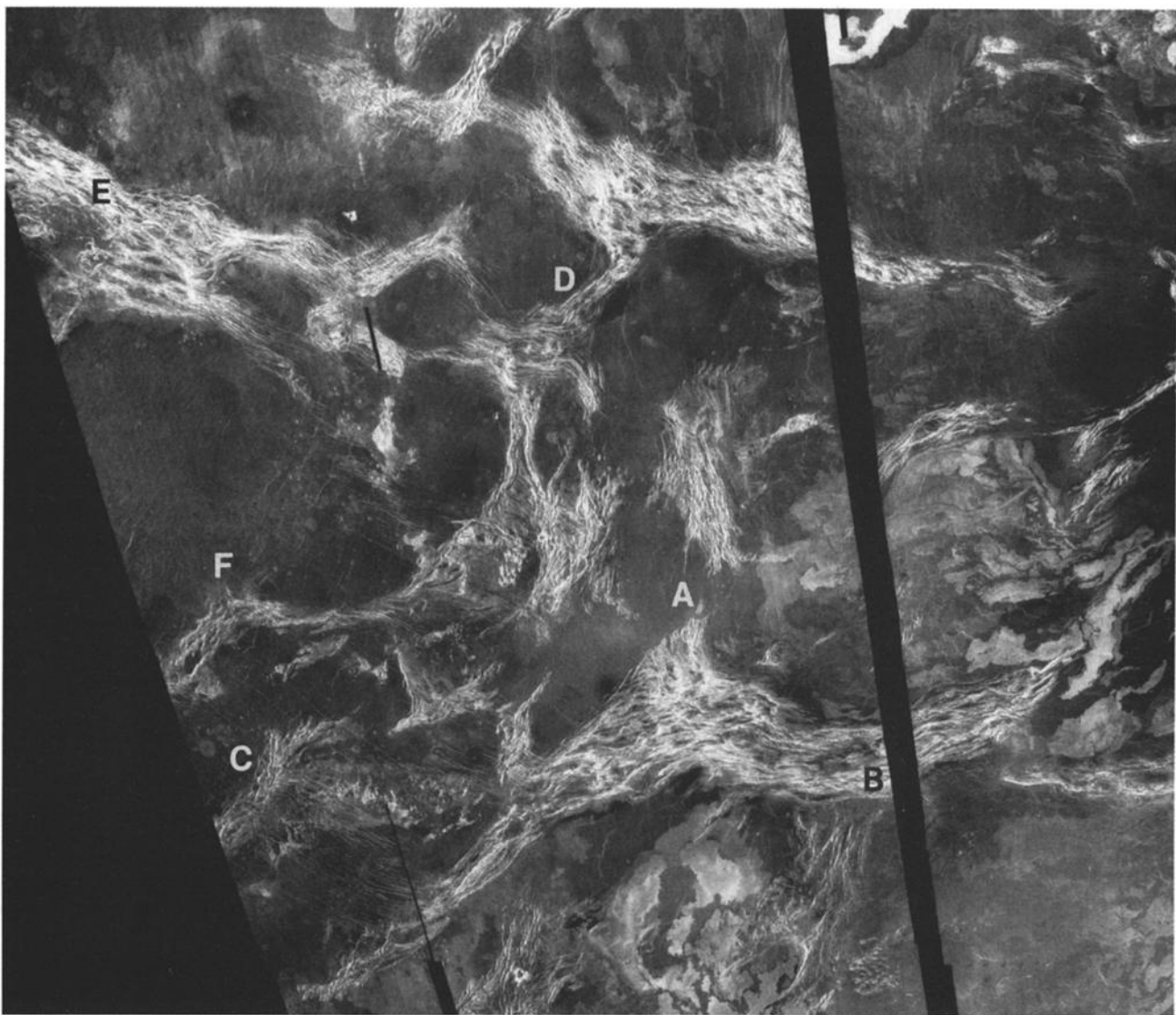


Fig. 26. Magellan radar image of ridge and fracture belts in Lavinia Planitia. The belts trending WNW contain graben or narrow fractures spaced 1–10 km apart; those trending NE contain narrow ridges about 5 km wide and 5–15 km apart. The image is centered at 45°S, 350°E and is 1850 km wide at the top. Letters denote areas discussed in the text.

algorithm used in precessing altimetric data is based on assumptions about the scattering law of the surface within the altimeter footprint [Pettengill *et al.*, 1991], and under certain circumstances, systematic differences in elevation can be obtained for areas with significantly different scattering properties.

The belt morphology may be a function of the orientation of the belt with respect to a regional stress field. Most of the plains of Lavinia Planitia are marked by a regular pattern of small wrinkle ridges and approximately orthogonal extensional grooves; the stress field that created these apparently coeval features must have been spatially and temporally uniform. Where deformation belts are parallel to the grooves, they tend to be fracture belts, and where they parallel the wrinkle ridges, they tend to be ridge belts; these relationships are particularly strong in western Lavinia Planitia [Squyres *et al.*, this issue (*a*), Figures 5 and 7].

An open question is whether or not the ridge belts and the fracture belts owe their origin to a similar mechanism. Evidence suggesting that they do includes the gross

geometric similarity of the two classes of belts (widths, heights, patterns traced across the plains) and the observation that a few belts undergo a transformation from ridge morphology to fracture morphology along their length (e.g., point F in Figure 26). Because of these gross similarities, and particularly because both types of belts are elevated, a reasonable working hypothesis is that both result from belt-normal crustal shortening and thickening [Solomon *et al.*, 1991]. If this view is correct, then the problem is in understanding the reasons for the very different morphologies of the two belt types.

The ridge belts of Lavinia Planitia appear to be fold belts, and an origin by horizontal shortening and crustal thickening is clearly indicated. The fracture belts, in contrast, have a morphology suggestive of at least near-surface stretching. One possibility is that fracture belts are dominantly extensional structures, perhaps localized into belts by patterns of lithospheric heating or igneous intrusion. Alternatively, if fracture belts are the result of horizontal compression and crustal thickening then their small-scale

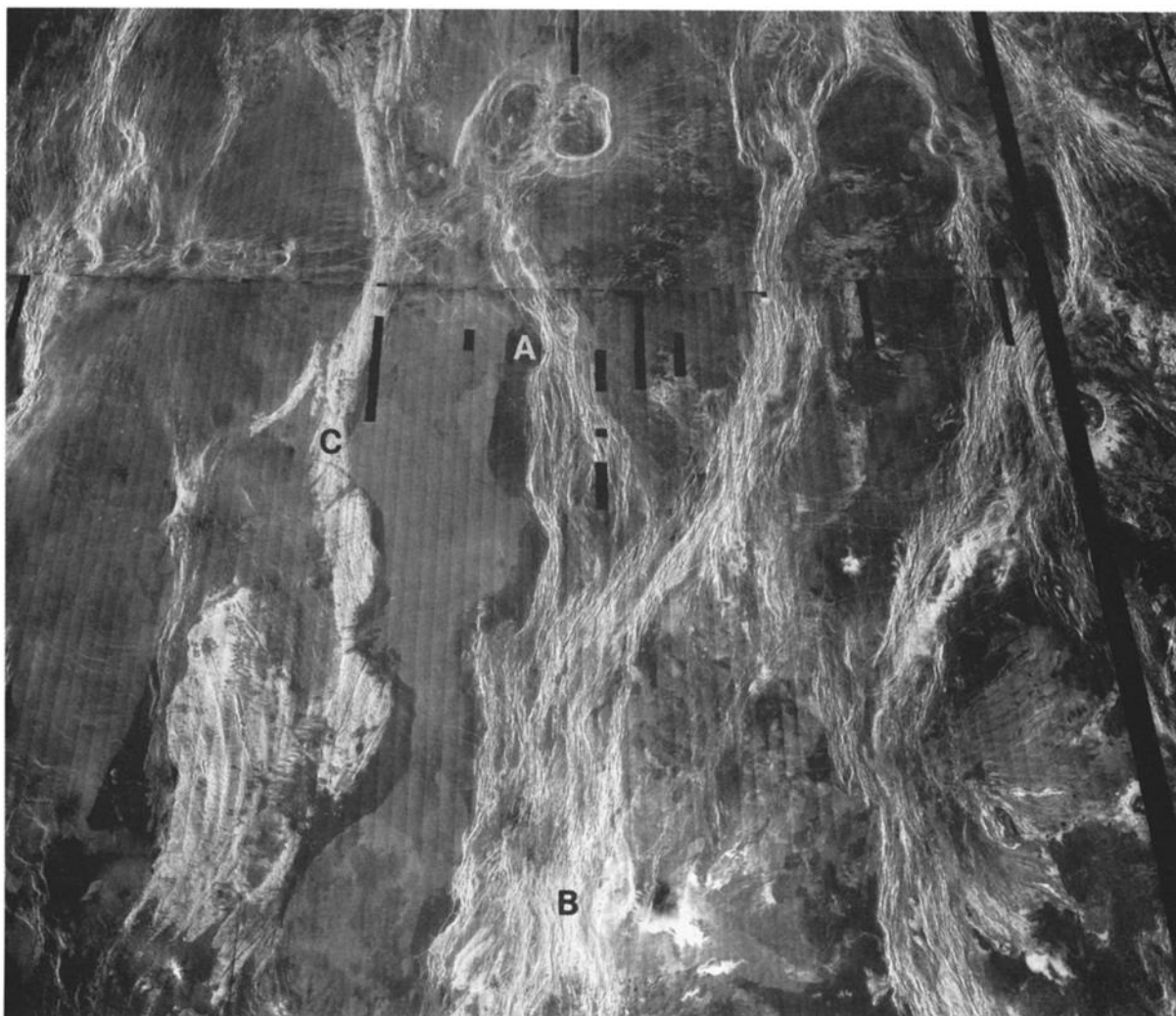


Fig. 27a. Magellan radar image of deformation belts in the Atalanta-Vinmara Planitiae area. The image is centered at 60°N, 208°E and is approximately 1850 km wide. Letters denote areas discussed in the text.

morphology may result from the stretching of a thin, brittle surface layer across the crest of a broad, archlike uplift formed by overall crustal shortening. The close association of fracture belts with widespread plains deposition and occasionally with fields of small volcanic shields [Solomon et al., 1991] is difficult to explain under the second hypothesis but would be an expected consequence of the first. Careful documentation of the history of deformation and magmatism within and near a number of ridge and fracture belts will be necessary if these hypotheses are to be distinguished.

Atalanta and Vinmara planitiae. The deformation belts of Atalanta and Vinmara planitiae show many similarities to those of Lavinia Planitia (Figures 27 and 28). Most of the belts run approximately N-S, but as in Lavinia Planitia they bifurcate and merge along strike to form an anastomosing pattern. Belts in Atalanta and Vinmara planitiae reach up to 250 km in width, and lengths well in excess of 1000 km are the norm. The belts are generally elevated by as much as 1 km above the surrounding plains, but a few sections of belts show almost no relief in Magellan altimetry (Figure 27b). Lukelong Dorsa, the prominent belt trending northwestward from the lower right corner of Figure 28, appears in the altimetry as a broad, low rise, but it is bounded on the west

by a shallow trough lying at a lower elevation than the adjacent plains; this trough (but not the low rise of the belt) was visible in earlier Venera 15-16 altimetry [Frank and Head, 1990].

A considerable range in morphology is observed among the Atalanta-Vinmara deformation belts. Several of the belts are similar to the Lavinia Planitia ridge belts. An example is shown in Figure 29 (also point A in Figure 27a). Here the belt consists primarily of subparallel, anastomosing ridges, although the ridges have a somewhat more irregular geometry than is typical in Lavinia Planitia. Other belts in Atalanta are more similar to fracture belts. A good example is shown in Figure 30 (also point B in Figure 27a). Note that this belt is the southward continuation of the ridge belt in Figure 29. Along this section of the belt some ridges are still apparent, but the morphology is dominated largely by fractures and faults, with a few faults paired to form graben. At this location, the belt is intermediate between the two extreme morphologic classes seen in Lavinia, but overall it is more like a fracture belt than a ridge belt. Further, as with the fracture belts in Lavinia Planitia, it displays more relief along this section than farther north where ridges dominate (Figure 27b). The variation in small-scale morphology along this

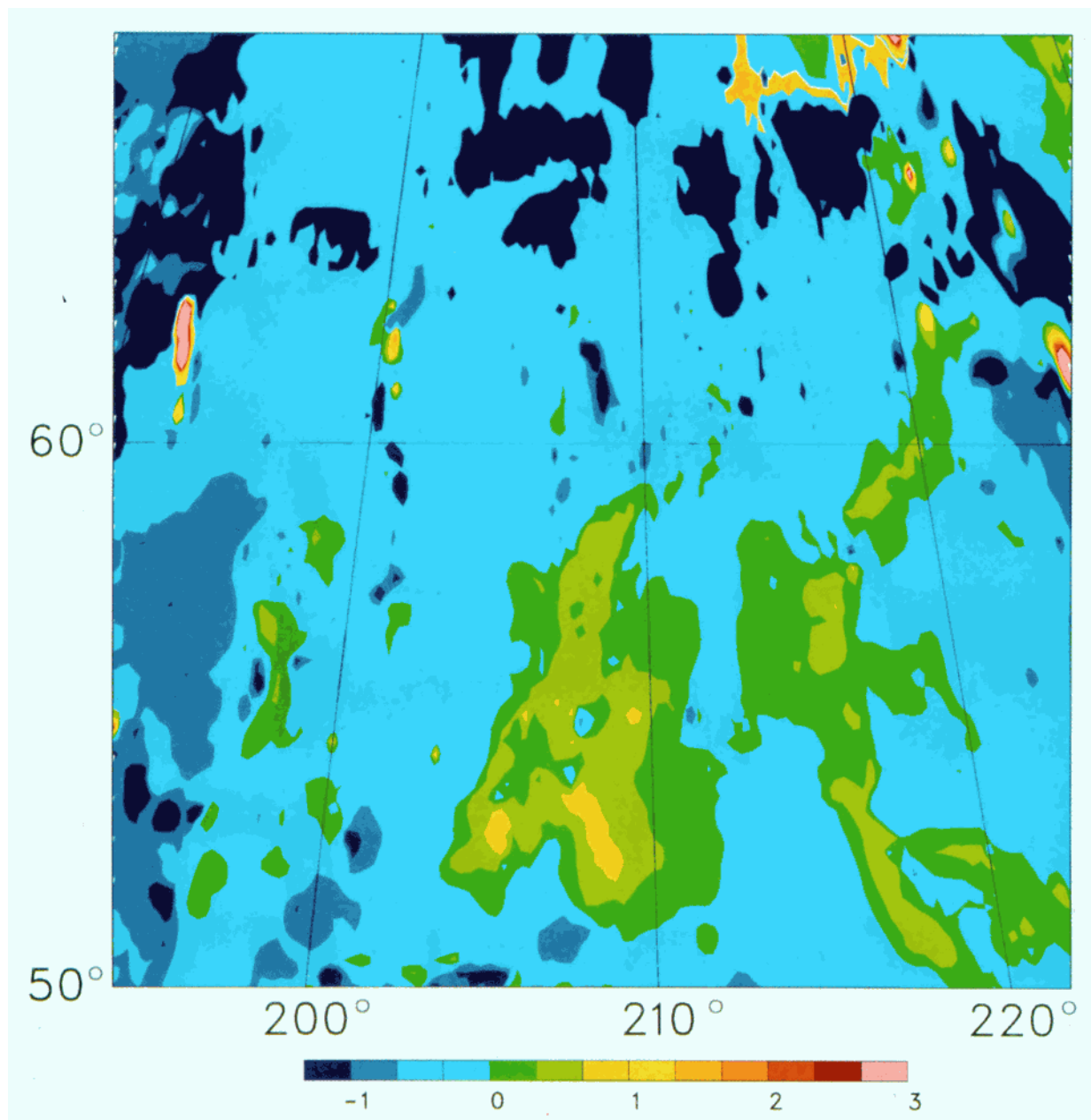


Fig. 27b. Altimetric contour map of the area shown in Figure 27a; map projection and boundaries are approximately the same; 0.33-km contour interval. The altimetric data points were regridded at 0.25° intervals of latitude and longitude.

single belt strengthens the case that ridge and fracture belts have a common origin. There is no significant change in the strike of this belt as it changes from one morphologic style to the other, however, in contrast to the strong correlation between the strike and style of the belts in Lavinia Planitia.

One of the most unusual deformation belts in the Atalanta-Vinmara Planitiae region is that at point C in Figure 27a. Instead of the subparallel ridges or faults seen elsewhere, this belt is characterized by an extremely fine, commonly rectilinear pattern of intersecting grooves and fractures. It is partially buried on its flanks by adjacent plains volcanic units, and along some of the grooves it is deeply embayed by plains material. The interior morphology of this belt is similar to that of tessera, or complex ridged terrain. Much of this belt shows positive relief in Magellan altimetry (Figure 27b), but the section near 60°N appears as a topographic trough;

as noted above, however, the topography may contain artifacts resulting from the locally large variations in radar backscatter. The intense deformation preserved within the belt interior appears at least partly to predate the formation of the belt as a large-scale structure. This feature may have formed when a long, curvilinear segment of older tessera terrain was uplifted slightly and then buried on both sides by volcanic plains material.

Deformational Sequence

Detailed studies of plains regions imaged early in the Magellan mission (Sedna, Navka, Guinevere, and Lavinia planitiae) indicate that the structural evolution of Venusian plains is complex. Within these plains regions there seems to be a first-order similarity in structural evolution.



Fig. 28. Magellan radar image of deformation belts in the Atalanta-Vinmara planitiae area. The belt extending from the center to lower right is Lukelong Dorsa. The image is centered at 75°N, 180°E and is about 1000 km wide at the base (sinusoidal projection, 164°E central meridian).

Reconnaissance of other plains areas on Venus suggests that this common structural evolution may characterize most plains regions, but further work is needed to establish this generalization firmly. We describe here the sequence in Lavinia Planitia [McGill, 1991; Squyres *et al.*, this issue (*a*)] and Guinevere Planitia (Figures 31-33) [McGill *et al.*, 1991]. Apparently similar examples from other plains regions are cited where appropriate.

In both Guinevere and Lavinia planitiae there are small inliers of radar-bright, complexly deformed terrain. Many of the inliers appear to be small exposures of complex ridged terrain, or tessera. Contact relationships with the surrounding plains indicate that these inliers are older than the plains materials (Figures 31 and 33). Commonly, the youngest structures affecting these inliers are sharply defined, straight to arcuate graben, some of which reach

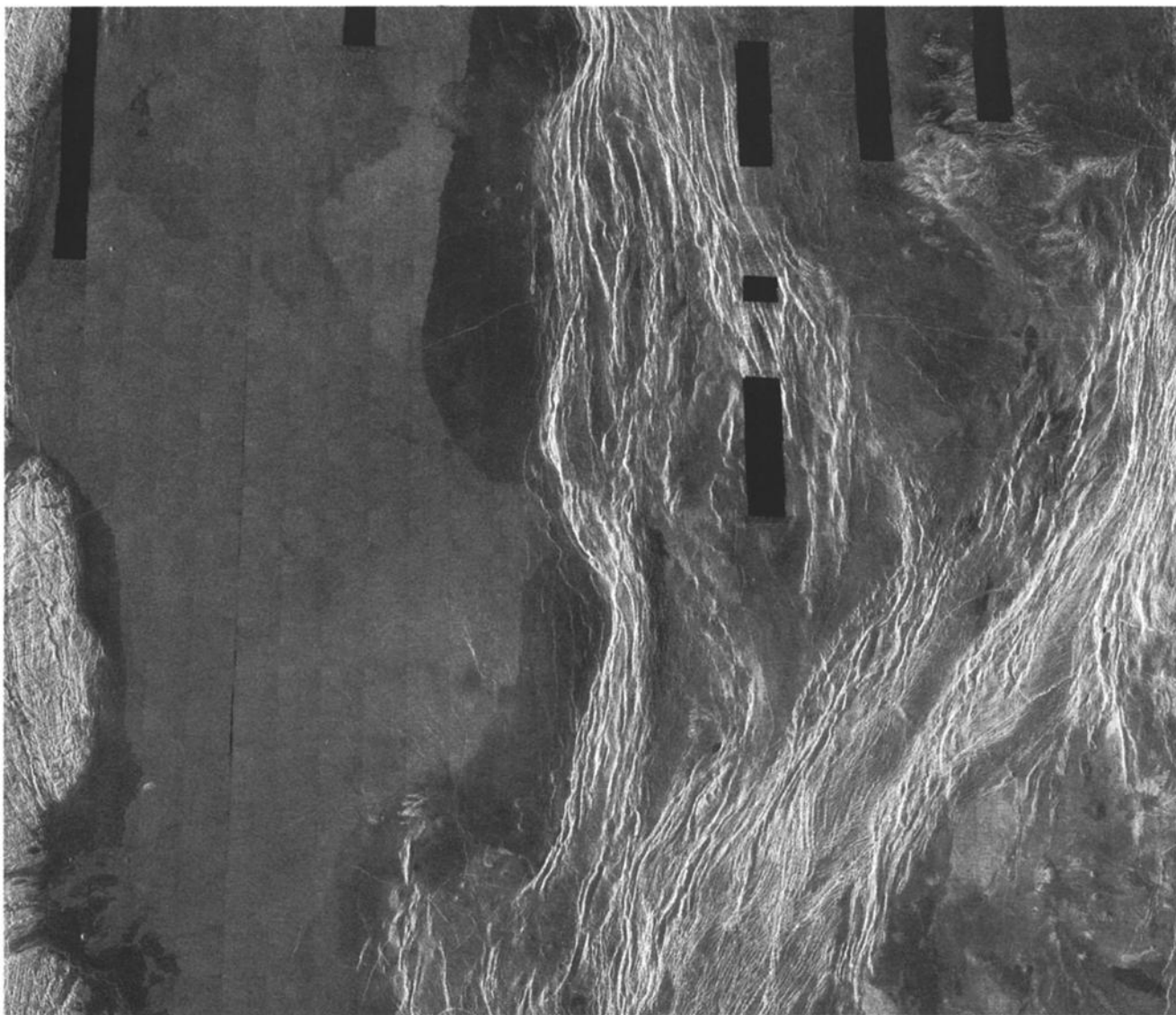


Fig. 29. Magellan radar image of the northern arms of the Pandrosos Dorsa deformation belt in Vinmara Planitia (from the center of the region shown in Figure 27). These two arms of this belt are similar in morphology to the ridge belts of Lavinia Planitia. The image is centered at 60°N, 207°E and is about 620 km wide.

widths of 10–15 km. Wherever these graben abut contacts between inliers and surrounding plains they are partially to completely flooded by plains materials [Squyres *et al.*, this issue (*a*), Figure 2] (Figure 33). The total length of some of these graben is hundreds of kilometers. Locally, there is discernible relief across the margins of graben buried beneath plains, suggesting that there has been minor fault movement after plains deposition. These relationships indicate that the time of formation of at least the largest of the graben-cutting tessera inliers overlaps with that of the early stages of plains deposition. The orientations of the large graben thus provide useful clues to stress orientations early in plains development. It also is possible to infer the presence of a deformed basement beneath the plains where large graben can be traced as "ghosts" (Figure 32) across plains areas.

In Lavinia Planitia, it is possible to demonstrate that true ridge belts (class 2) deform a bright "textured terrain" that is younger than the tessera inliers but older than plains materials [Squyres *et al.*, this issue (*a*)]. Textured terrain

exhibits a remarkably regular fabric that is penetrative at the scale of Magellan images [Squyres *et al.*, this issue (*a*), Figures 3 and 14]. This fabric is clearly truncated at contacts with plains materials, a relationship that supports the existence of the textured terrain as a unit older than these plains. Consequently, it is apparent that the ridges of at least some of the Lavinia ridge belts formed prior to the deposition of the typical widespread plains materials. Where textured terrain is mappable, this age relationship can be supported stratigraphically; where textured terrain cannot be distinguished from other plains, this age relationship depends on apparent embayment of ridge complexes by the other plains, a less definitive criterion of relative age. As noted above, there is some evidence of belt-parallel shear associated with the true ridge belts of Lavinia Planitia [Solomon *et al.*, 1991; Squyres *et al.*, this issue (*a*)], and where relative ages can be determined, this shearing preceded deposition of plains materials.

Most plains materials can be divided into two general

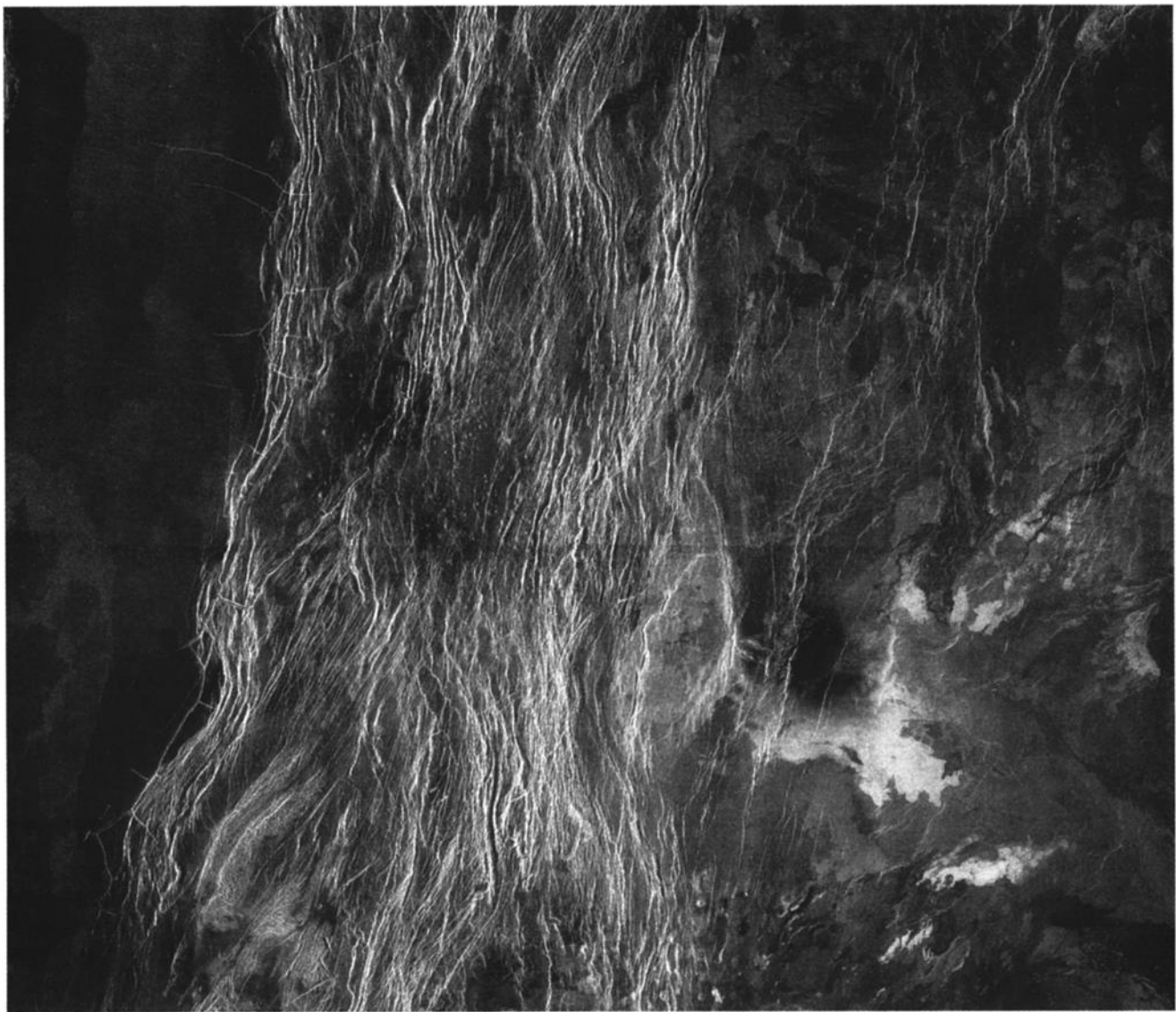


Fig. 30. Magellan radar image of the southward continuation from Figure 29 of Pandrosos Dorsa (also visible in the lower central region of Figure 27). This section of the deformation belt is most similar in morphology to the fracture belts of Lavinia Planitia. The image is centered at 55°N, 208°E and is about 620 km wide.

categories: "regional plains" and "digitate flows." Geological mapping demonstrates that in any given area it is possible to divide regional plains materials into mappable units distinguished from each other by differences in fine-scale surface texture, radar brightness, and the presence or absence of one or more sets of wrinkle ridges [McGill *et al.*, 1991]. There is no way at present to determine if these units resulted from discrete events widely separated in time or from essentially continuous depositional activity. In general, it is not possible to define more than two or three such units that can be mapped regionally; additional units commonly can be defined, but these are of local importance only (Figure 32). Contacts between the two areally important regional plains units in the region of Guinevere Planitia in Figure 32 indicate that many of the faults and fractures characteristic of Venusian plains developed after the older unit (Pd) but before the younger one (Pc). A similar relationship is present in Lavinia Planitia [Squyres *et al.*, this issue (*a*)]. Because many of these fractures and faults are closely associated with

the topographic rises and ridges visible in the altimetric data, the implication is that much or all of this topographic relief also developed between the depositional events or phases responsible for the two material units. In support of this inference is the common observation that the older regional plains unit appears to be continuous over rises and broad ridges, presumably because of postdepositional arching and uplift. Digitate flow complexes (e.g., unit Pa in Figure 32) show abundant evidence that fracture and ridge belts existed before their emplacement: they are superposed on almost all faults and fractures, their morphology implies that the flows were diverted by ridges and rises, and they are generally characterized by a very low abundance of wrinkle ridges.

Among the youngest structural features in the plains are widely spaced, bright lineations generally hundreds of kilometers long yet so narrow that their morphology cannot be resolved on full-resolution images except locally, where they appear to be troughs. In both Lavinia and Guinevere planitiae, these lineations trend WNW, but similar appearing

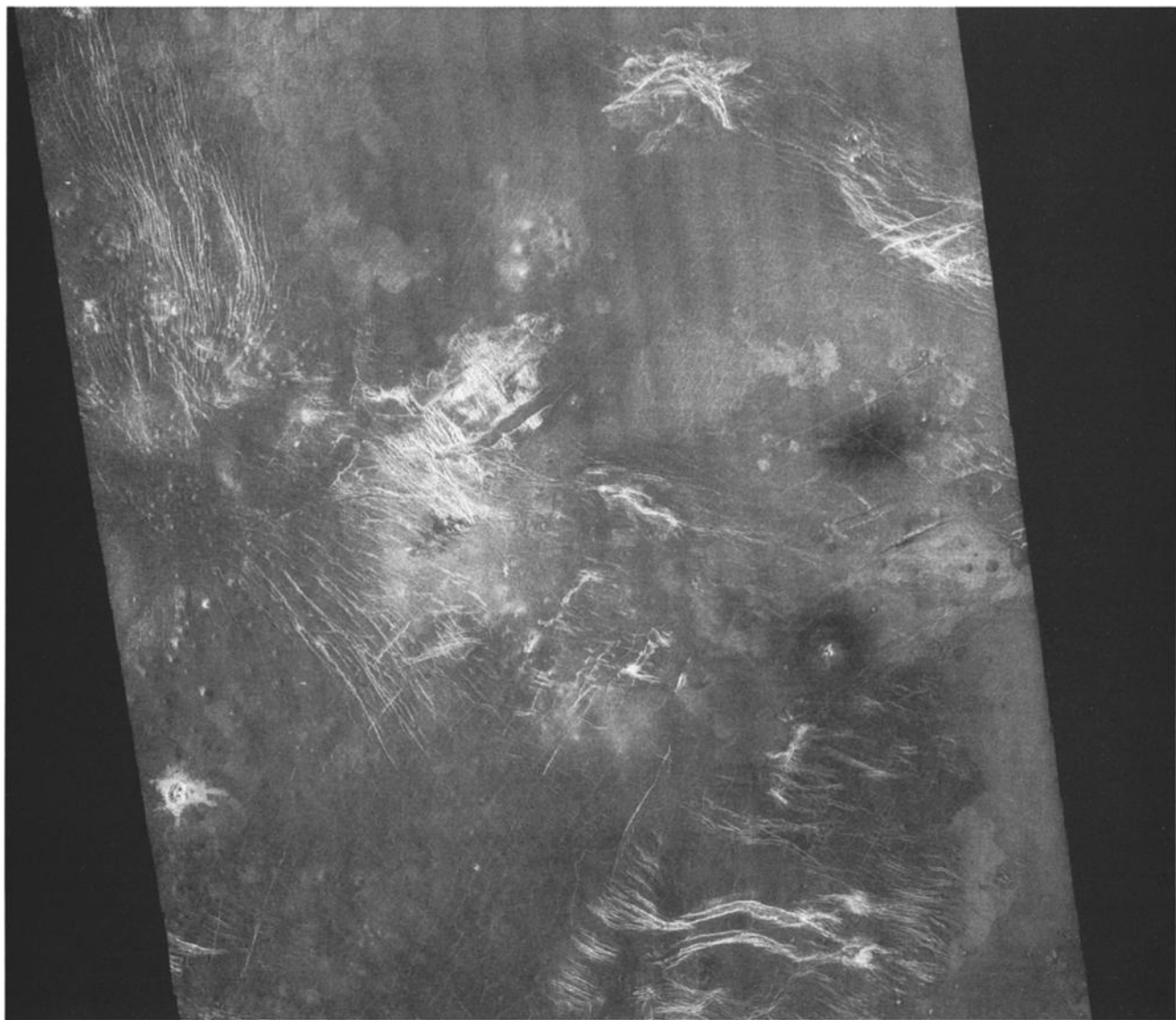


Fig. 31. Magellan radar image of a portion of the plains of southern Guinevere Planitia. The image is centered at 20°S, 337°E and is about 470 km wide.

lineations have different trends elsewhere on Venus. In Guinevere Planitia (Figure 32), only the areally limited, youngest plains unit (Pa) appears to be superposed on these fractures. In Lavinia Planitia [Squyres *et al.*, this issue (*a*)] these lineations do not cut digitate flows, but it is unclear if this is because the lineations are older or because they are areally restricted. Reconnaissance studies of other plains areas suggest that long, narrow, bright lineations are generally older than digitate plains flow complexes.

The fine, sinuous bright features interpreted as wrinkle ridges are very common in many plains regions but totally absent in others. Where they are common, they seem to have formed more or less continuously during plains evolution. All types of plains units have these features, including digitate plains. In Guinevere and Lavinia planitiae their abundance decreases markedly with decreasing relative age of the unit. The orientations of these features tend to be systematic in any given region; that is, the strike directions remain constant over a large area, or they maintain a consistent relationship to some major feature, such as a large

corona. Within the area shown in Figures 31 and 32, for example, the wrinkle ridges maintain a nearly constant NNE trend. In contrast, wrinkle ridges within a large area of eastern Aino Planitia define an arc concentric to Artemis Chasma. These systematic orientations persist regardless of the unit on which the wrinkle ridges occur and regardless of how abundant they are on that unit, implying that the stresses responsible for wrinkle ridge formation did not change orientation throughout the emplacement of all affected units.

A general kinematic sequence emerges from these observations. The earliest structures at least partially preserved in plains regions are large arcuate graben. These structures are largely buried now, but fragments of them are exposed in scattered tessera inliers, and their presence in the subsurface is locally revealed by subtle lineations on the plains surface. Ridge belts (class 2 belts) evidently formed next in Lavinia Planitia, deforming a locally distinctive, radar-bright terrain that may well be an early plains deposit. As discussed above, the morphology of the ridges in ridge belts

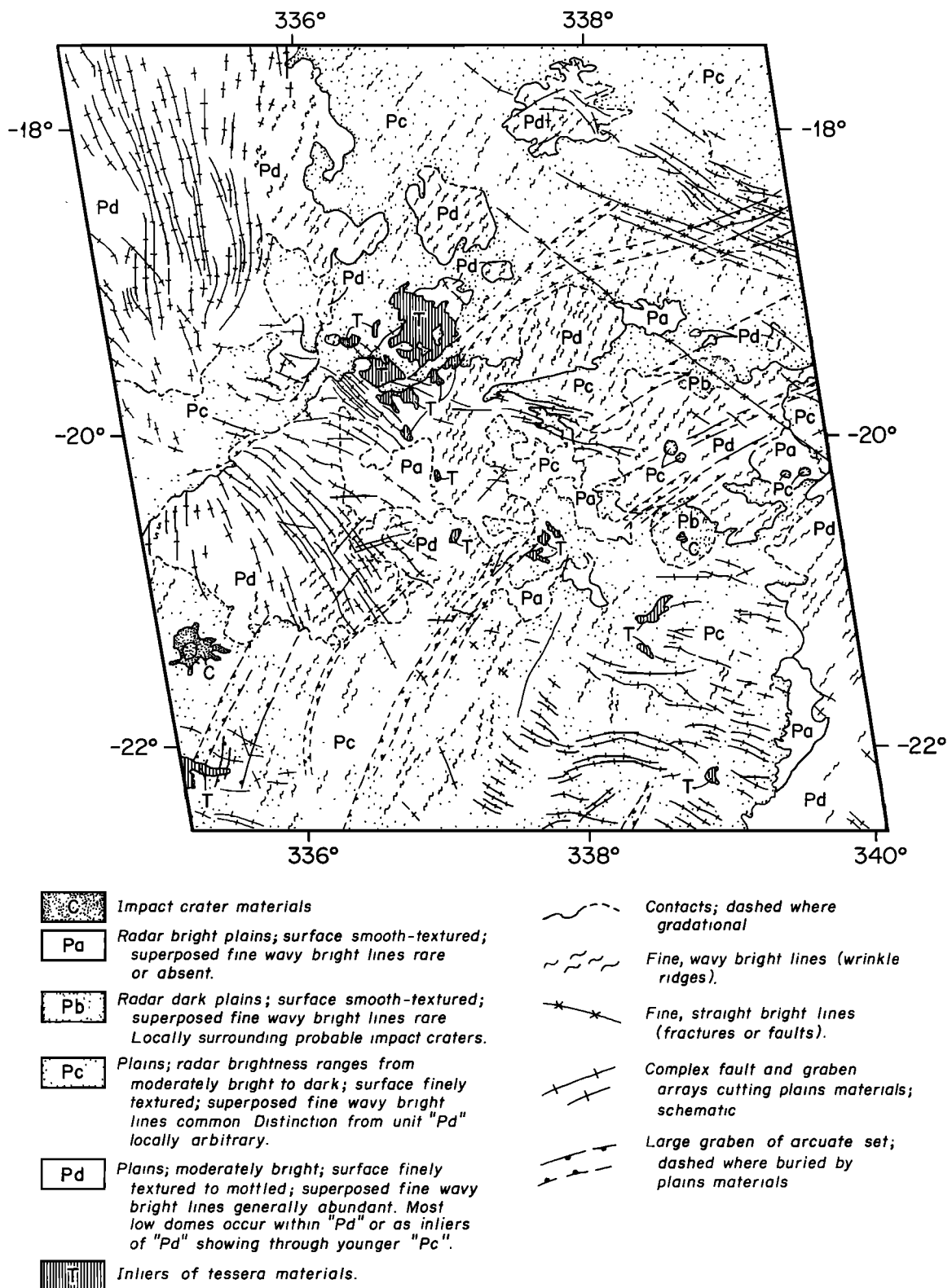


Fig. 32. Geologic map of the region in Figure 31 (by G. E. McGill). Truncation relationships demonstrate that faults and fractures are not all the same age. Evidence that large graben exist in the subsurface implies the presence of a deformed (tessera) basement beneath the plains.

supports a compressional origin, but there is also local evidence for belt-parallel shear during or following ridge formation [Solomon et al., 1991; Squyres et al., this issue (a)]. A really extensive regional plains materials embay the ridge

belts and truncate the shear zones, indicating that ridge belt development is an early phase of plains structural development. Much of the pervasive fracturing characteristic of plains, and also the associated topographic



Fig. 33. Magellan radar image of a portion of the center of Figure 31, showing a large graben (10 km wide) cutting an inlier of tessera. That the graben continues beneath the adjacent younger plains is indicated by the fine, radar-bright lines on the planes that are aligned with the edges of the exposed graben. The image is about 150 km wide.

rises and ridges, formed part way through plains development, after the oldest widespread plains deposits but before the youngest. Very long, narrow lineations with consistent orientations formed relatively late in plains development. Digitate flows clearly are younger than the rises and ridges and younger than most fractures and faults as well. Wrinkle ridges apparently formed more or less continuously throughout plains evolution, maintaining approximately constant orientations in any given locality throughout this history.

Although this kinematic sequence is based primarily on detailed studies in Guinevere and Lavinia planitiae, it appears as if much of it may apply to other plains regions as well. Straight to arcuate, undeformed graben are generally the youngest structures in tessera, and evidence can commonly be found for the continuation of large graben beneath plains adjacent to exposed tessera. Plains evolution seems everywhere characterized by a complex interplay of deposition and deformation that is kinematically similar to that in Guinevere and Lavinia planitiae. The most important possible exception is the timing of ridge belt development. Locally, ridge belts appear to be younger than at least some regional plains materials rather than older than all of them, as

seems to be the case in Lavinia Planitia. Furthermore, there are places where the distinction between ridge belts and wrinkle ridges is not easily drawn, suggesting that some ridge belts may simply be enlarged wrinkle ridges. It may well be that ridge belts are characteristically one of the oldest plains structures but that some plains regions are younger than others. This and other inferences concerning plains evolution on Venus must be tested with detailed studies of all plains regions.

The implications of the structural and stratigraphic sequence inferred for Guinevere and Lavinia planitiae for deformational processes are not fully understood. The large graben imply that the earliest phases of plains deposition in Guinevere Planitia were associated with pervasive crustal extension. Graben younger than tessera units in Lavinia Planitia suggest a similar early extensional phase there, but there are no large, throughgoing graben such as those present in Guinevere Planitia. In Lavinia Planitia there also is evidence for early ridge belt formation with crustal shortening and some shear, implying early compression. It is not clear whether these contrasting regimes occurred in sequence in one area or whether different subareas within a plains region had different early histories.

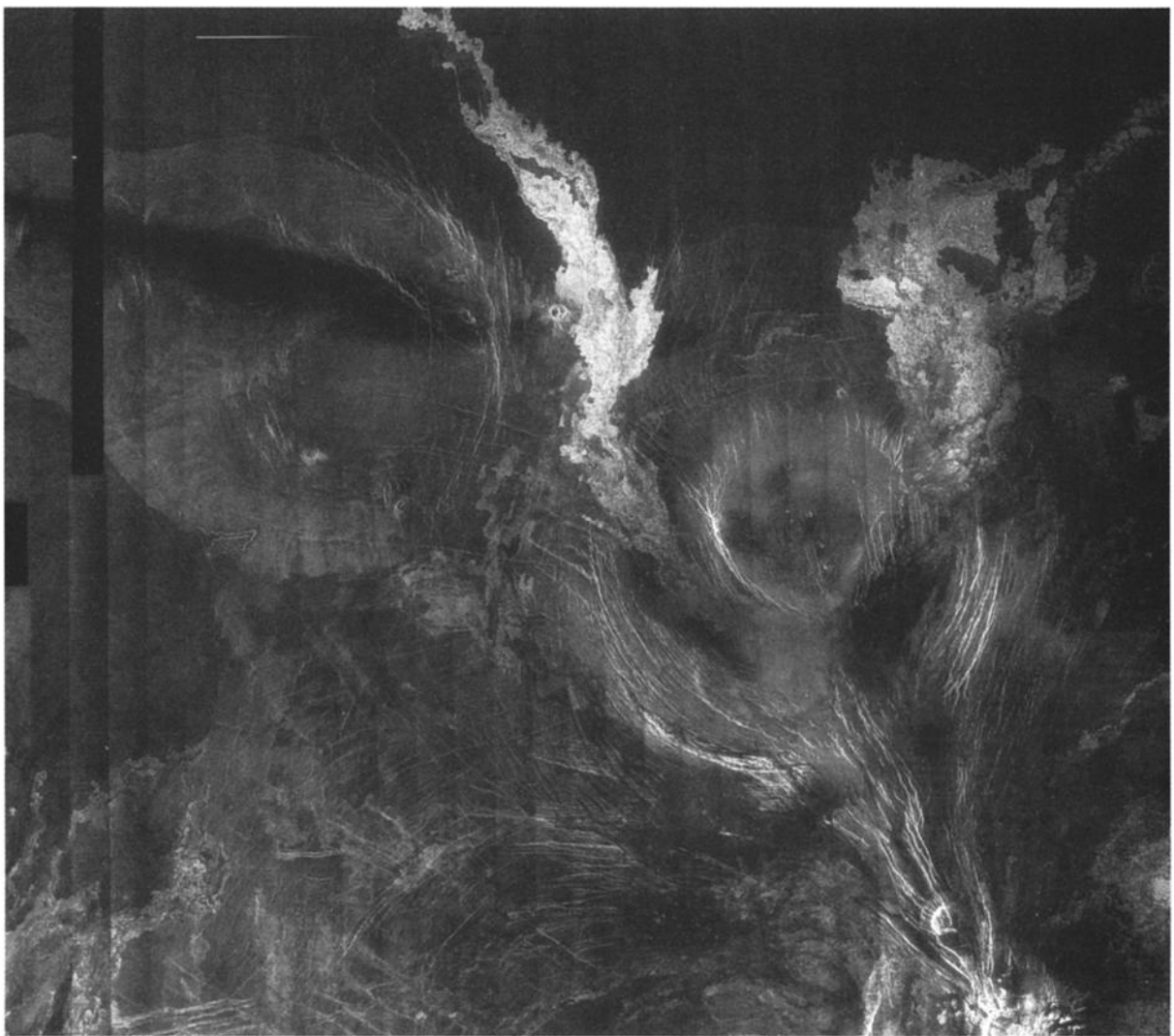


Fig. 34a. Magellan radar image of the corona Idem-Kuva, located at 25°N, 358°E. This corona is approximately 230 km in diameter and is notable for its association with Gula Mons (located about 300 km to the south) and for the radar-bright volcanic flows which emanate from topographic highs in the eastern and western portions of the structure.

CORONAE

Coronae are volcanotectonic structures unique to Venus and generally distinguished by a quasi-circular annulus, 100–2600 km in diameter, of concentric extensional faults and fractures and sometimes circumferential compressive ridges (Figure 34a). Topographically, the interiors of coronae generally stand higher than their surroundings and display domical or plateau-like shapes. Coronae sometimes have elevated rims and annular troughs or moats around their periphery (Figure 34b). Volcanic flows often cover large portions of the interior, fill the peripheral moat, and spill radially outward over the surrounding plains (Figure 34a and 34c). Coronae have been described from Venus 15-16 and Arecibo radar images by Barsukov *et al.* [1986], Basilevsky *et al.* [1986], Stofan and Head [1990] and Pronin and Stofan [1990]. Magellan radar images and topographic data have provided a significantly improved view of coronae, both in terms of the resolution of morphologic detail of individual structures and the global distribution of the population. The first discussions of coronae based on Magellan data focused on the tectonic [Solomon *et al.*, 1991]

and volcanic [Head *et al.*, 1991] characteristics of the third largest corona on Venus, Quatzalpetlatl, the first corona imaged by Magellan. The first detailed descriptions and analyses of other Venusian coronae using Magellan data appear in other papers in this issue by Squyres *et al.* [this issue (b)], Stofan *et al.* [this issue], Janes *et al.* [this issue], and Sandwell and Schubert [this issue]. Here we present an overview of the tectonics of coronae; an overview of the volcanic characteristics of coronae is given by Head *et al.* [this issue].

Tectonic Characteristics of Coronae

The tectonic features of coronae include extensional faults and graben oriented radially and circumferentially, as well as parallel to regional fault trends, and concentric compressional ridges (Figure 35). Circumferential faults and graben are mainly concentrated within a relatively narrow tectonic annulus, which is usually the most notable and distinctive characteristic of a corona. The tectonic annulus generally coincides approximately with the topographic rim and moat of the corona. Radial extensional faults extend outward

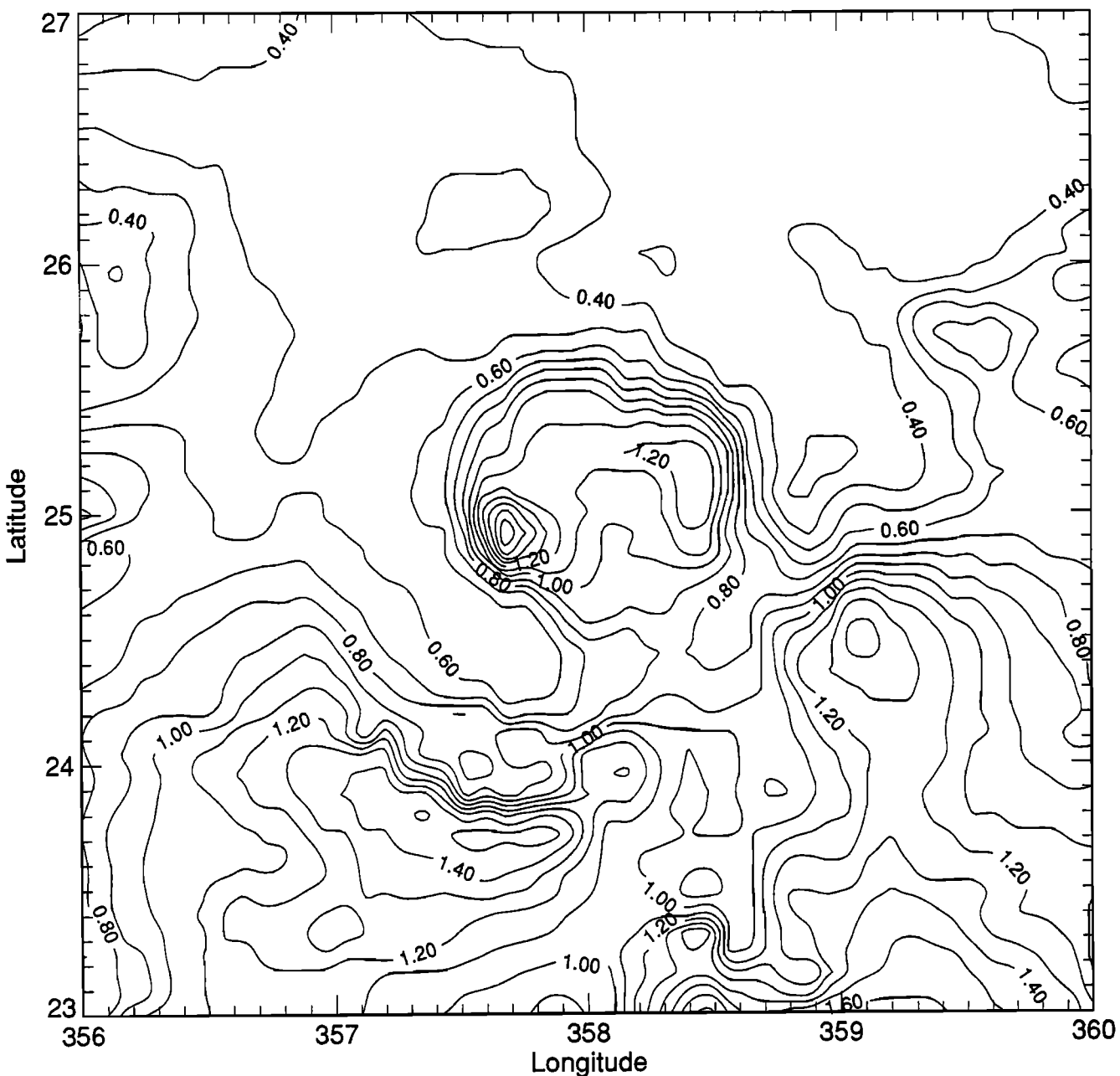


Fig. 34b. Topographic contour map of Idem-Kuva Corona. The contour interval is 100 m; the datum is a planetary radius of 6052.0 km. The eastern and western topographic highs within the corona interior appear to be sources of the radar-bright flows in Figure 34a. The regions at about 1.5 km elevation to the SSW and SE of the corona center are associated with the concentric graben which form the outer annulus of the corona.

from the center of some coronae (Figure 35a), often to large distances beyond the tectonic annulus. Obliquely striking extensional faults that parallel regional trends occur at all locations within coronae and are the most common tectonic features in the interior (Figure 35b). Compressional ridges are observed only rarely within coronae; when they do occur they are observed along portions of the rim (Figure 35c). Because volcanic flows often blanket large areas both inside and outside coronae, faults are generally best exposed on the rims and high-standing parts of the interior and in the unfilled parts of the moat and uncovered areas of the surrounding plains. In many instances, faults are superimposed on older volcanic flows. In some cases there is little volcanism to mask the tectonic features.

Tectonic annuli around coronae are very narrow compared with corona radii. Annuli are generally less than 100 km wide and have a tendency to be wider in larger coronae [Stofan et al., this issue]. The annulus of the largest corona, Artemis (about 2600 km in diameter), is only about 150 km wide. The tectonic annulus of Artemis coincides with its peripheral moat, as much as 3 km deep [Ford and Pettengill, this issue]. The extensional concentric faulting in the annulus around Artemis is likely a consequence of the flexural deformation of the elastic upper layer of the downwarped lithosphere in the moat [Sandwell and Schubert, this issue]. The general association of extensional concentric faults with the topographic moats and rims of coronae [Squyres et al., this issue (b)] implies that these faults

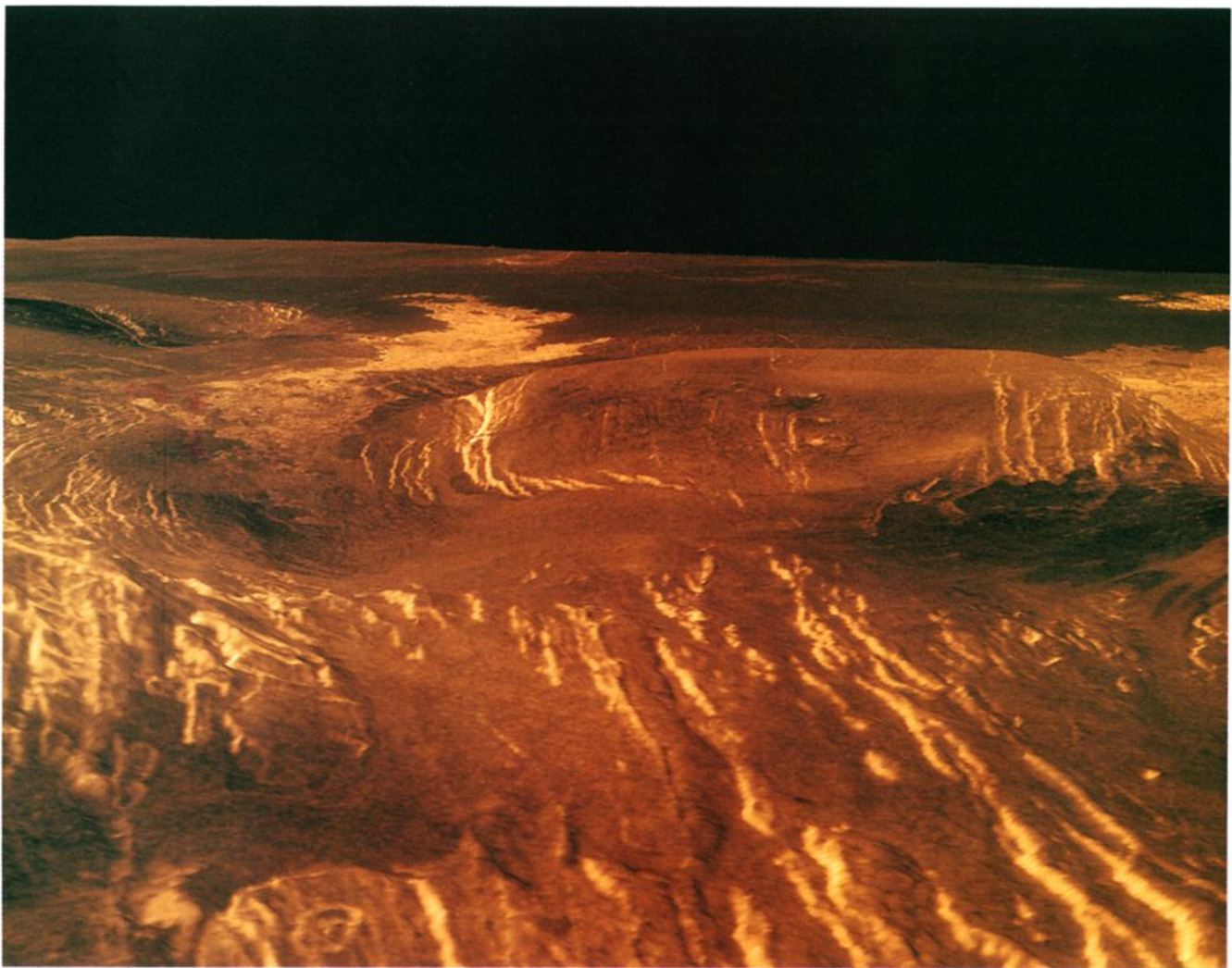


Fig. 34c. Perspective view of Idem-Kuva Corona as seen in combined false-color radar image and altimetry data.

form as a result of flexure of an elastic lithospheric layer forced to bend into the topographic moat-rim shape. This hypothesis is supported by a theoretical model of the thermoelastic effect of cooling and relaxation of a thermally isostatically supported plateau; the model can match the rim-moat topography and predicts predominantly radial extension in the moat and outward facing slope of the rim as the plateau subsides as a result of the cooling and thickening of the underlying lithosphere [Sandwell and Schubert, this issue]. Models of the viscous gravitational relaxation of a plateau can also match the rim-moat topography, with dominantly radial extension outward of the crest of the rim [Stofan et al., this issue; Janes et al., this issue]. Concentric extensional faults also occur on the inward facing slopes of some corona rims and in the slopes of coronalike features that are topographic depressions similar to calderas [Squyres et al., this issue (b)]. Like the concentric extensional faults of the caldera Sacajawea, the faults in the coronalike structures could also be caused by flexure of the elastic lithosphere forced to bend downward into the central depression.

The radial extensional faults and graben in coronae are presumably associated with the broad doming of coronae. Evidence that doming and radial fracturing may occur in the earliest stage of corona development is provided by coronalike features called novae. Novae are broad domes

with predominantly radial extensional faults and graben; they may constitute examples of this first stage of corona evolution [Squyres et al., this issue (b)]. Theoretical models of doming induced by the impingement of buoyant diapirs of hot mantle material on the base of the lithosphere provide good matches to topographic profiles across novae, and they predict surface stresses over the domes that are consistent with predominantly radial extensional faulting [Stofan et al., this issue; Janes et al., this issue]. The models also predict disorganized extensional faulting over the centers of the domes; examples of this behavior are found in coronae such as Aditi [Squyres et al., this issue (b)]. Shield volcanoes are also elevated structures with radial extensional faults, and some of the structures identified as novae may actually be volcanic shields; Squyres et al. [this issue (b)] identify Kunapipi as one such structure. The major difference between novae and volcanic shields is the relative importance of doming versus volcanic construction in the creation of the elevated topography. Since many novae have volcanic flows on their flanks (e.g., Tai Yuan [Squyres et al., this issue (b)]), it is sometimes difficult to distinguish between the two processes.

There are relatively few coronae that display compressional tectonic features; these occur as concentric ridges along segments of the tectonic annulus. One of these

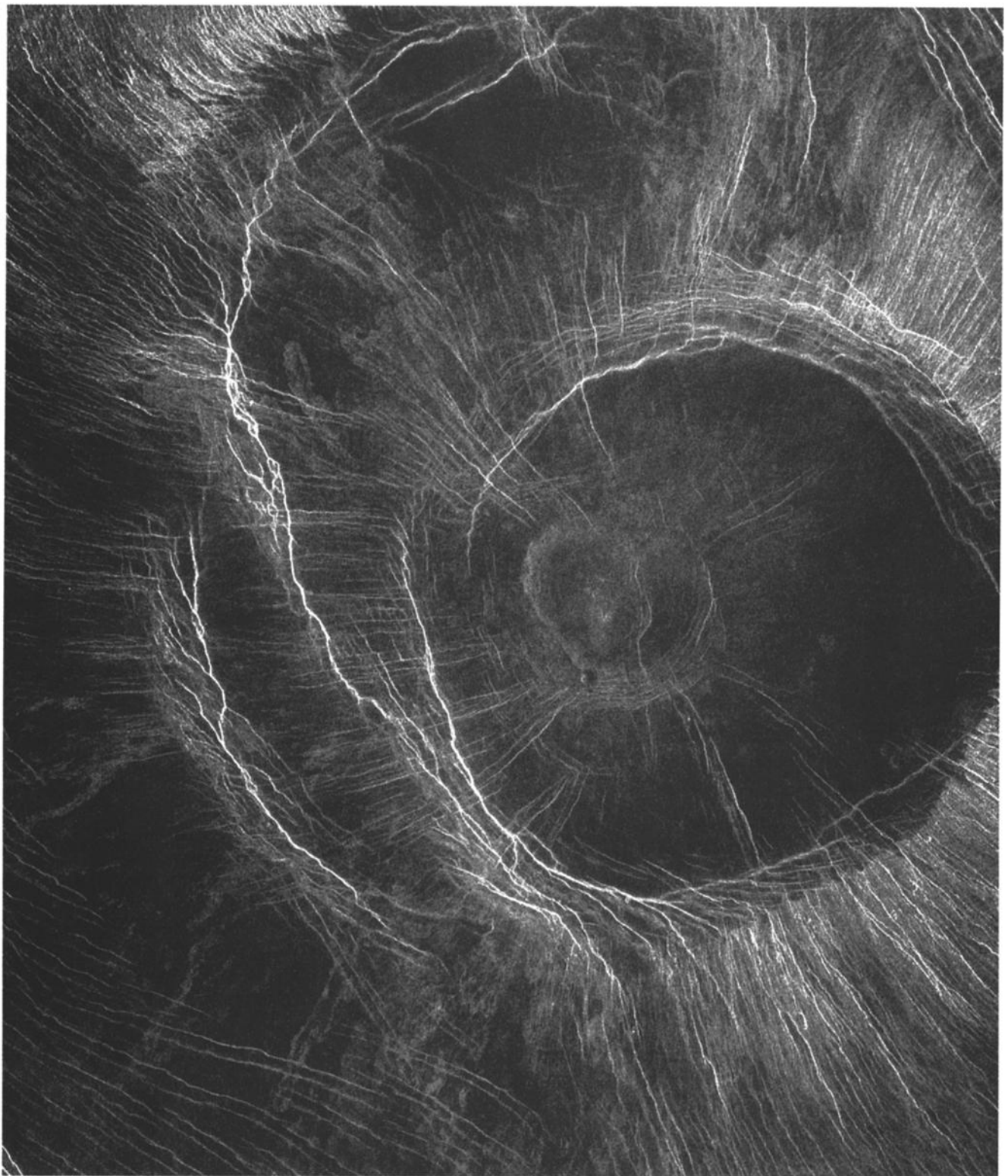


Fig. 35a. An example of a corona with both radial and concentric structures. The corona is at 18.5°S, 259°E; the image is 165 km wide.

is Quetzalpetlatl [Solomon et al., 1991]; other coronae with segments of concentric compressional ridges in their annuli are Ba'het and Tamfara [Squyres et al., this issue (*b*)]. No corona has been found to have an annulus composed entirely of compressional ridges. Predominantly radially compressive surface stresses can develop inward of the rim crest during the thermal or gravitational relaxation of a corona [Sandwell and Schubert, this issue; Stofan et al., this

issue; Janes et al., this issue]; perhaps these stresses can account for the occasional compressionally distorted segments of corona rims.

The formation of a corona, by whatever process, occurs in the presence of a regional stress field. Tectonic features basically intrinsic to coronae, e.g., the radial and concentric extensional faults, can be modified by regional stresses that add constructively or destructively to the stresses involved

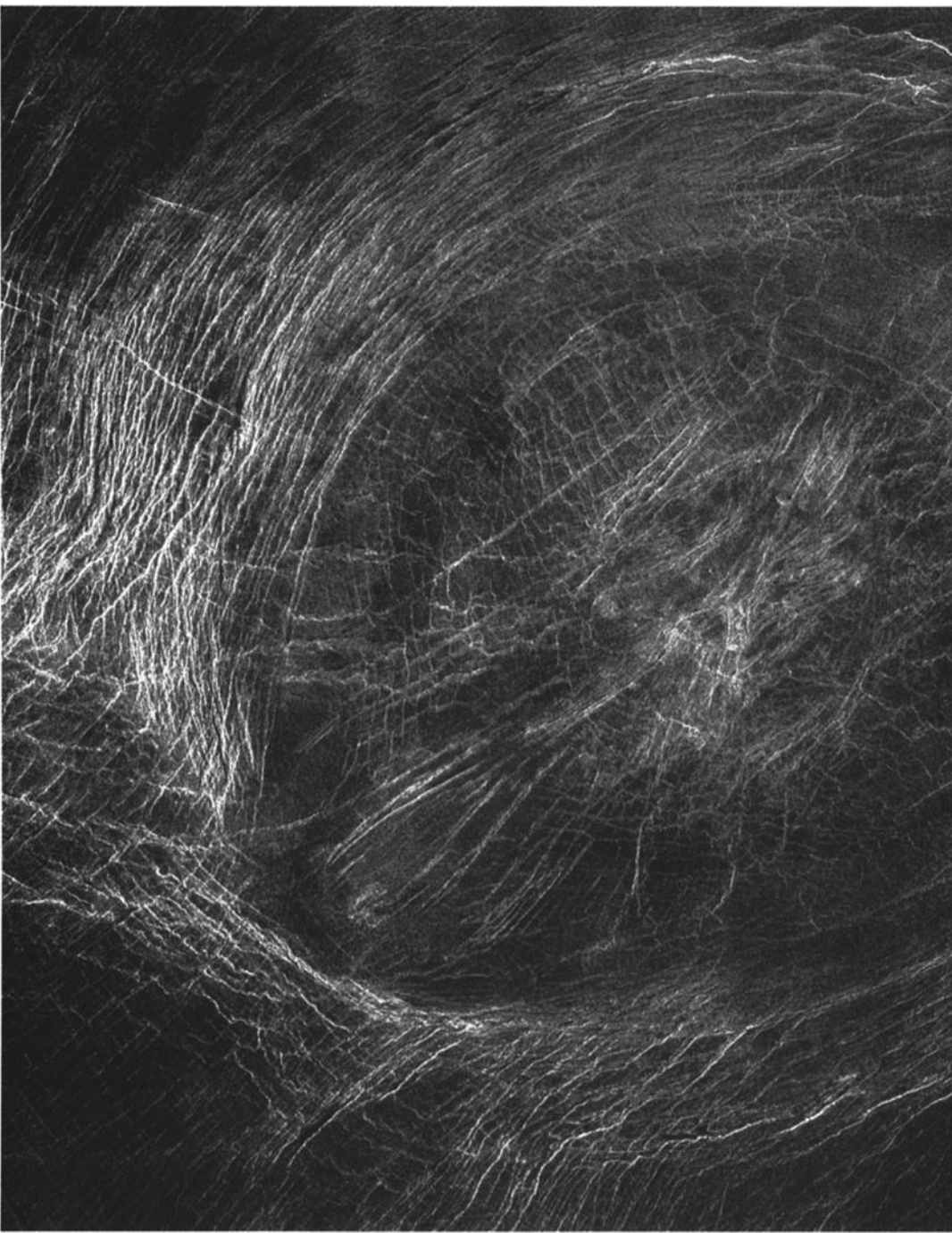


Fig. 35b A corona with obliquely-trending structures striking approximately NE-SW. This corona is at 31.5°N, 255°E; the image is 165 km wide.

in corona formation and evolution. Further, tectonic features associated with the regional stresses, such as extensional faults and graben oriented parallel to similar regional structures, can be superimposed on coronae. There are numerous examples of both of these effects [Squyres *et al.*, this issue (*b*)].

Models for Corona Formation and Evolution

On the basis of Venera 15-16 radar images of coronae, a generalized sequence of events in the formation and evolution of a typical corona was outlined by Stofan and

Head [1990]. Squyres *et al.* [this issue (*b*)] have confirmed this sequence on the basis of the more detailed Magellan observations of a large number of coronae and theoretical models of corona development [Stofan *et al.*, this issue; Janes *et al.*, this issue]. There are basically two stages in this generalized description of corona evolution. The initial stage involves domical upwarping and radial extensional faulting. The doming stage is followed by an extended period of modification in which gravitational relaxation plays an important role and in which most of the tectonic and topographic features of coronae are formed, including moats, rims, and tectonic annuli of concentric extensional faults and



Fig. 35c. Apparently compressional structures in the western rim annulus of Anahit Corona (77°N , 278°E). The image is about 225 km wide.

graben and compressional ridges. Volcanism can occur in both stages of corona development.

It has not yet proven possible to establish the relative timing of moat, rim, and annulus formation, but in coronae where these features and radial faults are present, the radial faults tend to be the oldest tectonic structures. If the moat, rim, and annulus are products of gravitational relaxation of coronae, then these features should have formed essentially contemporaneously, consistent with available observations. The existence of novae (domical uplifts with extensional radial faults), the theoretical prediction of extensional radial

faulting upon lithospheric upwarping, the elevated interior topography of coronae, the occurrence of old radial faults external to heavily modified coronae, the survival of high-standing radially faulted terrain in the interiors of heavily modified coronae, and the existence of coronae with both tectonic annuli and older radially faulted interiors and exteriors all combine to support the hypothesis that the nova is the initial stage in corona formation.

The morphology of coronae and the sequence of events in their evolution are consistent with corona formation by the ascent of a plume of hot mantle material to the base of the

lithosphere [Schubert et al., 1989, 1990; Stofan and Head, 1990; Squyres et al., this issue (b); Stofan et al., this issue; Janes et al., this issue; Schubert and Sandwell, this issue]. The nova stage corresponds to the initial arrival near the base of the lithosphere of the quasi-spherical plume head. The buoyancy of the plume head upwarps the lithosphere and creates the radial extensional faults. Following this initial stage, the plume head flattens against the overlying lithosphere, spreads radially outward, and thins the lithosphere above it, changing the topography into a more plateau-like shape. The radius of the corona increases with time during this stage. The final radius of the corona depends on the duration of plume activity and the supply of hot material to the flattened plume head. Some coronae may reach very large radii in this way (e.g., Artemis, Heng-O, and Quetzalpetlatl) and could still be growing at present. Flexural moats around coronae could occur at this stage as a radially expanding corona "eats" into and perhaps thrusts over the surrounding lithosphere [Sandwell and Schubert, this issue]. Eventually, the plume activity terminates, and the corona cools to the surface and relaxes gravitationally. The lithosphere thickens beneath the corona, the interior subsides, the rim develops, and the moat forms or develops further. Concentric extensional faulting in the tectonic annulus along the rim and moat occurs at this time, together with possible compressional deformation of the rim as well.

CONCLUDING DISCUSSION

Generalizations

With Magellan imaging and altimetry data now available for nearly the entire surface of Venus, we may make several generalizations about tectonic processes on both regional and global scales. The most obvious is that tectonic features on Venus are widespread and diverse. Comparatively few regions show no evidence of deformation; areas lacking tectonic features at Magellan resolution are restricted to what are probably among the youngest volcanic deposits and structures and the youngest impact craters and associated ejecta. Most of the surface, during at least some period over approximately the last 500 m.y. to 1 b.y. [Phillips et al., 1991a; Schaber et al., this issue], has experienced horizontal strain sufficient to fault or fold near-surface material.

Tectonic activity on Venus has continued until geologically recent time, and most likely the planet is tectonically active at present. Several arguments support this inference. The great relief and steep slopes of the mountains and plateau scarps of Ishtar Terra and of the equatorial chasm systems are difficult to reconcile with passive support by crustal strength for geologically significant lengths of time. Because of the high surface temperature on Venus, temperatures at which crustal rocks fail by ductile flow should be reached at much shallower depths than on Earth, as long as the temperature dependence of strength for crustal rocks is approximately similar on the two bodies [Weertman, 1979; Solomon and Head, 1984]. Numerical models suggest that areas of high relief and steep slope on Venus should spread under self-gravity by ductile flow of the weak lower crust on time scales less than about 10 m.y. [Smrekar and Solomon, this issue]. Thus the processes that build relief and

steepen slopes must have been active within the last 10 m.y. Further, a number of features produced by geological processes that have been operative more or less steadily during the past several hundred million years show evidence of subsequent tectonic activity. About one third of all preserved impact craters on Venus have throughgoing faults and fractures, and one in 12 are extensively deformed [Schaber et al., this issue]; tectonic activity appears to be capable of having removed at least some small craters from the current population of recognized impact structures. Some of the longest lava channels on the plains of Venus do not progress monotonically to lower elevations in the downstream direction, indicating that differential vertical motions have occurred since the channels were formed [Baker et al., this issue].

Compared with the Earth, horizontal displacements on Venus over the last 500 m.y. have been limited. Most of the tectonic features require modest strains and horizontal displacements of no more than a few tens to perhaps a few hundreds of kilometers. Plains thousands of kilometers across contain families of graben which cumulatively record horizontal strains of order 10^{-2} or less. The great rift systems of Beta and Atla regiones need have extended no more than a few tens of kilometers, on the basis of topographic profiles, features such as the rifted crater Somerville in Devana Chasma (Figure 5), and analogy with continental rifts on Earth [McGill et al., 1981]. For compressional structures, the amount of crustal thickening can be estimated under the simplifying assumption that the crust beneath a positive-relief feature has been isostatically thickened by thrusting and lower crustal flow; if valid, this approach provides only a lower bound on horizontal displacements if any crustal material is recycled into the mantle at zones of underthrusting. For ridge belts 100 km in width and with up to 1 km of relief, horizontal displacements of no more than 100 km are required if the crust is 10-20 km thick beneath the adjacent plains [Grimm and Solomon, 1988; Zuber and Parmentier, 1990]. Mountain belts are exceptional in that greater horizontal displacements are required. For a twofold to fourfold tectonic thickening of the crust beneath the 500 km width of Maxwell Montes, i.e., if at least half of the relief is supported by an Airy isostatic root, the implied minimum horizontal displacement is 1000-2000 km.

Unlike Earth, Venus does not show evidence for a global system of nearly rigid lithospheric plates with horizontal dimensions of 10^3 - 10^4 km separated by narrow plate boundary zones a few kilometers to tens of kilometers across. Predictions prior to Magellan that Aphrodite Terra would show features analogous to terrestrial spreading centers and oceanic fracture zones [Head and Crumpler, 1987, 1990] are now seen to be incorrect. Evidence for shear is present in the ridge and fracture belts and in the mountain belts, but the shearing tends to be broadly distributed and to accompany horizontal stretching or shortening. Few clear examples have yet been documented of long, large-offset strike-slip faults such as those typical of oceanic and many continental areas on Earth; two such features have been identified in the interior of Artemis Corona [McKenzie et al., this issue]. A number of the chasm systems of Venus have arcuate planforms, asymmetric topographic profiles, and high relief [Ford and Pettengill, this issue] and have been likened to

deep-sea trenches on Earth [McKenzie *et al.*, this issue]. These include arcuate segments of Dali and Diana chasmata [McKenzie *et al.*, this issue] and the moat structure of Artemis Corona [Sandwell and Schubert, this issue]; such trenches may be products of limited underthrusting or subduction of lithosphere surrounding large coronae [Sandwell and Schubert, this issue]. Elsewhere, however, chasm systems of comparable to somewhat lesser relief display more linear segments and more nearly symmetric topographic profiles, such as Devana Chasma, and on the basis of small-scale morphology are clearly extensional rifts. Further analysis of the highest-resolution images and topography as well as gravity measurements to be made later in the Magellan mission should help to resolve whether chasms on Venus are produced by compressional as well as extensional processes.

Much of the tectonic behavior on Venus appears to be more reminiscent of actively deforming continental regions than of oceanic regions on Earth. In particular, as in tectonically active continental areas, deformation is typically distributed across broad zones one to a few hundred kilometers wide separated by comparatively stronger and less deformed blocks having dimensions of hundreds of kilometers. On Earth, the continental lithosphere in tectonically active areas is weaker than typical oceanic lithosphere because of the greater thickness of more easily deformable crust. As noted above, because of the higher surface temperature on Venus, the likely comparable lithospheric thermal gradients on Venus and Earth [Solomon and Head, 1982; Phillips and Malin, 1984], and the strong temperature dependence of ductile behavior, the lithosphere on Venus should behave in a weak manner for crustal thicknesses less than those typical of continental regions on Earth.

Characteristic Scales of Deformation

Examples of both horizontal shortening and horizontal extension occur at a variety of scales on Venus, ranging from the 1-km scale that characterizes the spacing between tectonic features in a number of regions to the 1000-km scale that governs the large-scale physiography of major structures and the spatial coherence of many smaller-scale patterns of strain. These various scales of deformation likely arise from the complicated mechanical and dynamical structure of the Venus interior. The 10–30 km scale is plausibly attributed to the response of a strong upper crustal layer, while the deformation of a strong upper mantle layer can account for tectonic features with characteristic scales of a few hundred kilometers [Zuber, 1987; Banerdt and Golombek, 1988; Zuber and Parmentier, 1990]. The scale of a few hundred to a few thousand kilometers, particularly where evident in the long-wavelength gravity as well as the topography, is likely dominated by mantle convection and its associated dynamic stresses and heat transport [Phillips, 1986, 1990]. The scale of a few kilometers and less involves either internal deformation of the upper crust or tectonic disruption of a thin surficial layer decoupled thermally or mechanically from the remainder of the otherwise strong upper crust.

Because our understanding of the thermal structure of the Venus interior is based entirely on theoretical models and analogy with Earth, direct observational tests of mechanical and thermal models for the Venus lithosphere are crucial. The

most straightforward of such tests is to estimate the thickness of the elastic lithosphere of Venus from the flexural response to lithospheric loads [McNutt, 1984]. Prior to Magellan, the most likely identified case of flexure was where the lithosphere of the north polar plains was interpreted as having underthrust Ishtar Terra along Uorsar Rupes [Head, 1990a]. The flexural length scale indicated by Venera 15–16 topographic profiles implied an elastic lithosphere 11–18 km thick, consistent with a thermal gradient of 15–25 K/km and a heat flow of 50–70 mW/m² [Solomon and Head, 1990a]. These values of thermal gradient and heat flow are in the range expected for the global averages of these quantities [Solomon and Head, 1982; Phillips and Malin, 1984], and the north polar plains stand at an elevation near the modal value for the planet, consistent with the premises that global heat loss on Venus may be estimated by scaling from Earth and that the majority of the heat transport through the outer layers of the planet occurs by lithospheric conduction [Solomon and Head, 1982, 1991; Morgan and Phillips, 1983].

Several additional estimates of elastic lithosphere thickness have been made from Magellan data. Sandwell and Schubert [this issue] fit flexural models to Magellan topographic profiles exterior to Uorsar Rupes and to three large corona structures. For the flexure of the north polar plains beneath northern Ishtar Terra at Uorsar Rupes, Sandwell and Schubert [this issue] obtained an elastic lithosphere thickness of 10–25 km and a thermal gradient of 10–25 K/km, values essentially equivalent to those obtained from Venera data [Solomon and Head, 1990a]. For the coronae Heng-O and Artemis, and for the Latona structure consisting of paired arcuate segments of Dali and Diana chasmata (Figure 15), however, Sandwell and Schubert [this issue] obtained significantly greater elastic lithosphere thicknesses (30–60 km) and correspondingly lesser lithospheric thermal gradients (3–9 K/km). For a fourth corona, Eithinoha, they obtained a smaller elastic lithosphere thickness (10–30 km range, 15 km best fitting value), comparable to that for the north polar plains. From the radial distances of graben to the NW of and approximately concentric to Gula Mons, Grimm and Phillips [this issue] estimated that the elastic lithosphere would have to have been at least 50 km thick at the time of graben formation if the faults formed as a result of flexural loading.

Taken at face value, these large values for elastic lithosphere thickness pose a challenge to presently accepted thinking about the thermal structure of Venus. The implied thermal gradients are remarkably low, particularly for regions near coronae and a major volcano, areas that should be sites of heat flow at least as great as the global average. The failure of one of two key assumptions in the flexural analysis, however, may render the derived thermal gradients incorrect. First, if the lower lithosphere and underlying asthenosphere are viscoelastic, then topographic profiles obtained during the time-dependent response to surface loading by volcanism or underthrusting may mimic that due to flexure of an elastic plate overlying an inviscid interior [e.g., Smrekar and Solomon, this issue], and the derived flexural parameter may not readily be relatable to temperature at depth. Second, if because of the low water content of the lower Venus atmosphere the Venus crust and upper mantle are very dry, then crustal and mantle rocks on Venus may be considerably

more creep-resistant at a given temperature than would be indicated by flow laws for ductile creep derived from laboratory experiments on terrestrial samples. In that situation the thermal gradients derived from elastic lithosphere thicknesses could be greater than indicated above. Further analysis of these issues is warranted. If such analysis supports the flexural and thermal interpretations as cited, then interior heat production and global heat flow on Venus may be substantially less than current estimates.

For the flexural studies discussed above it has been presumed that much of the flexural strength of the Venus lithosphere is provided by the layer of strong mantle material lying immediately beneath the crust. The upper crust should also behave as a strong layer on geological times scales [Zuber, 1987; Banerdt and Golombek, 1988; Zuber and Parmentier, 1990]. Because crustal rocks lose strength at temperatures only slightly higher than the Venus surface temperature, however, the strong upper crustal layer may be quite thin, perhaps only a few kilometers or less [Solomon and Head, 1984]. The surface temperature on Venus varies with elevation at a rate of about 8 K/km [Seiff et al., 1980], so that the highest elevations are as much as 80 K cooler than at the mean planetary radius. Suppe and Connors [this issue] have measured the relief on Venus fold belts, the difference in elevation between the toe of the fold belt wedge and the crest of the belt, and have documented a linear relationship between such relief and absolute elevation. They interpret this linear relationship as evidence for an influence of surface temperature on the thickness of the strong upper crustal layer.

Status of Models for Interior Dynamics

A major challenge in unravelling the tectonic evolution of Venus is to understand the interaction between mantle convection and the lithosphere. As discussed above, the hotspot and the coldspot models for the formation and evolution of major highlands on Venus are distinguishable on the basis of the predicted sequence of events and the time-dependent relationship between topography and gravity. Both models face difficulties in their present forms, however, at least partly because both the rheology of the upper crust of Venus and the observed patterns of magmatism and deformation are more complex than in current models for the deformation and magmatic response of the crust to mantle flow. Any model for the formation of highlands on Venus, of course, must also consider the formation of lowlands as part of an internally consistent global paradigm. For both the coldspot and hotspot models for the origin of highlands, the large apparent depths of isostatic compensation in the lowlands [Phillips et al., 1991b] must be interpreted, for self-consistency, in terms of dynamic support. A successful model must also account for volcanism in the lowlands, including volcanism more recent than much of the compressional deformation accommodated by deformation belts, as in Lavinia Planitia. The ultimate fate of lowlands in the two classes of models differs because of strong secondary crustal flow in the coldspot model.

All dynamical models to date require special pleading to explain Ishtar Terra. As explained above, the hotspot model appeals to lateral variations in lithospheric strength to explain the formation of the mountain belts on the periphery

of Lakshmi Planum [Grimm and Phillips, 1990, 1991]. In the coldspot model, Ishtar Terra must overlie a region of anomalously vigorous downwelling to explain both the elevation of the plateaus and the origin and maintenance of the mountain belts [Bindschadler et al., this issue (b)]. A successful model must also explain the volcanism that is observed on Lakshmi Planum and on several outward plateaus, as well as the large amount of potential energy stored in the downwelling plume that is required to satisfy the gravity field under the coldspot model [Grimm and Phillips, 1991].

Both the Beta-type highlands and coronae are generally regarded as sites of upwelling mantle flow and magma generation by pressure-release partial melting of mantle material. These two classes of features have very different tectonic and morphological manifestations at the Venus surface. While coronae are greater in number by two orders of magnitude and most coronae are less than 400 km in diameter [Stofan et al., this issue], the horizontal dimensions of the largest coronae (up to 2600 km for Artemis) overlap those of such smaller Beta-type highlands as Bell Regio. If both Beta-type highlands and coronae are products of mantle upwelling, then multiple scales of mantle convection are indicated and the different morphologies of the two classes of features may be related to differences in the geometry, buoyancy flux, or duration of flow in the two types of upwelling regions. It has also been suggested that the smaller coronae are not the result of plumes formed by instabilities in the lower thermal boundary layer of mantle convection but arise from another process, such as Rayleigh-Taylor instabilities in layers of melt distributed within broader zones of mantle upwelling [Tackley and Stevenson, 1991].

We have hardly begun the process of assessing existing dynamical models for the tectonic evolution of Venus in the context of Magellan data, much less developing the next generation of models. Such an assessment will require an understanding of geological relationships at all scales, from the highest resolution available to global patterns. High-resolution measurements of the global gravity field later in the Magellan mission, particularly at high-latitude regions such as Ishtar Terra, are needed to provide key data for testing and refining models. The current hotspot and coldspot models are, at best, highly simplified idealizations. The Magellan mission has provided a rich new data set on the complex inner workings of Venus. A challenge to terrestrial and planetary geophysicist alike is ultimately to understand these new data in terms of a generalized theory for the interior dynamics of terrestrial planets.

Acknowledgments. We are indebted to Linda Meinke for assistance with the preparation of the altimetry figures. We also thank Peter Ford for providing early access to Magellan altimetry data, Susan Yewell and the Magellan Data Management and Archive Team for help with the photographic reproduction of Magellan images, Matt Golombek and Ken Tanaka for constructively reviewing an earlier manuscript draft, and the many members of the Magellan science team who freely shared ideas and preprints of papers. This research has been supported by the Magellan Project under contract JPL 957070 from the Jet Propulsion Laboratory to MIT and additional contracts to the institutions of the coauthors.

REFERENCES

- Arvidson, R. E., V. R. Baker, C. Elachi, R. S. Saunders, and J. A. Wood, Magellan: Initial analysis of Venus surface modification, *Science*, 252, 270–275, 1991.

- Baker, V. R., G. Komatsu, T. J. Parker, V. C. Gulick, J. S. Kargel, and J. S. Lewis, Channels and valleys on Venus: Preliminary analysis of Magellan data, *J. Geophys. Res.*, this issue.
- Banerdt, W. B., and M. P. Golombek, Deformational models of rifting and folding on Venus, *J. Geophys. Res.*, 93, 4759-4772, 1988.
- Barsukov, V. L., et al., The geology and geomorphology of the Venus surface as revealed by the radar images obtained by Veneras 15 and 16, *Proc. Lunar Planet. Sci. Conf. 16th*, Part 2, *J. Geophys. Res.*, 91, suppl., D378-D398, 1986.
- Basilevsky, A. T., Structure of central and eastern areas of Ishtar Terra and some problems of Venusian tectonics, *Geotectonics*, 20, 282-288, 1986.
- Basilevsky, A. T., A. A. Pronin, L. B. Ronca, V. P. Kryuchkov, A. L. Sukhanov, and M. S. Markov, Styles of tectonic deformations on Venus: Analysis of Venera 15 and 16 data, *Proc. Lunar Planet. Sci. Conf. 16th*, Part 2, *J. Geophys. Res.*, 91, suppl., D399-D411, 1986.
- Bindschadler, D. L., and J. W. Head, Diffuse scattering on the surface of Venus: Origin and implications for the distribution of soils, *Earth Moon Planets*, 42, 133-149, 1988.
- Bindschadler, D. L., and J. W. Head, Characterization of Venera 15/16 geologic units from Pioneer Venus reflectivity and roughness data, *Icarus*, 77, 3-20, 1989.
- Bindschadler, D. L., and J. W. Head, Tessera terrain, Venus: Characterization and models for origin and evolution, *J. Geophys. Res.*, 96, 5889-5907, 1991.
- Bindschadler, D. L., and E. M. Parmentier, Mantle flow tectonics: The influence of a ductile lower crust and implications for the formation of topographic uplands on Venus, *J. Geophys. Res.*, 95, 21,329-21,344, 1990.
- Bindschadler, D. L., M. A. Kreslavsky, M. A. Ivanov, J. W. Head, A. T. Basilevsky, and Yu. G. Shkuratov, Distribution of tessera terrain on Venus: Prediction for Magellan, *Geophys. Res. Lett.*, 17, 171-174, 1990a.
- Bindschadler, D. L., G. Schubert, and W. M. Kaula, Mantle flow tectonics and the origin of Ishtar Terra, Venus, *Geophys. Res. Lett.*, 17, 1345-1348, 1990b.
- Bindschadler, D. L., A. deCharon, K. K. Beratan, S. E. Smrekar, and J. W. Head, Magellan observations of Alpha Regio: Implications for formation of complex ridged terrains on Venus, *J. Geophys. Res.*, this issue (a).
- Bindschadler, D. L., G. Schubert, and W. M. Kaula, Coldspots and hotspots: Global tectonics and mantle dynamics of Venus, *J. Geophys. Res.*, this issue (b).
- Campbell, D. B., J. W. Head, J. K. Harmon, and A. A. Hine, Venus: Identification of banded terrain in the mountains of Ishtar Terra, *Science*, 221, 644-647, 1983.
- Campbell, D. B., J. W. Head, J. K. Harmon, and A. A. Hine, Venus: Volcanism and rift formation in Beta Regio, *Science*, 226, 167-170, 1984.
- Campbell, D. B., D. A. Senske, J. W. Head, A. A. Hine, and P. C. Fisher, Venus southern hemisphere: Geologic character and age of terrains in the Themis-Alpha-Lada region, *Science*, 251, 180-183, 1991.
- Crumpler, L. S., J. W. Head, and D. B. Campbell, Orogenic belts on Venus, *Geology*, 14, 1031-1034, 1986.
- Dewey, J. F., and K. Burke, Hot spots and continental break-up: Implications for collisional orogeny, *Geology*, 2, 57-60, 1974.
- Ford, P. G., and G. H. Pettengill, Venus topography and kilometer-scale slopes, *J. Geophys. Res.*, this issue.
- Frank, S. L., and J. W. Head, Ridge belts on Venus: Morphology and origin, *Earth Moon Planets*, 50/51, 421-470, 1990.
- Grimm, R. E., and R. J. Phillips, Tectonics of Lakshmi Planum, Venus: Tests for Magellan, *Geophys. Res. Lett.*, 17, 1349-1352, 1990.
- Grimm, R. E., and R. J. Phillips, Gravity anomalies, compensation mechanisms, and the geodynamics of western Ishtar Terra, Venus, *J. Geophys. Res.*, 96, 8305-8324, 1991.
- Grimm, R. E., and R. J. Phillips, Anatomy of a Venusian hot spot: Geology, gravity, and mantle dynamics of Eistla Regio, *J. Geophys. Res.*, this issue.
- Grimm, R. E., and S. C. Solomon, Viscous relaxation of impact crater relief on Venus: Constraints on crustal thickness and thermal gradient, *J. Geophys. Res.*, 93, 11,911-11,929, 1988.
- Grimm, R. E., and S. C. Solomon, Tests of crustal divergence models for Aphrodite Terra, Venus, *J. Geophys. Res.*, 94, 12,103-12,131, 1989.
- Head, J. W., Formation of mountain belts on Venus: Evidence for large-scale convergence, underthrusting, and crustal imbrication in Freyja Montes, Ishtar Terra, *Geology*, 18, 99-102, 1990a.
- Head, J. W., Venus trough-and-ridge tessera: Analog to Earth oceanic crust formed at spreading centers?, *J. Geophys. Res.*, 95, 7119-7132, 1990b.
- Head, J. W., III, and L. S. Crumpler, Evidence for divergent plate-boundary characteristics and crustal spreading on Venus, *Science*, 238, 1380-1385, 1987.
- Head, J. W., and L. S. Crumpler, Venus geology and tectonics: Hotspot and crustal spreading models and questions for the Magellan mission, *Nature*, 346, 525-533, 1990.
- Head, J. W., D. B. Campbell, C. Elachi, J. E. Guest, D. McKenzie, R. S. Saunders, G. G. Schaber, and G. Schubert, Venus volcanism: Initial analysis from Magellan data, *Science*, 252, 276-288, 1991.
- Head, J. W., L. S. Crumpler, J. C. Aubele, J. E. Guest, and R. S. Saunders, Venus volcanism: Classification of volcanic features and structures, associations, and global distribution from Magellan data, *J. Geophys. Res.*, this issue.
- Herrick, R. R., and R. J. Phillips, Blob tectonics: A prediction for western Aphrodite Terra, Venus, *Geophys. Res. Lett.*, 17, 2192-2132, 1990.
- Herrick, R. R., B. G. Bills, and S. A. Hall, Variations in effective compensation depth across Aphrodite Terra, Venus, *Geophys. Res. Lett.*, 16, 543-546, 1989.
- Janes, D. M., D. L. Bindschadler, G. Baer, G. Schubert, V. L. Sharpton, S. W. Squyres, and E. R. Stofan, Geophysical models for the formation and evolution of coronae on Venus, *J. Geophys. Res.*, this issue.
- Janle, P., D. Jannsen, and A. T. Basilevsky, Morphologic and gravimetric investigations of Bell and Eisila regiones on Venus, *Earth Moon Planets*, 39, 251-273, 1987.
- Janle, P., D. Jannsen, and A. T. Basilevsky, Tepev Mons on Venus: Morphology and elastic bending models, *Earth Moon Planets*, 41, 127-139, 1988.
- Kaula, W. M., D. L. Bindschadler, R. E. Grimm, V. L. Hansen, K. M. Roberts, and S. E. Smrekar, Styles of deformation in Ishtar Terra and their implications, *J. Geophys. Res.*, this issue.
- Kiefer, W. S., and B. H. Hager, Geoid anomalies and dynamic topography from convection in cylindrical geometry: Applications to mantle plumes on Earth and Venus, *Geophys. J. Int.*, 108, 198-214, 1992.
- Klose, K. B., J. A. Wood, and A. Hashimoto, Mineral equilibria and the high radar reflectivity of Venus mountain tops, *J. Geophys. Res.*, this issue.
- Kryuchkov, V. P., Ridge belts on the plains of Venus, 1 (abstract), *Lunar Planet. Sci.*, 19, 649-650, 1988.
- Markov, M. S., et al., The geologic and morphological structure of the Bell Region (A photographic map of the surface of Venus, Plate V-23), *Solar Syst. Res.*, 21, 8-14, 1987.
- Masursky, H., E. Eliason, P. G. Ford, G. E. McGill, G. H. Pettengill, G. G. Schaber, and G. Schubert, Pioneer Venus radar results: Geology from images and altimetry, *J. Geophys. Res.*, 85, 8232-8260, 1980.
- McGill, G. E., Structural evolution of Venusian plains (abstract), *Eos Trans. AGU*, 72 (17), Spring Meeting Suppl., 173, 1991.
- McGill, G. E., S. J. Steenstrup, C. Barton, and P. G. Ford, Continental rifting and the origin of Beta Regio, Venus, *Geophys. Res. Lett.*, 8, 737-740, 1981.
- McGill, G. E., J. L. Warner, M. C. Malin, R. E. Arvidson, E. Eliason, S. Nozette, and R. D. Reasenberg, Topography, surface properties, and tectonic evolution, in *Venus*, edited by D. M. Hunten, L. Colin, T. M. Donahue, and V. I. Moroz, pp. 69-130, University of Arizona Press, Tucson, 1983.
- McGill, G. E., E. R. Stofan, R. S. Saunders, and P. G. Ford, Depositional and structural sequence revealed by mapping on Magellan radar images, Eistla Regio/Guinevere Planitia area, Venus (abstract), *Lunar Planet. Sci.*, 22, 877-878, 1991.
- McKenzie, D., P. G. Ford, C. Johnson, B. Parsons, D. Sandwell, S. Saunders, and S. C. Solomon, Features on Venus generated by plate boundary processes, *J. Geophys. Res.*, this issue.
- McNutt, M. K., Lithospheric flexure and thermal anomalies, *J. Geophys. Res.*, 89, 11,180-11,194, 1984.
- Morgan, P., and R. J. Phillips, Hot spot heat transfer: Its application to Venus and implications to Venus and Earth, *J. Geophys. Res.*, 88, 8305-8317, 1983.

- Pettengill, G. H., E. Eliason, P. G. Ford, G. B. Loriot, H. Masursky, and G. E. McGill, Pioneer Venus radar results: Altimetry and surface properties, *J. Geophys. Res.*, 85, 8261-8270, 1980.
- Pettengill, G. H., P. G. Ford, and B. D. Chapman, Venus: Surface electromagnetic properties, *J. Geophys. Res.*, 93, 14,881-14,892, 1988.
- Pettengill, G. H., P. G. Ford, W. T. K. Johnson, R. K. Raney, and L. A. Soderblom, Magellan: Radar performance and data products, *Science*, 252, 260-265, 1991.
- Phillips, R. J., A mechanism for tectonic deformation on Venus, *Geophys. Res. Lett.*, 13, 1141-1144, 1986.
- Phillips, R. J., Convection-driven tectonics on Venus, *J. Geophys. Res.*, 95, 1301-1316, 1990.
- Phillips, R. J., and M. C. Malin, The interior of Venus and tectonic implications, in *Venus*, edited by D. M. Hunten, L. Colin, T. M. Donahue, and V. I. Moroz, pp. 159-214, University of Arizona Press, Tucson, 1983.
- Phillips, R. J., and M. C. Malin, Tectonics of Venus, *Annu. Rev. Earth Planet. Sci.*, 12, 411-443, 1984.
- Phillips, R. J., W. M. Kaula, G. E. McGill, and M. C. Malin, Tectonics and evolution of Venus, *Science*, 212, 879-887, 1981.
- Phillips, R. J., R. E. Arvidson, J. M. Boyce, D. B. Campbell, J. E. Guest, G. G. Schaber, and L. A. Soderblom, Impact craters on Venus: Initial analysis from Magellan, *Science*, 252, 288-297, 1991a.
- Phillips, R. J., R. E. Grimm, and M. C. Malin, Hot-spot evolution and the global tectonics of Venus, *Science*, 252, 651-658, 1991b.
- Plescia, J. B., and M. P. Golombek, Origin of planetary wrinkle ridges based on the study of terrestrial analogs, *Geol. Soc. Am. Bull.*, 97, 1289-1299, 1986.
- Pronin, A. A., The structure of Lakshmi Planum, an indication of horizontal asthenospheric flow on Venus, *Geotectonics*, 20, 271-281, 1986.
- Pronin, A. A., and E. R. Stofan, Coronae on Venus: Morphology, classification, and distribution, *Icarus*, 87, 452-474, 1990.
- Roberts, K. M., and J. W. Head, Lakshmi Planum, Venus: Characteristics and models of origin, *Earth Moon Planets*, 50/51, 193-249, 1990.
- Sandwell, D. T., and G. Schubert, Flexural ridges, trenches, and outer rises around coronae on Venus, *J. Geophys. Res.*, this issue.
- Saunders, R. S., R. E. Arvidson, J. W. Head, III, G. G. Schaber, E. R. Stofan, and S. C. Solomon, An overview of Venus geology, *Science*, 252, 249-252, 1991.
- Schaber, G. G., Venus: Limited extension and volcanism along zones of lithospheric weakness, *Geophys. Res. Lett.*, 9, 499-502, 1982.
- Schaber, G. G., R. G. Strom, H. J. Moore, L. A. Soderblom, R. L. Kirk, D. J. Chadwick, D. D. Dawson, L. R. Gaddis, J. M. Boyce, and J. Russell, Geology and distribution of impact craters on Venus: What are they telling us?, *J. Geophys. Res.*, this issue.
- Schubert, G., Numerical models of mantle convection, *Annu. Rev. Fluid Mech.*, 24, 359-394, 1992.
- Schubert, G., D. Bercovici, P. J. Thomas, and D. B. Campbell, Venus coronae: Formation by mantle plumes (abstract), *Lunar Planet. Sci.*, 20, 968-969, 1989.
- Schubert, G., D. Bercovici, and G. A. Glatzmaier, Mantle dynamics in Mars and Venus: Influence of an immobile lithosphere on three-dimensional mantle convection, *J. Geophys. Res.*, 95, 14,105-14,129, 1990.
- Seiff, A., D. B. Kirk, R. E. Young, R. C. Blanchard, J. T. Findlay, G. M. Kelly, and S. C. Sommer, Measurements of thermal structure and thermal contrasts in the atmosphere of Venus and related dynamical observations: Results from the four Pioneer Venus probes, *J. Geophys. Res.*, 85, 7903-7933, 1980.
- Senske, D. A., Geology of the Venus equatorial region from Pioneer Venus radar imaging, *Earth Moon Planets*, 50/51, 305-327, 1990.
- Senske, D. A., J. W. Head, E. R. Stofan, and D. B. Campbell, Geology and structure of Beta Regio, Venus: Results from Arecibo radar imaging, *Geophys. Res. Lett.*, 18, 1159-1162, 1991.
- Senske, D. A., G. G. Schaber, and E. R. Stofan, Regional topographic rises on Venus: Geology of western Eistla Regio and comparison to Beta Regio and Atla Regio, *J. Geophys. Res.*, this issue.
- Sjogren, W. L., B. G. Bills, P. W. Birkeland, P. B. Esposito, A. R. Konopliv, N. A. Mottinger, S. J. Ritke, and R. J. Phillips, Venus gravity anomalies and their correlations with topography, *J. Geophys. Res.*, 88, 1119-1128, 1983.
- Smrekar, S., and R. J. Phillips, Gravity-driven deformation of the crust on Venus, *Geophys. Res. Lett.*, 15, 693-696, 1988.
- Smrekar, S. E., and R. J. Phillips, Venusian highlands: Geoid to topography ratios and their implications, *Earth Planet. Sci. Lett.*, 107, 582-597, 1991.
- Smrekar, S. E., and S. C. Solomon, Gravitational spreading of high terrain in Istar Terra, Venus, *J. Geophys. Res.*, this issue.
- Solomon, S. C., and J. W. Head, Mechanisms for lithospheric heat transport on Venus: Implications for tectonic style and volcanism, *J. Geophys. Res.*, 87, 9236-9246, 1982.
- Solomon, S. C., and J. W. Head, Venus banded terrain: Tectonic models for band formation and their relationship to lithospheric thermal structure, *J. Geophys. Res.*, 89, 6885-6897, 1984.
- Solomon, S. C., and J. W. Head, Lithospheric flexure beneath the Freyja Montes foredeep, Venus: Constraints on lithospheric thermal gradient and heat flow, *Geophys. Res. Lett.*, 17, 1393-1396, 1990a.
- Solomon, S. C., and J. W. Head, Tepev Mons and the elastic lithosphere of Venus: An assessment of flexure models (abstract), *Lunar Planet. Sci.*, 21, 1180-1181, 1990b.
- Solomon, S. C., and J. W. Head, Fundamental issues in the geology and geophysics of Venus, *Science*, 252, 252-260, 1991.
- Solomon, S. C., J. W. Head, W. M. Kaula, D. McKenzie, B. Parsons, R. J. Phillips, G. Schubert, and M. Talwani, Venus tectonics: Initial analysis from Magellan, *Science*, 252, 297-312, 1991.
- Squyres, S. W., D. G. Jankowski, M. Simons, S. C. Solomon, B. H. Hager, and G. E. McGill, Plains tectonism on Venus: The deformation belts of Lavinia Planitia, *J. Geophys. Res.*, this issue (a).
- Squyres, S. W., D. M. Janes, G. Baer, D. L. Bindschadler, G. Schubert, V. L. Sharpton, and E. R. Stofan, The morphology and evolution of coronae on Venus, *J. Geophys. Res.*, this issue (b).
- Stofan, E. R., and J. W. Head, Coronae of Mnemosyne Regio: Morphology and origin, *Icarus*, 83, 216-243, 1990.
- Stofan, E. R., J. W. Head, D. B. Campbell, S. H. Zisk, A. F. Bogomolov, O. N. Rzhiga, A. T. Basilevsky, and N. Armand, Geology of a rift zone on Venus: Beta Regio and Devana Chasma, *Geol. Soc. Am. Bull.*, 101, 143-156, 1989.
- Stofan, E. R., V. L. Sharpton, G. Schubert, G. Baer, D. L. Bindschadler, D. M. Janes, and S. W. Squyres, Global distribution and characteristics of coronae and related features on Venus: Implications for origin and relation to mantle processes, *J. Geophys. Res.*, this issue.
- Sukhanov, A. L., Parquet: Regions of areal plastic dislocations, *Geotectonics*, 20, 294-305, 1986.
- Sukhanov, A. L., et al., Geomorphic/geologic map of part of the northern hemisphere of Venus, Map I-2059, U.S. Geol. Surv., 1989.
- Suppe, J., and C. Connors, Critical taper wedge mechanics of fold-and-thrust belts on Venus, *J. Geophys. Res.*, this issue.
- Tackley, P. J., and D. J. Stevenson, The production of small Venusian coronae by Rayleigh-Taylor instabilities in the uppermost mantle (abstract), *Eos Trans. AGU*, 72 (44), Fall Meeting Suppl., 287, 1991.
- Vorder Bruegge, R. W., and J. W. Head, Fortuna Tessera, Venus: Evidence of horizontal convergence and crustal thickening, *Geophys. Res. Lett.*, 16, 699-702, 1989.
- Watters, T. R., Wrinkle ridge assemblages on the terrestrial planets, *J. Geophys. Res.*, 93, 10,236-10,254, 1988.
- Weertman, J., Height of mountains on Venus and the creep properties of rock, *Phys. Earth Planet. Inter.*, 19, 197-207, 1979.
- Zuber, M. T., Constraints on the lithospheric structure of Venus from mechanical models and tectonic surface features, *Proc. Lunar Planet. Sci. Conf. 17th*, Part 2, *J. Geophys. Res.*, 92, suppl., E541-E551, 1987.
- Zuber, M. T., and E. M. Parmentier, On the relationship between isostatic elevation and the wavelengths of tectonic surface features on Venus, *Icarus*, 85, 290-308, 1990.

D. L. Bindschadler, W. M. Kaula, and G. Schubert, Department of Earth and Space Sciences, University of California, Los Angeles, CA 90024-1567.

R. E. Grimm, Department of Geology, Arizona State University, Tempe, AZ 85287.

G. E. McGill, Department of Geology and Geography, University of Massachusetts, Amherst, MA 01003.

R. J. Phillips, Department of Earth and Planetary Sciences, Washington University, St. Louis, MO 63130.

R. S. Saunders and E. R. Stofan, M/S 230-225, Jet Propulsion Laboratory, 4800 Oak Grove Drive, Pasadena, CA 91109.

S. E. Smrekar and S. C. Solomon, Building 54-520, Department of Earth, Atmospheric, and Planetary Sciences, Massachusetts Institute of Technology, Cambridge, MA 02139.

S. W. Squyres, Center for Radiophysics and Space Research, 428 Space Sciences Building, Cornell University, Ithaca, NY 14853.

(Received November 27, 1991;
revised June 19, 1992
accepted June 19, 1992.)